Institute for Water and Energy Sciences (incl. Climate Change)

Master Dissertation

Submitted in partial fulfilment of the requirements for the degree of

Master of science in

WATER ENGINEERING

Presented by

Jeannette NIYONSABA

FLOOD RISK ASSESSMENT AND HYDROLOGICAL MODELING USING HEC-HMS: SEBEYA CATCHMENT , RWANDA

Defended on 20th/04/ 2025 Before the Following Committee:

Chair	Hartani Tarek	Prof. National Higher School of Agronomy
Supervisor	Umaru Garba WALI	Prof. University of Rwanda
External Examiner	Franco Matías FRANCISCA	Prof. National University of Cordoba
Internal Examiner	BENTALHA Chakib	Dr. University of Tlemcen

APPROVAL SHEET

The undersigned confirm that they have reviewed the document and hereby endorse its submission to the Pan African University of Water and Energy Sciences, including Climate Change (PAUWES) research thesis titled **FLOOD RISK ASSESSMENT AND HYDROLOGICAL MODELING IN SEBEYA CATCHMENT USING HEC-HMS-RWANDA**, in partial fulfilment of the requirements for the award of **MASTER OF SCIENCE IN WATER ENGINEERING.**

DECLARATION

I, Jeannette NIYONSABA , affirm that I have authored this submission independently. To the best of my understanding and conviction, it does not include any content previously published or authored by anyone nor does it incorporate material acknowledged for the attainment of any other University or higher education degree. Any instances where I have drawn upon external sources are appropriately acknowledged in the text and reference list.

Signature :  Date : 20/04/2025

Name : Jeannette NIYONSABA

Reg. N^0 : PAUWES/2023/MWE03

This thesis is Jeannette NIYONSABA's own work. The candidate displayed strong research skills, a keen analytical mind and the capacity to think critically and creatively. She has successfully navigated the complexity of her chosen research issue by doing extensive literature reviews, creating rigorous techniques and collecting and analysing data efficiently. The thesis was written with our help and supervision. It has been submitted for review with our consent as the official University Supervisor.

Signature:  Date: 20/04/2025

Prof. Umaru Garba WALI

Professor of Water and Environmental Engineering,

Dean, School of Engineering, College of Science and Technology

University of Rwanda.

DEDICATION

I would like to express my heartfelt gratitude to my mentors for their unwavering support and guidance throughout this journey. My deepest appreciation goes to my Supervisor, Prof. Umaru Garba Wali, as well as Dr. Hussein Bizimana and Mr. Manasse Ntakirutimana, for their valuable expertise, insightful advice, and continuous encouragement, which were instrumental in the successful completion of this thesis.

I am also sincerely thankful to the staff of the Rwanda Water Resources Board for their professional assistance and collaboration, which greatly enriched my research.

A special note of appreciation goes to my beloved husband, Mr. Pierre Kwizera, whose patience, love, and support kept me grounded. I am equally grateful to my parents for their unwavering belief in me, and to my colleagues and dear friends—Amans Tiwangye, Mutuyemariya Alexia, and Anthia Sarah Carmel Irakoze—for their encouragement, motivation, and companionship throughout this journey. To all my friends, brothers, and sisters, thank you for standing by me with your kindness and support.

ACKNOWLEDGEMENTS

This thesis would not have been possible without the significant efforts and assistance of many persons. I appreciate the African Union Commission and PAUWES Staff's financial support for the Pan African University research grant. In addition, I am grateful to the African Union Commission for providing me with the chance to pursue a Master of Science degree in Water Engineering at Pan African University, Algeria. I would like to express my heartfelt gratitude to my supervisor, Prof. Umaru Garba Wali, for his consistent direction, continual availability, and instructional comments, all of which contributed considerably to the achievement of this project. I am profoundly appreciative for his assistance. My gratitude also goes to the Algerian government, PAUWES stakeholders, the people of Tlemcen, and the Algerian community in general for their encouragement and generosity in sponsoring my education. I must thank Prof. Dr. Abdellatif Zerga, the Institute Director of PAUWES, and the entire PAUWES personnel for their assistance and for providing an enriching learning atmosphere. I enjoy the time I spent with my Water Engineering 9th Cohort classmates. Finally, I would want to express my profound gratitude to my family, relatives, friends, and everyone else who helped bring this project to conclusion, both locally and internationally. Your encouragement and assistance were vital throughout my academic career. Thank you all very much.

ABBREVIATION AND ACRONYMS

CN: Curve Number

DEM: Digital Elevation Model

GIS: Geographical Information System

HEC-HMS: Hydrologic Engineering Center- Hydrologic Modelling System.

HEC-RAS: Hydrologic Engineering Center- River Analysis System.

LULC: Land Use and Land Cover

MIDIMAR: Ministry of Disaster and Refugee Affairs of Rwanda

NIDM: Indian, National Institute of Disaster Management.

NISR: National Institute of Statistics of Rwanda

NGO's: Non-Government Organizations

NLA: National Land Authority.

PAUWES: Pan African University Institute of Water and Energy Sciences including Climate Change.

RWB: Rwanda Water Resources Board

SCS: Soil Conservation Service.

SHG: Hydrological Soil Group

TIN: Triangular Irregular Network.

UNISDR: United Nations International Strategy for Disaster Risk Reduction

Table of Contents

IST OF TABLES

LIST OF FIGURES

ABSTRACT

Flooding remains one of the most devastating natural disasters globally, affecting nearly 80% of the population and causing widespread economic, social, and environmental damage. This study aims to support flood risk management efforts in Rwanda through a comprehensive flood risk assessment of the Sebeya Catchment, using the Hydrologic Engineering Center's Hydrologic Modeling System (HEC-HMS). A continuous hydrological model was developed in HEC-HMS to estimate runoff in the catchment using appropriate methods tailored to the local conditions. The model was calibrated using meteorological and hydrological data from 2014 to 2018, and validated with daily data from 2019 to 2021. The simulation results demonstrated good agreement between observed and modeled hydrographs, with performance metrics indicating satisfactory accuracy (Nash-Sutcliffe Efficiency (NSE) = 0.66, R^2 = 0.76, and RMSE = 0.6). In parallel, a social assessment was conducted through questionnaires to capture local community perceptions and experiences related to flooding. Respondents reported common impacts such as loss of life, destruction of agricultural land, damage to infrastructure, and losses in livestock, homes, and commercial properties. A significant proportion of the population resides within 100 to 500 meters of rivers due to limited financial capacity to relocate, exposing them to high flood risk. Government interventions identified include relocation efforts, construction of dams, retaining walls, gabions, and use of sandbags. Flood hazard mapping was carried out using ArcGIS to visualize flood characteristics including water depth, flow velocity, surface elevation, and inundation extent. The analysis showed that flood extent increases with return period, corresponding with higher peak discharges. Compared to the 5-year return period, inundated areas increased by 1.4%, 2.1%, and 3.3% for return periods of 10, 20, and 50 years, respectively. The most flood-prone areas were identified as Mahoko, Nyundo, Pfunda, Kanama, Rugerero, Nyakiriba, and Karambo. Overall, the findings provide critical insights into runoff behavior, flood dynamics, and community vulnerability, offering valuable guidance for integrated watershed management and future flood mitigation planning in the Sebeya Catchment.

INTRODUCTION

1.1 Background

Flooding is a major natural disaster affecting approximately 80% of the global population, causing significant economic, social, and environmental impacts. About 40% of the damage from natural disasters is attributed to flooding (Alexander, 1993). Several studies demonstrate that population expansion, urbanization, and climate change will cause a considerable increase in flooding in the coming decades (Nsangou et al., 2022). According to the World Meteorological Organization (WMO), floods are responsible for more than half of all weather-related disasters, resulting in extensive damage and loss of life (WMO, 2021). In Rwanda, the problem of flooding is particularly acute due to the country's hilly terrain, high rainfall variability and rapid urbanization. The Sebeya Catchment, located in the Western Province of Rwanda, is one of the most flood-prone areas in the country. Frequent flooding in this region disrupts livelihoods, damages infrastructure, and hampers agricultural productivity, which is vital for local communities' sustenance.

According to EM-DAT, from 1979 to 2019, weather, climate and water-related hazards accounted for 50% of all documented disasters, 56% of deaths, and 75% of economic losses. Tropical cyclones, drought, riverine floods, and heatwaves are among the most destructive risks (UNDRR, 2020). Over one-third of the world's land area has been estimated to be vulnerable to flooding (Rutagengwa et al., 2020). Currently, a major environmental concern is the conversion of natural grasslands and forests for urban growth and agricultural intensification as a result of the world's fastest population increase (Karamage, Shao, et al., 2016). Growth in urbanization increases impermeable surfaces, which lowers the capacity of infiltration and causes downstream flooding, erosion of stream banks, increased turbidity (muddiness caused by agitated sediment) from erosion, destruction of habitats, combined sewer overflows, damage to infrastructure, and contaminated rivers, streams, and coastal water (Karamage et al., 2017). In recent decades, Rwanda has experienced an increase in disasters, resulting in physical, social, and economic damages and losses (MIDIMAR, 2015) . Most natural catastrophes that affect Rwanda are caused by floods and droughts. Floods mainly happen between April and May and during the rainy seasons, which last from September to November (Asumadu-Sarkodie, 2015). Anthropogenic activity and climate change have led to an increase in floods, especially in Rwanda's northern and western regions (Hirwa et al., 2023).

Stormwater runoff presents major environmental and public health concerns in Rwanda, where severe floods, landslides, soil erosion, and water pollution are becoming more common issues (Karamage et al., 2017). The Sebeya catchment experiences abundant rainfall exceeding 1200 mm annually and a singularly short dry season from June to August. It encompasses four districts, namely Rubavu, Nyabihu, Ngororero, and Rutsiro, each exhibiting varying degrees of vulnerability to hazards (MoE, 2024).

1.2 Problem Statement

Rwanda is one of Africa's most densely populated countries, with a population density of 470.6 people per km² and an annual growth rate of 2.7%. In comparison, the World and Eastern Africa have mean population densities of 56.5 and 59.2 people per km², respectively. The Rwandan economy heavily relies on primitive agriculture, with approximately 83.4% of the population dependent on subsistence farming (Karamage, Zhang, et al., 2016).

Flooding, especially flash floods triggered by intense precipitation, is the leading cause of weather-related disruptions in road transportation (Ntakiyimana et al., 2022). Intense rainfall, coupled with unregulated land cover and land use changes, exacerbates issues like erosion, flooding, landslides, and water contamination (Karamage, 2016). According to a report by the Ministry of Emergency Management (MINEMA, 2018),storms, floods and landslides in 2018 affected over 15,000 households, resulting in 222 deaths and numerous injuries. The disasters caused extensive damage to homes and infrastructure, with financial losses nearing 204 billion Rwandan Francs across the 15 most affected districts.

In 2023, MINEMA reported that disasters damaged 100 segments of transportation infrastructures, including roads and bridges, incurring substantial rehabilitation costs. Additionally, over 15,000 hectares of cultivated land were destroyed, posing significant threats to food security (MINEMA, 2023). According to Karamage et al. (2017), land use changes have significantly impacted runoff, leading to a national average increase in runoff depth of 2.33 mm per year (0.38% annually). Although precipitation changes influenced annual runoff variations, long-term trends were primarily driven by land use changes districts such as Rubavu, Nyabihu, Ngororero, Gakenke, and Musanze have seen annual runoff depth increases exceeding 3.8 mm per year over the past 27 years, due to extensive deforestation (62% to 85%) and cropland expansion (123% to 293%).

Rwanda faces a high risk of inland flooding, with an annual probability exceeding 20%. Without adequate flood protection, a 10-year flood event has a 10% chance of occurring in any given year, potentially causing over $6.1 million in urban damage, $865.6 million in lost GDP, and affecting 837,200 people (Asumadu-Sarkodie, 2015) . It is crucial to focus on runoff control in areas where rainy season runoff is three times greater than during the dry season (Karamage et al., 2017).

Given the persistent flooding challenges in Rwanda, particularly in the Sebeya Catchment, prioritizing research is essential. This research provides critical insights for planners and disaster risk management sectors, helping them understand the impacts, occurrences, and potential future events. Such knowledge is fundamental for effective forecasting, risk prediction, early warning systems, and monitoring of extreme weather events across the catchment area.

1.3 Research questions

1. How can the hydrological model of the Sebeya Catchment be created using HEC-HMS, incorporating local hydrological, meteorological, and geographical data for accurate simulation of watershed processes?
2. How do local communities perceive flood risk in the Sebeya Catchment, and how can their knowledge and experiences be integrated with hydrological modeling?
3. How can flood-prone areas be identified and mapped based on the assessment findings?

1.4 Objectives

1.4.1 Main objective

To contribute to flood risk management in Rwanda by conducting a comprehensive flood risk assessment in the Sebeya Catchment, utilizing the Hydrologic Engineering Center's Hydrologic Modeling System (HEC-HMS) to inform effective flood risk management and mitigation strategies.

1.4.2 Specific objectives

1. To create the hydrological model of the Sebeya Catchment using HEC-HMS, incorporating local hydrological, meteorological, and geographical data for accurate simulation of watershed processes.

2. To evaluate the community's perception of flood risk in the Sebeya Catchment by integrating local knowledge and experiences with hydrological modeling results
3. To identify and map flood-prone areas based on the assessment findings.

1.5 Relevance Of Study

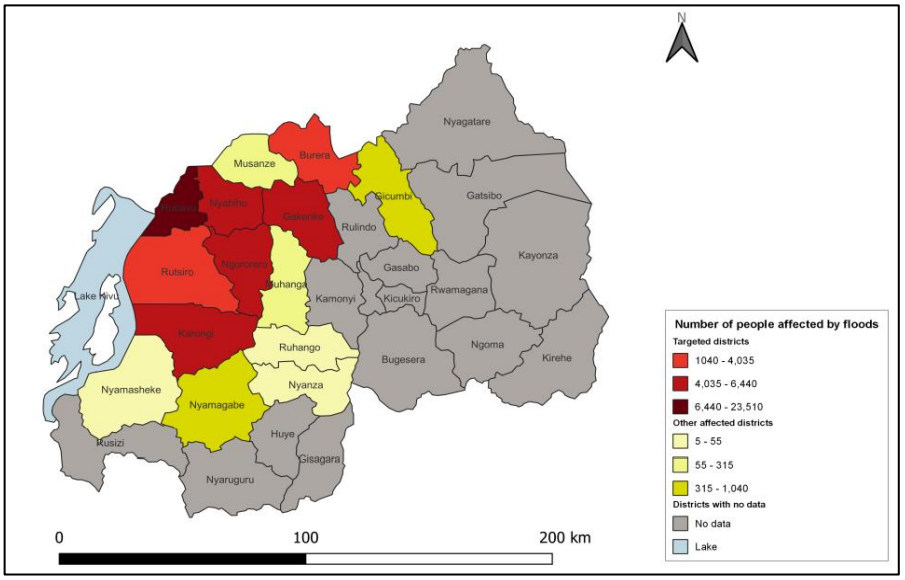

Figure 1.1: Flood status in Rwanda (IFRC, 2023)

Figure 1.2: Effects of flooding in Rwanda (Source: Davies, 2023)

Rwanda has been affected by the devastating flooding and landslides on May 02 and 03, 2023, as a result of heavy rain is still rising. 14 persons have died in the Karongi districts, 26 in

Rutsiro, 18 in Rubavu, 19 in Nyabihu, and 18 in Ngororero as a result of this incident. The fall of houses has caused several injuries and several missing persons to be feared missing in the impacted districts (Davies, 2023). To conduct research on the flood hazard assessment and hydrological modelling findings in Sebeya catchment such as vulnerabilities of communities, infrastructures and ecosystem, flood prone map, current, future volume and runoff will help in land use planning, infrastructure development, and the development of appropriate mitigation strategies which can contribute in decision making processes. In addition, Sebeya catchment is the one of the catchments contributing to high flood risks to economic, health and environmental issues such as loss of life, economic crisis, destruction of infrastructures, ecosystems loss and water quality deterioration. Meanwhile, no research conducted related to prediction of flood magnitude using HEC-HMS in this catchment in order to have deep knowledge and understanding on flow mechanisms to assist planners and decision makers to establish system monitoring and develop early flood warning in this catchment.

1.6 Thesis Chapter Outline

This thesis composed of five chapters, references and appendixes, each addressing a critical aspect of the research on flood risk assessment and hydrological modeling in the Sebeya Catchment using HEC-HMS. The chapters are structured to provide a logical flow from the introduction of the problem to the presentation of findings and recommendations.

Chapter 1: Introduction - This chapter provide a comprehensive overview of flooding as a global issue, with specific focus on Rwanda and the Sebeya Catchment. It outlined the background of the study, emphasizing the significance of flood risk management in the context of climate change and increasing flood events. The chapter will include:

- Background and Context: Overview of global, national, and local flood scenarios.
- Problem Statement: Clear articulation of the flooding issues in the Sebeya Catchment.
- Objectives: Detailed description of the study's aims.
- Scope and Limitations: Definition of the study’s boundaries and potential constraints.
- Significance of the Study: Explanation of the importance of the research for local communities, policy-makers, and the scientific community.

Chapter 2: Literature review -This chapter critically examined previous research and theoretical frameworks relevant to the study. It covered:

- Flooding impacts and causes: Examination of the primary factors contributing to floods and their effects on communities and ecosystems.
- Hydrological modelling: Overview of hydrological model and hydraulic model, with a focus on HEC-HMS and HEC RAS and its applications in flood risk assessment.
- Geographical Information System (GIS) Applications: Discussion on the role of GIS in hydrological modeling and flood risk mapping.
- Integration of Hazard, Exposure, and Vulnerability Analysis: Review of methodologies for integrating these components in flood risk assessment.
- Case Studies and Previous Work: Summary of similar studies and their findings to identify research gaps.

Chapter 3: Research methodology - This chapter described the research design, methods, and procedures used to achieve the study's objectives. It included:

- Study area description: Detailed description of the Sebeya Catchment, including its geography, climate, hydrology, and socio-economic context.
- Data collection: Methods and sources of data, including hydrological, meteorological, topographical, land use, and soil data.
- Materials and methods: Tools and techniques used for data analysis and modelling, including HEC-HMS for hydrological modelling and GIS for spatial analysis.
- Model development: Steps in setting up, calibrating, and validating the hydrological model.

Chapter 4: Results and Discussion - This chapter present the findings of the study and provide a detailed analysis in the context of the research objectives. It covers:

- Hydrological model results: Presentation of model calibration and validation results.
- Flood hazard analysis: Results of the flood simulations, including inundation maps
- Discussion: Interpretation of results, comparison with previous studies, and implications for flood risk management.

Chapter 5: Conclusion and Recommendations - This chapter summarize the key findings of the study and provide practical recommendations. It includes:

- Conclusions: Summary of the main findings in relation to the study's objectives.

- Recommendations: Suggestions for flood risk management and mitigation strategies, including structural and non-structural measures.
- Future research directions: Identification of areas for further research to enhance flood risk assessment and management.

Chapter 6: References - This section provides a comprehensive list of all sources cited in the thesis, following an appropriate academic referencing style.

Chap 7: Appendix - This section will include supplementary materials that support the research. It covers:

- Sample questionnaire: Example of a questionnaire used for collecting primary data from local communities.
- Additional data and maps: Any additional data, charts, maps, or tables that are relevant to the study but not included in the main chapters.
- Official letters such permission to conduct research and internship certificate.

LITERATURE REVIEW

2.1 Introduction

Flooding is a natural phenomenon that happens when water collects on an impermeable surface and can not quickly disappear (Ntakiyimana et al., 2022)**.** According to the UNDRR report, between 1997 and 2017, 88 million people across nations were affected by multi-hazard disasters, including 76 million population due to severe floods. Natural disasters continue to be the most common cause of displacement, relocating about 24 million people annually over the past decade (UNDRR, 2019).

2.2 Flooding Impacts and Causes

2.2.1 Causes of floods

Floods can be caused by a variety of hydrological extremes including severe precipitation and flows that occur naturally, as well as by human activities. Various factors including heavy rainfall, Rwanda's hilly and mountainous topography, population pressure, and the growth of agriculture on steep slopes, contribute to the country's high likelihood of soil erosion (Karamage, Zhang, et al., 2016), (Majoro et al., 2021). The erosive force of runoff from highland places reaches 18.7%, which causes stream bank erosion. In the Sebeya catchment, high rainfall impacts account for 69.33% of the total natural causes of soil erosion, while steep slopes account for 28% (Majoro et al., 2021). Extreme flooding is the result of the interactions between human activities, basin hydrological processes, and atmospheric processes. Floods are produced by rainfall, melting snow or ice, or the structural failure of water-containing structures, especially underground structures (Du et al., 2010). Intense and long-lasting rainfall is typically the primary factor that triggers severe floods. Rapid urbanization and geographic variations lead to changes in land use, resulting in an increase in the runoff coefficient. This, in turn, amplifies runoff generation, leading to higher flood peaks and volumes in rivers. Fluvial flooding happens when rivers exceed their banks or when dams/dikes rupture (O'Connell et al., 2007). Pluvial flooding occurs when rainfall exceeds infiltration and drainage capacity, causing urban areas to flood. Additionally, landslide-formed barrier lakes in hilly locations may collapse, causing severe floods downstream (Sharafati et al., 2021). Flash floods are usually caused by heavy rain, but they can also be triggered by dam or levee failures in rivers during the winter and spring months (Oleyiblo & Li, 2010). Human susceptibility to floods has risen

globally due to changes in land use patterns and acceleration of population growth (Dewan, 2015). Floods can cause direct mortality and morbidity, as well as indirect displacement and significant damage to agriculture, infrastructure, and property (Doocy et al., 2013). The deforestation and increasing of populations are the among of major causes of floods. Every year, floods kill thousands of people, leave millions homeless, and inflict substantial damage to properties and infrastructures around the world (Dewan, 2015). The frequency of floods is increasing as a result of climate change and global warming (Peker et al., 2024). Worldwide population growth increases flash flooding risk. A large amount of runoff, which can quickly damage buildings and roadways, originates from impermeable surfaces like concrete or compacted bare soils (Rehman et al., 2021). Floods in developing countries endanger more people's lives, health, and well-being than in developed countries. In general, two-thirds of flood-related deaths are caused by drowning, and one-third by physical trauma, heart attack, and electrocution (Du et al., 2010).

Floods are described as "the condition that occurs when water overflows the natural or artificial confines of a stream, river, or other body of water, or accumulates by drainage over low-lying areas." At the end of the twenty-first century, the relative global flood displacement risk is expected to increase by approximately 350%, compared to an increase of 150% without the contribution of population change. Projected population shifts will accelerate these increases internationally and in most world regions (Kam et al., 2021). Every year, millions of people worldwide are displaced from their homes as a result of climate-related calamities. River flooding accounts for a significant portion of this displacement, and the river flood risk is predicted to change as a result of global warming and its effects on the hydrological cycle (Kam et al., 2021). Extreme and disastrous floods can have a wide range of negative impacts, including economic losses, social problems, and environmental implications (Yu et al., 2022).

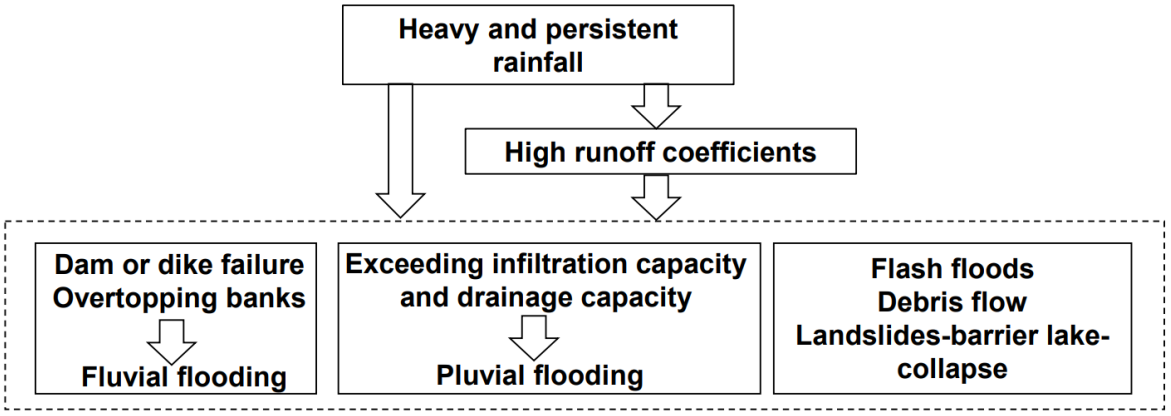

Figure 2.1: Causes of floods (Source (Yu et al., 2022))

2.2.2 Factors affecting river floods

Watershed characteristics significantly shape flood dynamics by influencing water movement, storage, and runoff patterns. Key factors include the size and shape of the watershed, which determine water accumulation and flow rates, with circular watersheds often leading to faster runoff. Steeper slopes increase surface runoff by reducing infiltration, while low-lying areas promote water pooling. Urbanization and reduced vegetation cover escalate runoff and flooding by limiting water absorption, whereas natural vegetation mitigates flood risks. Soil type also plays a critical role, as permeable soils reduce runoff while clayey soils increase it. Lastly, dense stream networks can rapidly distribute water, potentially intensifying flooding (Gaál et al., 2012). Land use characteristics, precipitation, erosion and sedimentation also leads to the river flood. Floods may also be caused by natural drainage failing. The replacement of natural landscape features with non-absorbent infrastructure, such as urban expansion or the removal of wetlands, results in reduced absorption of water. Poorly designed or insufficient drainage systems in new construction or clogged drainage systems from trash or waste buildup can also contribute to impaired drainage (Du et al., 2010). Flooding and population vulnerability have increased in recent decades due to factors such as land-use changes, urbanization of flood-prone areas, squatter settlements, substandard construction, and increased household density (Guarín et al., 2015).

2.2.3 Impacts of floods

Floods are the most common, economically and socially significant geohazard on Earth. On average, river and coastal floods kill over 25,000 people, affect 520 million people, and leave 3.2 million homeless, affecting the global economy more than $60 billion every year (Jakob & Church, 2011).

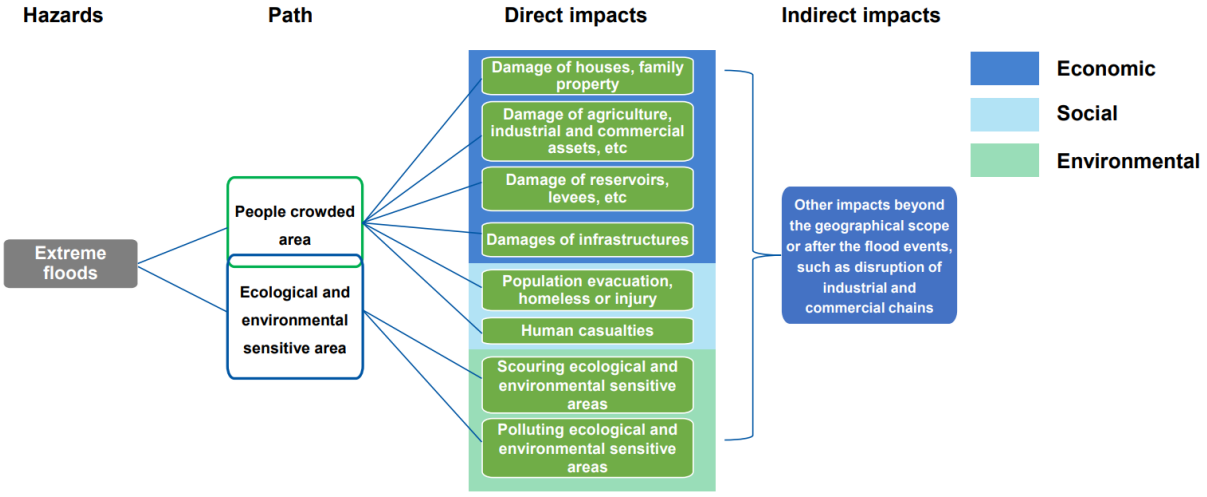

Figure 2.2: Direct and indirect impacts of floods (Source(Yu et al., 2022))

Social impacts

Social impacts are quantified by the projected number of individuals affected inside the inundated region, as safeguarding human lives is the major objective of flood prevention and emergency management. Comprehending the magnitude of affected populations is a necessary condition for making decisions regarding flood management, as well as for offering assistance in terms of personnel evacuation, emergency rescue operations, and the provision of medical and food relief. Furthermore, many forms of damages are intricately linked to human productivity and existence. The patterns of impacted individuals might provide insights into the effects and detriments of socio-economic activities and assets that are intimately associated with floods. Social consequences mostly encompass those who are affected by the evacuation, homelessness, injury, and the possibility of human casualties (Yu et al., 2022).

Environmental impacts

When extreme floods pass across exposed potential pollutant sources, they can cause contaminant leakage or the release of organic loads in water bodies. Environmental hazards from extreme floods include nature reserves and other sensitive places such as protected surface

and groundwater (Yu et al., 2022). Extreme floods can have detrimental effects on vulnerable ecological areas, including protected surface and groundwater resources and nature reserves. The environmental impact encompasses soil erosion, habitat degradation, and potential risks to biodiversity, presenting continuing challenges to the biological equilibrium of the basin (Hahirwabasenga et al., 2024).

Economic impacts

Direct economic costs, such as residential building losses, residential inventory damage, farm losses, losses to industrial companies, traffic and roadways, and hydraulic engineering losses in the flooded area, represent the economic negative consequences (Yu et al., 2022). Droughts and floods can reduce the region's medium-term economic growth by 1 and 0.5 percentage points each year, respectively (Zeufack et al., 2021). Severe floods can result in severe impacts, including physical harm to humans, significant damage or destruction of livelihoods, and even the interruption of global supply lines (Alexander, 2020). Economic consequences encompass the destruction of residential properties, agricultural lands, industrial and commercial assets, as well as the impairment of vital infrastructures, including transportation, water supply, power supply, and communication systems (Yu et al., 2022). Climate consequences on the poor include loss of life and livelihood, damage to critical infrastructure and interruption of services, poor health and malnutrition, and an increase in distress-driven migration (Zeufack et al., 2021). Extreme weather events (droughts and floods) can contribute to maternal and child malnutrition in the absence of effective social protection programs by reducing food intake, triggering decisions to pull children out of school, or causing poor households to sell productive assets, perpetuating and deepening inequalities (Zeufack et al., 2021). For example, natural hazards have the potential to raise food insecurity levels by 5-20 percentage points in Ethiopia, Malawi, Mali, Nigeria, and Tanzania. Climate-related health problems and decreased school attendance would exacerbate gender inequality and diminish future earning opportunities (Zeufack et al., 2021).

2.3 Hazard, Exposure and Vulnerability Analysis

2.3.1 Hazard

A hazard, in its broadest sense, is a threat to people and the things they value. It is possible that a hazard will occur, but it also includes the actual impact of an event on people or places. Hazards are caused by the interaction of social, technical, and natural systems (Chaudhary & Piracha, 2021). This definition of hazard suggests that the crucial factor in transforming a natural process into a hazard is the interaction between the natural and social systems. It is important to note that a hazard, in and of itself, is not harmful, but rather a potential threat that has the capacity to cause harm. The Federal Emergency Management Agency (FEMA) defines hazards as events or physical conditions that have the potential to result in fatalities, injuries, property damage, infrastructure damage, agricultural loss, damage to the environment, interruption of business, or other forms of harm or loss. Similarly, the United Nations International Strategy for Disaster Reduction (UNISDR) provides a definition of a natural hazard as "any natural process or phenomenon that has the potential to result in loss of life, injury, health impacts, property damage, loss of livelihoods and services, social and economic disruption, or environmental damage" (Chaudhary & Piracha, 2021). The natural environmental dangers that have been recognized include geologic events such as earthquakes, volcanic eruptions, landslides, and avalanches. Atmospheric hazards include tropical cyclones, tornadoes, and hail storms. Hydrologic hazards include river floods and coastal floods. Lastly, biologic hazards include epidemic diseases and wildfires (Khan et al., 2014).

2.3.2 Exposure

The Cambridge Dictionary defines exposure as "the fact of experiencing something or being affected by it as a result of being in a specific situation or location." In the context of natural disaster management, exposure refers to the collection of items (such as people, property, systems, or services) in an area that are at risk of being affected by hazard events (Chaudhary & Piracha, 2021). Therefore, if there are no human or capital resources present in a location that is susceptible to natural hazard(s), then the possibility of a natural disaster occurring is eliminated. Exposure to a hazard is a necessary but not sufficient condition for a disaster to occur. For example, an asset could be exposed to a hazard but may possess adequate capacity to tolerate the hazard without damage, thereby avoiding a disaster (Kayode et al., 2017).

2.3.3 Vulnerability

Vulnerability refers to the sensitivity to human death, bodily damage, or economic loss of livelihoods and assets when exposed to hazard events (Kayode et al., 2017). The level of vulnerability is determined by the design, susceptibility, weaknesses, inherent capabilities, or fragility of the elements that are exposed (Thywissen, 2006).

2.3.4 Risk

Risk is defined as the potential for loss, injury, or other unfavorable circumstances; a chance or condition that entails such potential. Risk is the probability of an event occurring multiplied by the impact of that event, should it occur (Chaudhary & Piracha, 2021). It can be articulated in the formula below:

$$\text{Risk(R)} = \text{Hazard(H)} \times \text{Vulnerability(V)}$$

Risk depends on the combination of hazard, vulnerability, and exposure. Risk is the estimated impact that a hazard would have on people, services, infrastructure, and physical assets in a community. It refers to the likelihood of a hazard event becoming a disaster. Wisner et al. modified the relationship presented in (2) by including personal protection capacity (C) and larger scale risk mitigation measures at the societal level (M) (Wisner, 2018).He proposed the following mnemonic relationship between these variables:

$$R = H \times [(\frac{V}{C}) - M]$$

2.4 Hydrological Modeling

2.4.1 HEC- HMS model

The Hydrologic Engineering Center-Hydrologic Modelling System(HEC-HMS) demonstrates proficiency to simulate rain fall runoff relations for dendritic watersheds in space and time (Gebre, 2015).The HEC-HMS is based on semi-distributed modeling and commonly used in hydrological research due to its convenience of use and compatibility with standard methodologies (Janicka & Kanclerz, 2023). The HEC-HMS model has been successfully applied to catchment modelling in several river basins worldwide (Janicka & Kanclerz, 2023; Koneti et al., 2018). HEC-HMS utilizes rainfall and watershed features as input parameters to calculate the flow. The watershed characteristics encompass morphometric features, land use patterns, and soil conditions. HEC-HMS is commonly used with ArcGIS 10.5 software for

spatial-based hydrological simulation using distributed data, continuous flow models, and calibration facilities. This software performs initial calculations for losses, hydrograph unit transformation, baseflow, and flood routing. The HEC-HMS software, also known as the Hydrologic Engineering Centre-Hydrologic Modeling System, was created by the U.S. Army Corps of Engineering. The mathematical model aims to simulate rainfall runoff in a dendritic watershed system. It incorporates basin and meteorologic models as well as control requirements and data input. HEC-HMS employs a synthetic unit hydrograph computation technique that incorporates both observed and simulated flood hydrographs (Bunganaen et al., 2021). Floods are among the most damaging natural disasters in terms of both socioeconomic impact and casualties. However, flood modeling undertaken prior to the occurrence of a flood can be used to control and mitigate the effects of these natural disasters (Peker et al., 2024). HEC-HMS is a simple conceptual model that has been successfully developed by multiple researchers throughout the world. The semi-distributed modeling approach makes it more effective than the Revitalized Flood Hydrograph model for simulating peak flow. The soil moisture accounting model, which is based on the natural hydrological cycle in natural catchments, is thought to be appropriate for rural catchments (Nadeem et al., 2022).

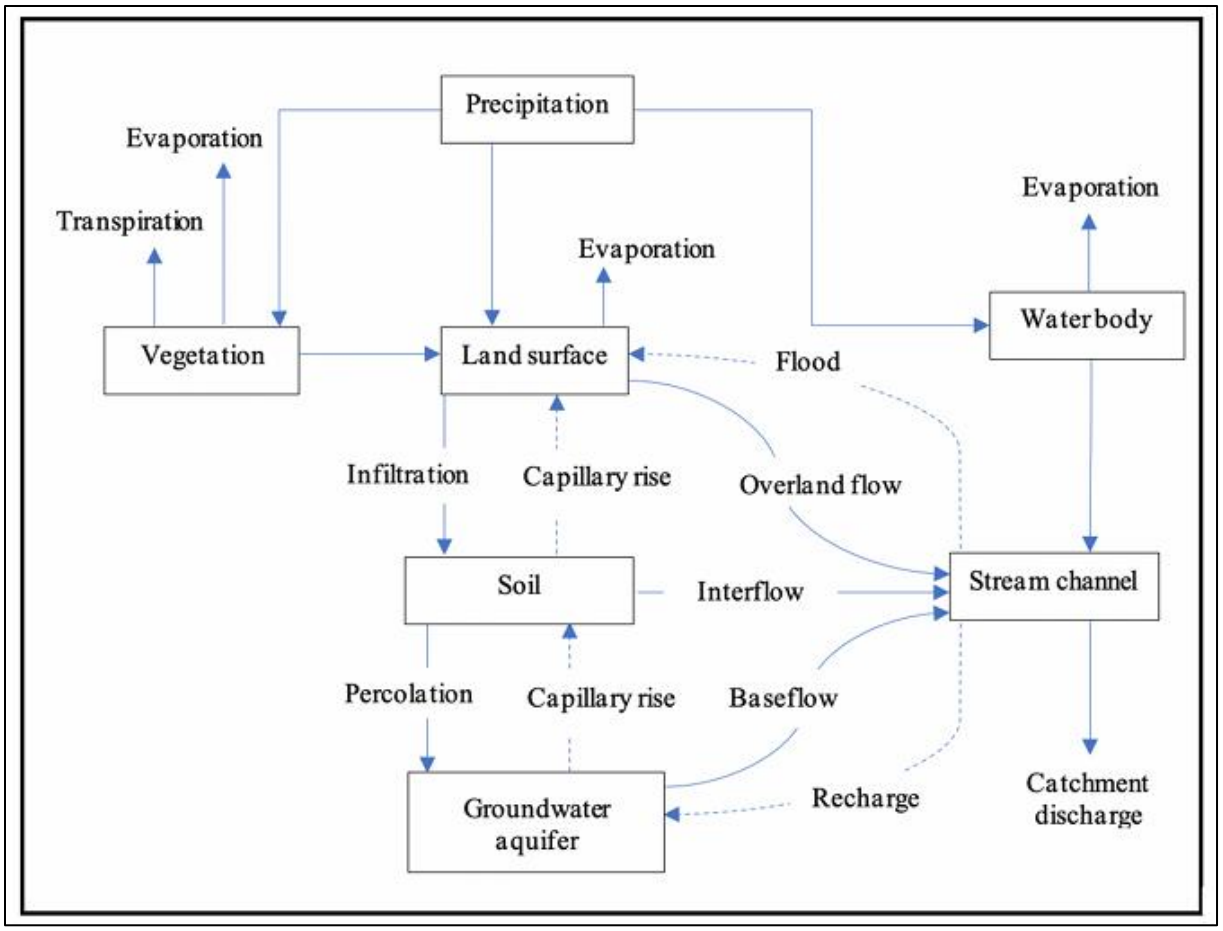

Figure 2.3: Hydrological representation of catchment in HEC-HMS model (USACE HEC, 2022b).

2.4.2 HEC-RAS Model

The HEC-RAS model is among the most frequently employed software for flood modeling in hydrodynamic simulations. This model has been developed to execute 1D steady flow and 2D unsteady flow simulations for river flow studies, in addition to sediment transport and water temperature/quality modeling. The model employs geometric data representation and computational processes for hydraulic analysis of both natural and artificial river systems (Dasallas et al., 2019).

One-Dimensional River Flow Modeling

In one-dimensional river hydraulic modeling, all water flows are considered to move in a longitudinal direction. One-dimensional models show the landscape as a series of cross-sections and simulate flow to determine characteristics such as flow velocity and water depth. To facilitate computation, HEC-RAS presumes a level water surface at each cross-section

perpendicular to the flow direction, resulting in ignoring the momentum exchange between the channel and the floodplain (Brunner, 2010). The equations of motion in one dimension subsequently transform into:

$$\frac{\partial A}{\partial t} + \frac{\partial(\Phi Q)}{\partial x_c} + \frac{\partial[(1-\Phi)Q]}{\partial x_f} = 0$$

$$\frac{\partial Q}{\partial t} + \frac{\partial\left(\Phi^2 Q^2 / A_c\right)}{\partial x_c} + \frac{\partial\left[(1-\Phi)^2 Q^2 / A_f\right]}{\partial x_f} + gA_c\left[\frac{\partial Z}{\partial x_c} + S_{fc}\right] + gA_f\left[\frac{\partial z}{\partial x_f} + S_{ff}\right] = 0$$

where Q is the total flow, A is the flow area, Φ is the quotient of channel conveyance over the total conveyance, z is the elevation of water surface, and Sf is the friction slope, in which the subscripts c and f refers to the channel and floodplain, respectively.

Two-Dimensional Flood Inundation Modeling

Two-dimensional flood models deliver water flow in both longitudinal and lateral directions, whereas velocity is considered unimportant in the vertical direction. It utilizes shallow water equations to characterize water movement through depth-averaged two-dimensional velocity and water depth. The diffusion wave approximation method is employed to calculate the flow field in the 2D mesh, as it results in reduced calculation time and may mitigate model instability. The model region is divided into grid cells, and HEC-RAS produces a comprehensive hydraulic property table for each cell and its corresponding faces. The water surface profiles generated by the model, utilizing various hydraulic design elements, can assist decision-makers in allocating resources efficiently to mitigate disasters and enhance quality of life by assessing the magnitude of flooding and flood inundation areas (Vashist & Singh, 2023). In contrast to one-dimensional models, these models depict the terrain as a continuous surface utilizing a mesh or grid. To enhance computational efficiency, HEC-RAS employs a sub-grid methodology that utilizes a relatively coarse computational grid with finer-scale topographical data (Dasallas et al., 2019). The sub-grid bathymetry equations are formulated using comprehensive shallow water and diffusion wave equations. Assuming the governing equation applies to an incompressible fluid, the unsteady differential version of mass conservation is expressed as:

$$\frac{\partial H}{\partial t} + \frac{\partial(hu)}{\partial x} + \frac{\partial(hv)}{\partial y} + q = 0$$

where t is time, q is the source/sink term, and the u and v are velocity components in x- and y-directions,

respectively. The water surface elevation H is defined as the sum of the surface elevation z(x, y) and water depth h(x, y, t).

2.5 Geographical Information System (GIS) And Remote Sensing

Geographic Information Systems (GIS) and remote sensing technologies play a significant part in planning and management for flood risks in watersheds. For instance, geospatial technology, offers optimal capabilities for analyzing and delivering necessary outcomes crucial for timely and efficient flood-related decision-making (Ogato et al., 2020).

Remote sensing and geographical information system (GIS) are effective tools for both qualitative and quantitative research of drainage networks within a watershed. They have been utilized for the purpose of prioritizing watersheds and managing them based on drainage factors (Jamal & Ali, 2023). Remote sensing is an effective technique for flood mapping and suitability assessment, as well as for emergency response and catastrophe preparedness (Uddin et al., 2013). Remote sensing technology extracts flood region features and provides information on upcoming disasters and event issues. Flood risk maps can be generated using acquired images and remote sensing data (Munawar et al., 2022). Remote sensing methods collect data about items and infrastructure on the Earth's surface without physical contact, utilizing a range of recording sensors (Shah et al., 2019). As a result, it is useful in environments where no physical or intimate touch is possible. Some examples of these technologies include Synthetic Aperture Radar (SAR), imaging platforms in space, and satellites. This strategy speeds up data collection (Anusha & Bharathi, 2020). Geographic Information Systems (GIS), has become crucial in hydrologic studies because it allows for the analysis of the spatial aspects of the factors and rainfall that impact hydrologic processes. The utilization of geographic information systems (GIS) is essential in the parameterization of distributed hydrologic models. GIS applications are used to extract hydrologic data, including flow direction, flow accumulation, watershed boundaries, and stream networks, from a digital elevation model (DEM) (Nadeem et al., 2022).

METHODOLOGY

The methodology adopted in this study is divided into different main tasks as illustrated in the figure below:

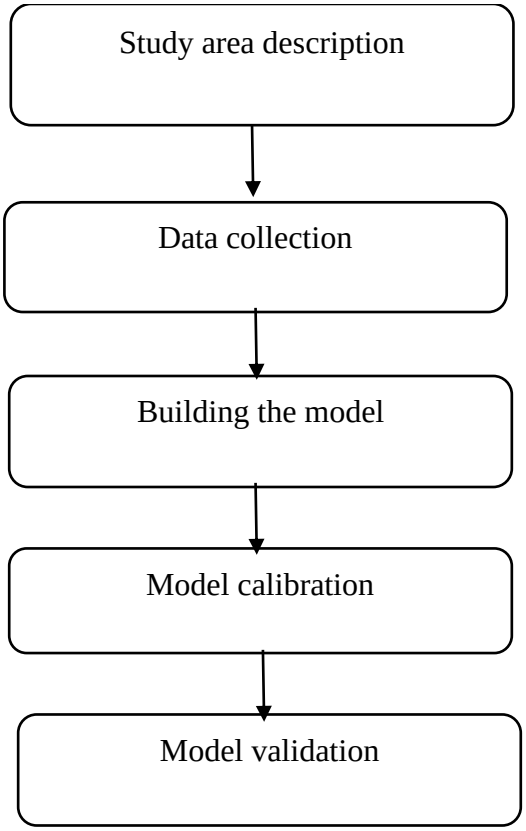

Figure 3.1: Methods adopted for model in the research

3.1 Study Area Description

Sebeya is a level 2 catchment within the broader Level 1 catchment of Lake Kivu. Sebeya, located on the western side of the Congo-Nile divide, is one of the most upstream areas in the Congo River basin, with a total surface area of 336.4 km^2. It has a total surface area of 336.4 km^2, accounting for 1.4% of Rwanda's total area of 26,338 km^2 (IWRM, 2018; MoE, 2024). The upstream region constitutes 80% of the catchment area and is distinguished by steep slopes and significant erosion, resulting in elevated sediment loads in the rivers. The downstream section constitutes 20% of the catchment area and is characterized by a flatter topography, lower elevation, and greater soil permeability compared to the upstream section (Hahirwabasenga et al., 2024). The Sebeya catchment falls into four administrative subdivisions: Rubavu, Nyabihu, Rutsiro, and Ngororero Districts. The principal river within this catchment is the Sebeya, which

originates from the Rutsiro mountains and spans a length of 48 kilometers. The recurrent floods usually are in its downstream part. The population density in Sebeya catchment is 644 hab/km2, while Rwanda's average density is around 415 hab/km2. Situated within the high elevation zone of the country, the catchment experiences altitudes ranging from 1,462 meters to 2,979 meters above sea level. It has steep slopes and receives significant rainfall (1,200 mm to 1,700 mm per year) (Majoro & Wali, 2022). The largest overlapped area between Rubavu and the Sebeya watershed is 44.6%. The highest overlapping area, amounting to 41.3%, is found between the Rutsiro and Sebeya catchments (Majoro et al., 2020).

Table 3.1: Overlap between Districts and Sebeya catchment (Majoro et al., 2021)

Districts			The overlap between District and Catchment		
District name	Area in km^2	Population	The overlapped area in km^2	% of Catchment	Overlapped population
Ngororero	679	403,662	37	11%	156,054
Rutsiro	1,157	294,740	139	41.3%	21,053
Nyabihu	532	324,654	38	11.3%	39,003
Rubavu	388	333,713	150	44.6%	18,185
Total			363	100%	234,295

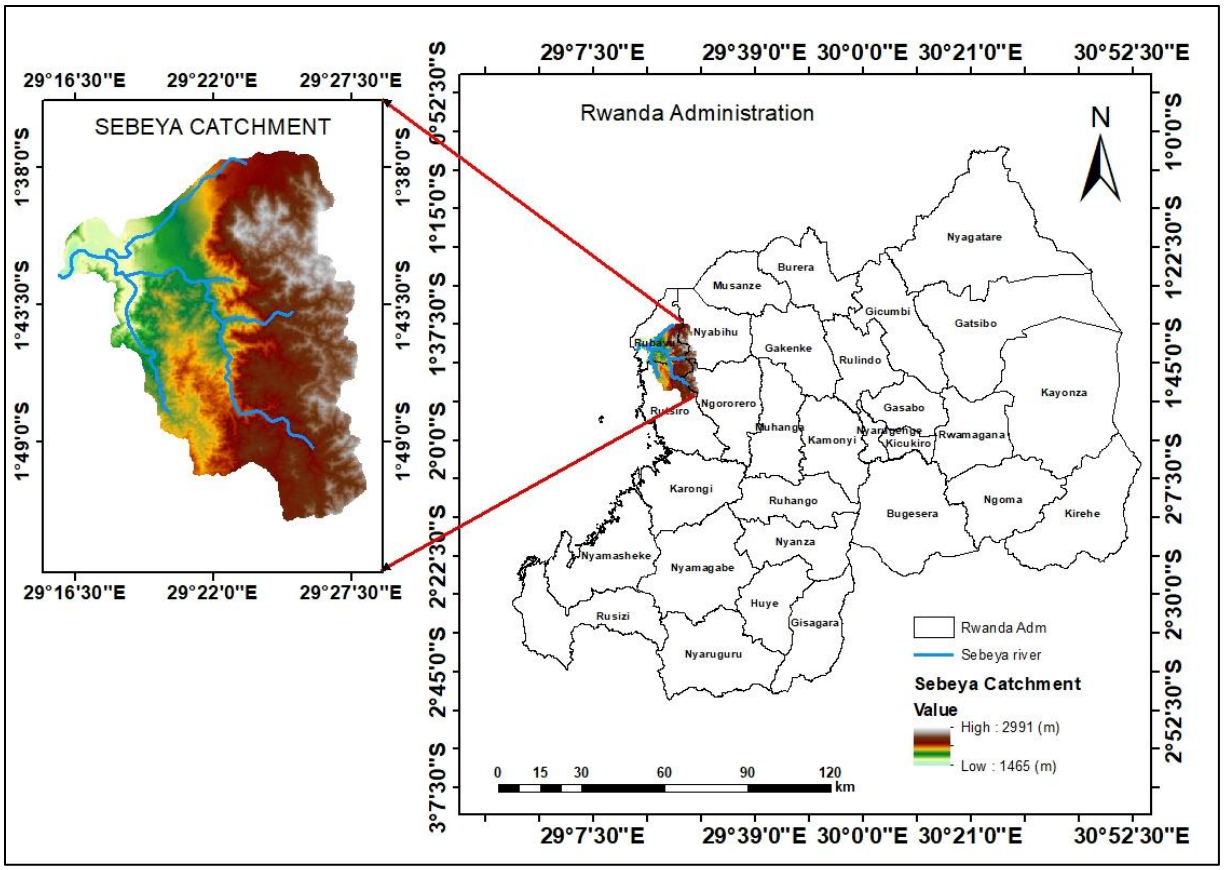

Figure 3.2: Sebeya catchment location and elevation

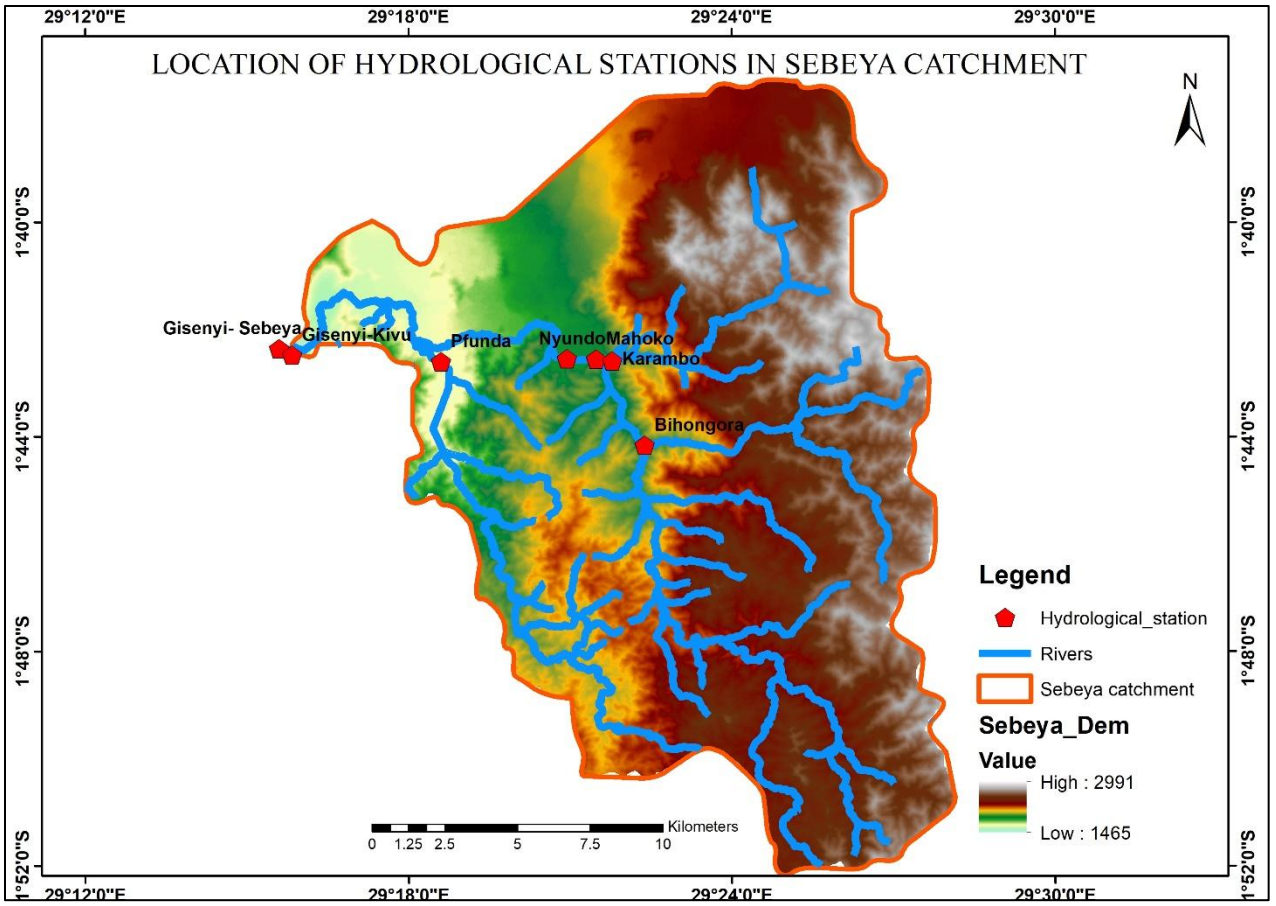

Figure 3.3: The hydrological station within Sebeya catchment

3.1.1 Topography

Topography is a factor that influences the spatial and temporal variability of hydrologic processes. It can be expressed using a digital elevation model suitable for computer utilization. This allows for the analysis of territorial structural features such as watershed boundaries and their characteristics, slope mapping, and the extraction of the hydrographic network (Mendas, 2010). Digital elevation model was downloaded from Shuttle Radar Topography Mission(STRM) with 30m resolution. Therefore, Sebeya catchment has topography which varies between 1465 m and 2991 m above mean sea level as shown in fig 3.4.

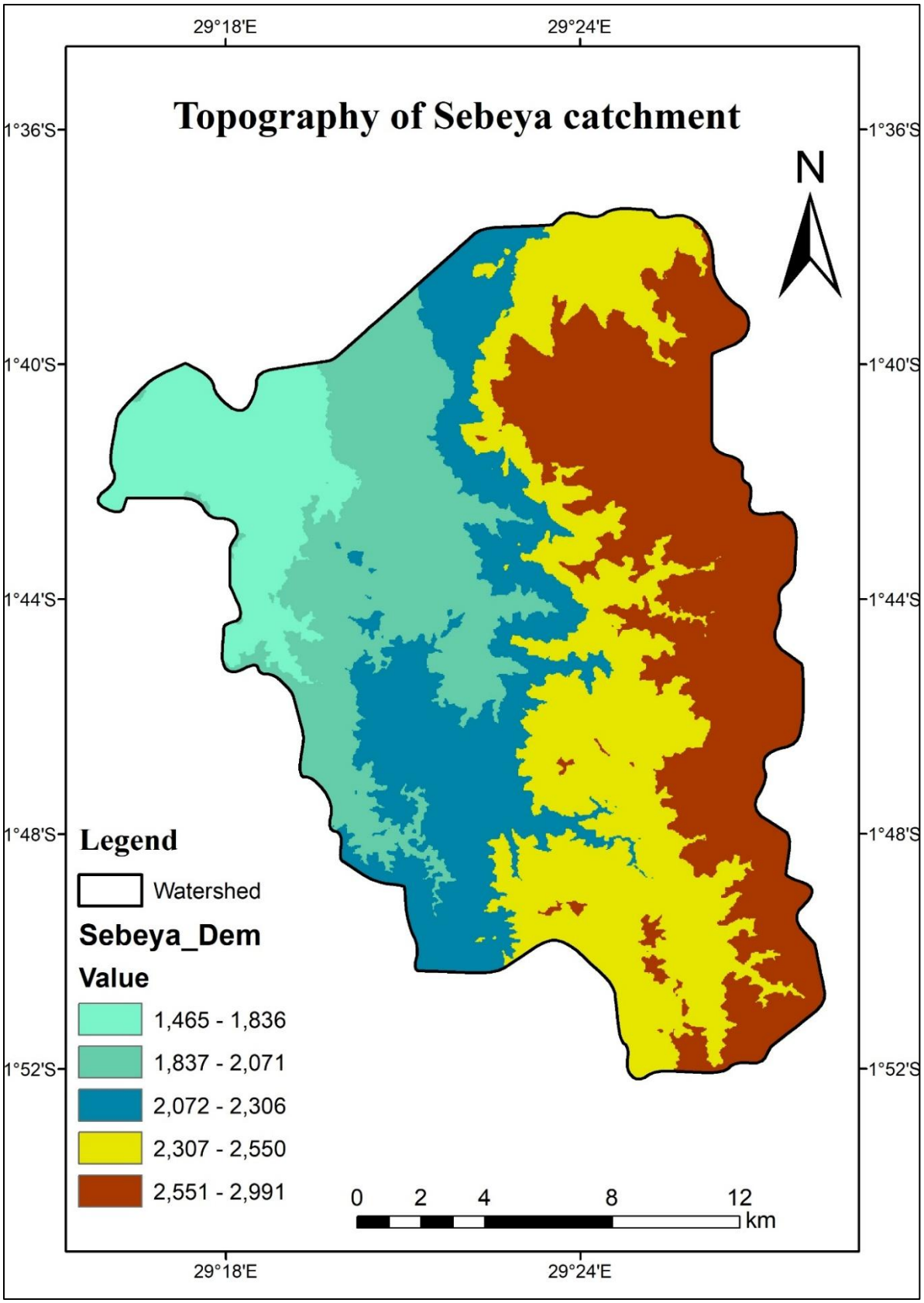

Figure 3.4: The elevation in the catchment

3.1.2 Hydrology and watershed characteristics

The hydrological response to rainfall within a catchment is determined largely by land morphology. The Sebeya catchment is a mountainous area with hardly any land below the 1,620 m elevation (Lake Kivu level is about 1,470 m) (MoE, 2024). Surface water flows are sustained during the dry season (July and August) and there is a very restrained hydrological response during the short rainy season (September to December), when infiltration to groundwaters significantly reduces direct runoff. During the long rainy season (February to May), monthly flows show a greater increase, indicating that groundwater reserves are completely replenished at this time. It should be noted that instantaneous peak flow levels in this period are often significantly higher than the monthly average flow levels. This happens when the infiltration capacity of the soil is not sufficient to absorb heavy rain due to large scale deforestation in favour of agriculture and urbanization, infiltration capacity has decreased over time and surface runoff (and related soil erosion) has increased (IWRM, 2018). The water in the catchment is a vital resource for the rapidly urbanizing regions surrounding the city of Rubavu district and the adjacent valley in the downstream section of the sub-catchment. The primary water users include hydropower plants, domestic water producers, irrigation systems, and commercial entities like as mining operations, fish farms, and other manufacturers, including the Bralirwa brewery (MoE, 2024). The primary economic activities in the catchment area are tourism at Gishwati National Park, Volcanoes National Park, and around Lake Kivu, as well as hydropower generation and agricultural pursuits. Hydropower has been recognized as a significant catalyst for economic progress in Rwanda, where half of its electricity is generated from hydropower (RoR, 2020). Agriculture constitutes the predominant land use, accounting for 62% of the catchment, followed by grazing pastures and various mining sites, particularly in the upstream section of the catchment (Hahirwabasenga et al., 2024). The catchment has small tributaries that drain in the main river called Sebeya with 8 major hydrological stations. The figure below shows the catchment with its tributaries.

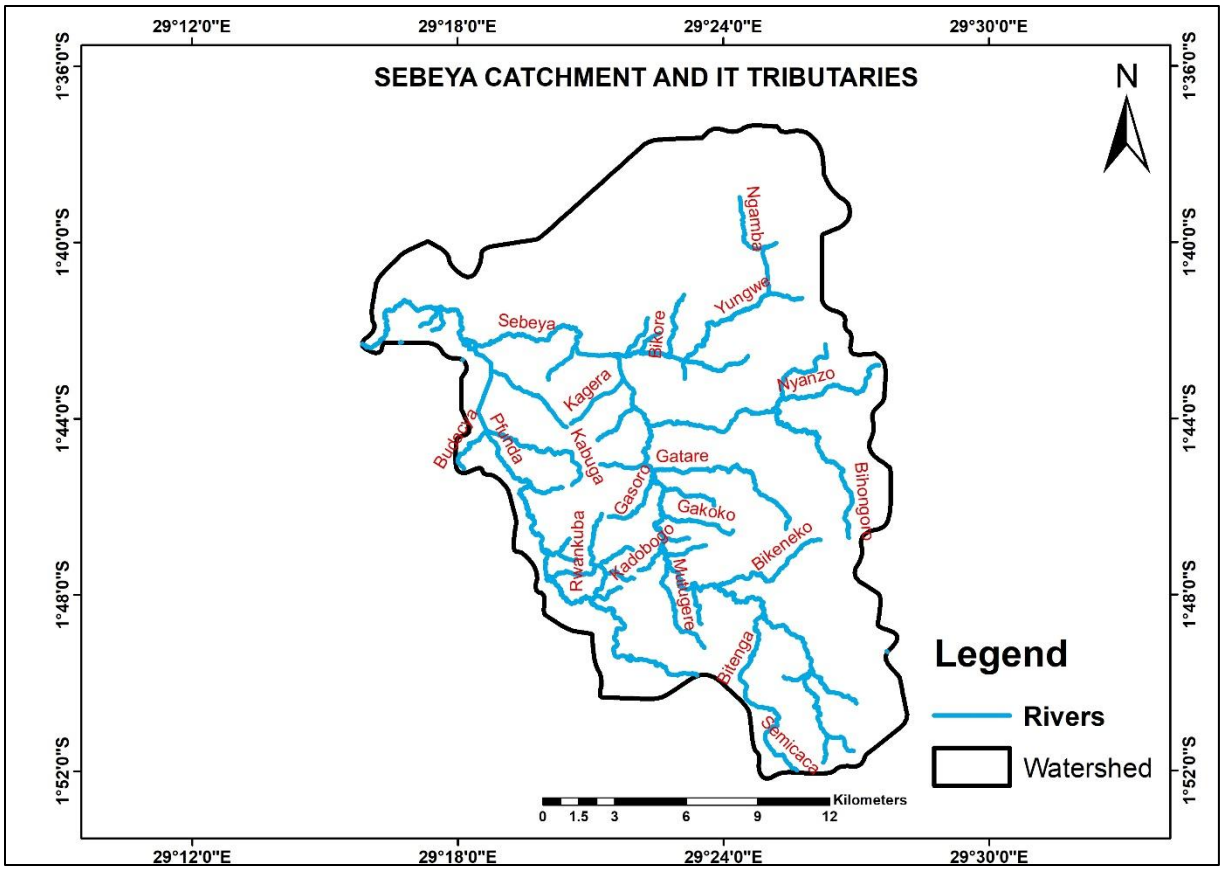

Figure 3.5: Sebeya catchment with its tributaries

3.1.3 Land use and Land cover

Land cover of the catchment Land use is one of the drivers of hydrology of a watershed. Land use and Land cover data was obtained from Rwanda National Land Authority(NLA) for the country. ArcGIS 10.4 Version was used to obtain the land use and land cover for Sebeya catchment . The TIF format was introduced in ArcGIS and a shapefile of the catchment was added in the data and the data management tools(raster processing tool-clip) was used to get the land use and landcover for the study area. The land use is dominated by Agriculture, grassland, and build up areas as shown by Fig 3.6.

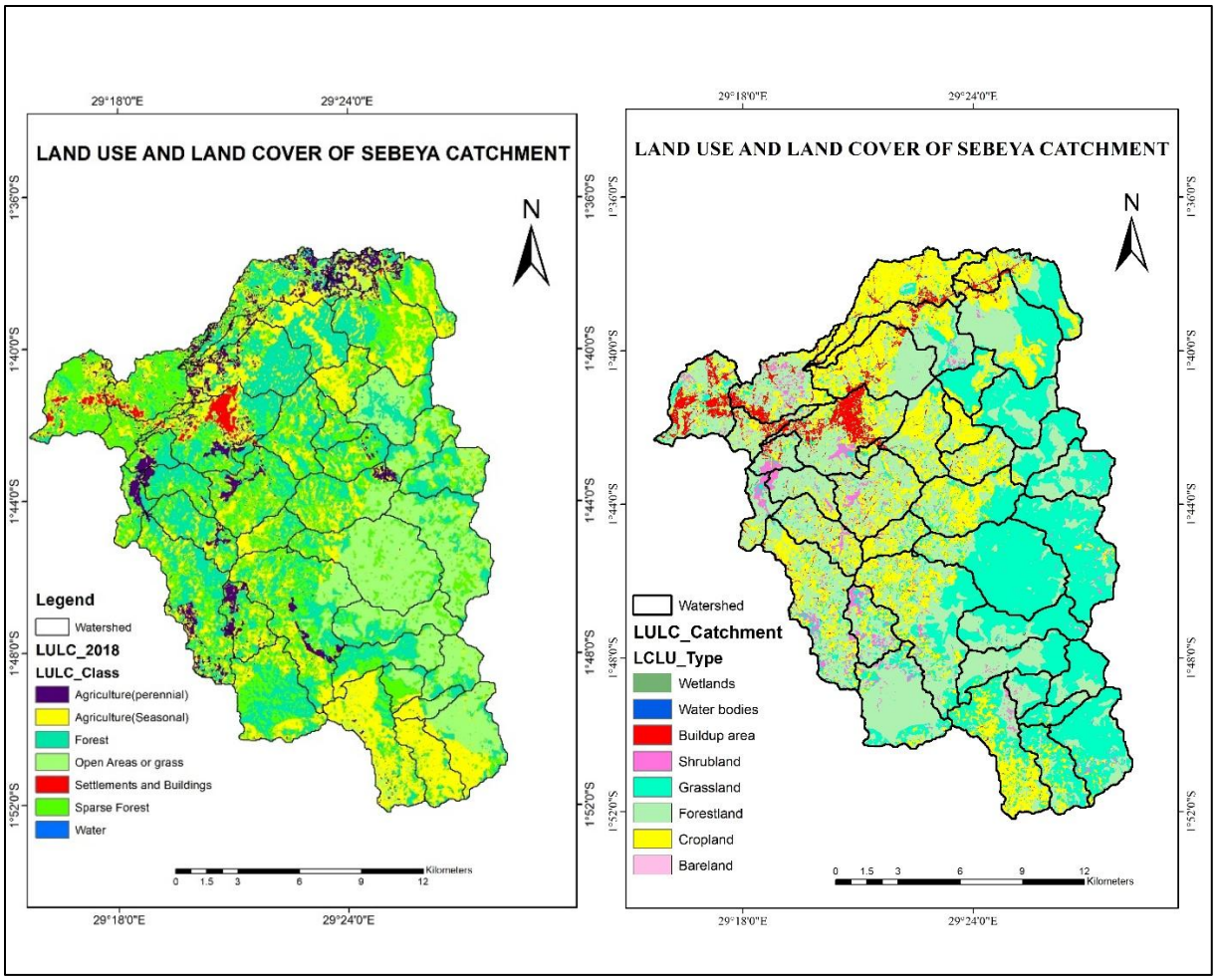

Figure 3.6: The Land use Land cover for 2018 and 2021in the Sebeya catchment

3.1.4 Soil of the catchment

Soil data has been provided by Rwanda National Land Authority(NLA). The dominant soil types which are highly dominating are andosols, alisols and cambisols. The soil texture as a factor of generating the runoff has been found mostly to be clay where is highly dominating in upstream and downstream part of the catchment followed by sandy clay and clay loam as shown in figure3.7.

Table 3.2: Soil domain in Sebeya catchment

Soils Domain	Area(km^2)	Area (%)
Alisols	21.86	5.99
Regosols	1.36	0.37
Acrisols	37.14	10.17
Alisols	76.05	20.82
Andosols	120.03	32.87
Cambisols	52.34	14.33
Ferralsols	10.66	2.92
Gleysols	0.93	0.25
Histosols	3.14	0.86
Luvisols	21.94	6.01
Phaeozems	8.82	2.42
Regosols	10.94	3.00

Table 3.3: Soil texture in Sebeya catchment

Soil Texture	Area(km^2)	Area in (%)
Clay	173.39	47.48
Clay loam	47.21	12.93
Loam	30.41	8.33
Sandy clay	55.76	15.27
Sandy clay loam	31.07	8.51
Sandy loam	8.51	2.33
Silt loam	17.86	4.89
Silty clay	1.01	0.28

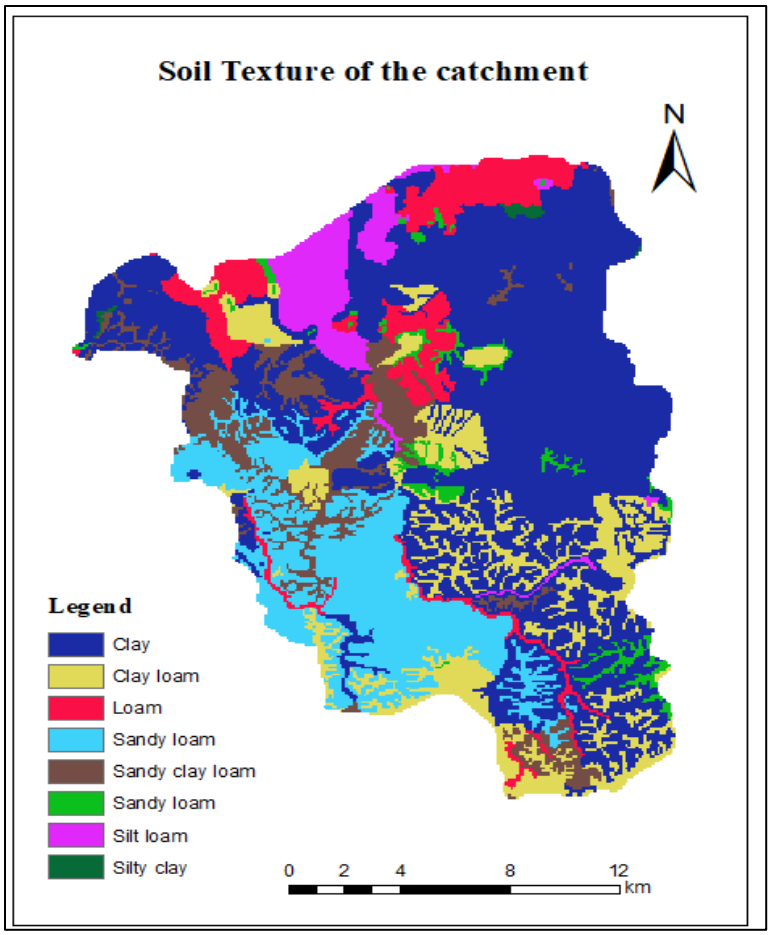

Figure 3.7: Soil texture in Sebeya catchment

3.1.5 River flow

Historical Flow data and water level for 30 years starting from 1991 to 2021 was obtained from the river gauging station at Nyundo from Rwanda Water Resources Board(RWB).This data had a significant missing value in different years from 2011to 2021 which was completed using XL Stat in excel using multiple imputation method (Monte Carlo method) due its accuracy. The imputation approach(MCMC) is employed to evaluate incomplete data by estimating the most accurate value for a missing variable (Ingsrisawang & Potawee, 2012). Many of recent flow data were unavailable and also with many missing values between 1991 to 2010 due to the flooding and limited measuring instruments. The daily maximum flow of main river between 2011-2021 stands at **47.5 m^3/s** which was obtained at Nyundo hydrological station considered in this research for calibration and validation of the model.

3.1.6 Evapotranspiration

ET comprises two processes which are transpiration from plants and evaporation from surfaces. It is important to consider as a key component of continuous hydrologic models. ET removes water from the soil and transmits it to the atmosphere, which can create a moisture deficit prior to flood events that reduces or eliminates direct runoff early during a precipitation event. HMS can simulate surface evaporation, plant canopy evaporation, and plant (USACE, 2000). Deficits created through ET from significant moisture which is lost to the atmosphere. This data was obtained from https://data.apps.fao.org/wapor/?lang=en&share=f-695af678-d13a-46dd-9199-e4a3728fb686.and used as the input for the model. The average amount of ET with in the catchment is 58.03mm. The figure below presents the average ET within the Sebeya catchment obtained from 2011 to 2018.

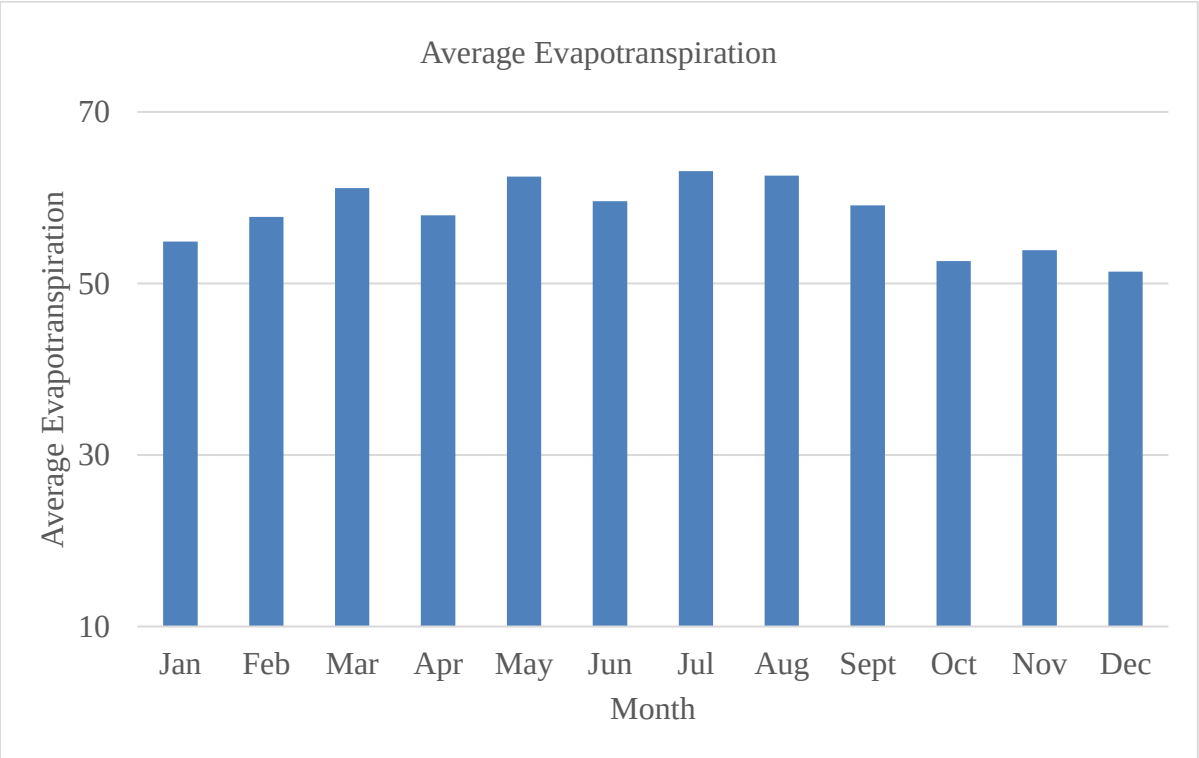

Figure 3.8: Average Evapotranspiration from 2014 to 2018 within the catchment

3.1.7 Rainfall

The Rwanda Meteorological Agency (METEO) is responsible for measuring, storing, and managing meteorological factors in Rwanda. The METEO has supplied the rainfall time series data for 30 years from 1991 to 2021. The provided figure 3.9 presents the precise locations of

meteorological stations within or close to the Sebeya catchment, where rainfall measurements are conducted. A preliminary visual assessment of the data revealed missing values for 13 days in the rainfall records. Thus, the collected rainfall data were obtained daily. Out of the 25 rainfall stations available, only 5 were selected for analysis, this was obtained using Thiessen polygons found in ArcGIS as they encompass the Sebeya catchment area. The selected meteorological station for this study were Kivumu, Kanama, Nyundo ,Bigogwe and Murunda.

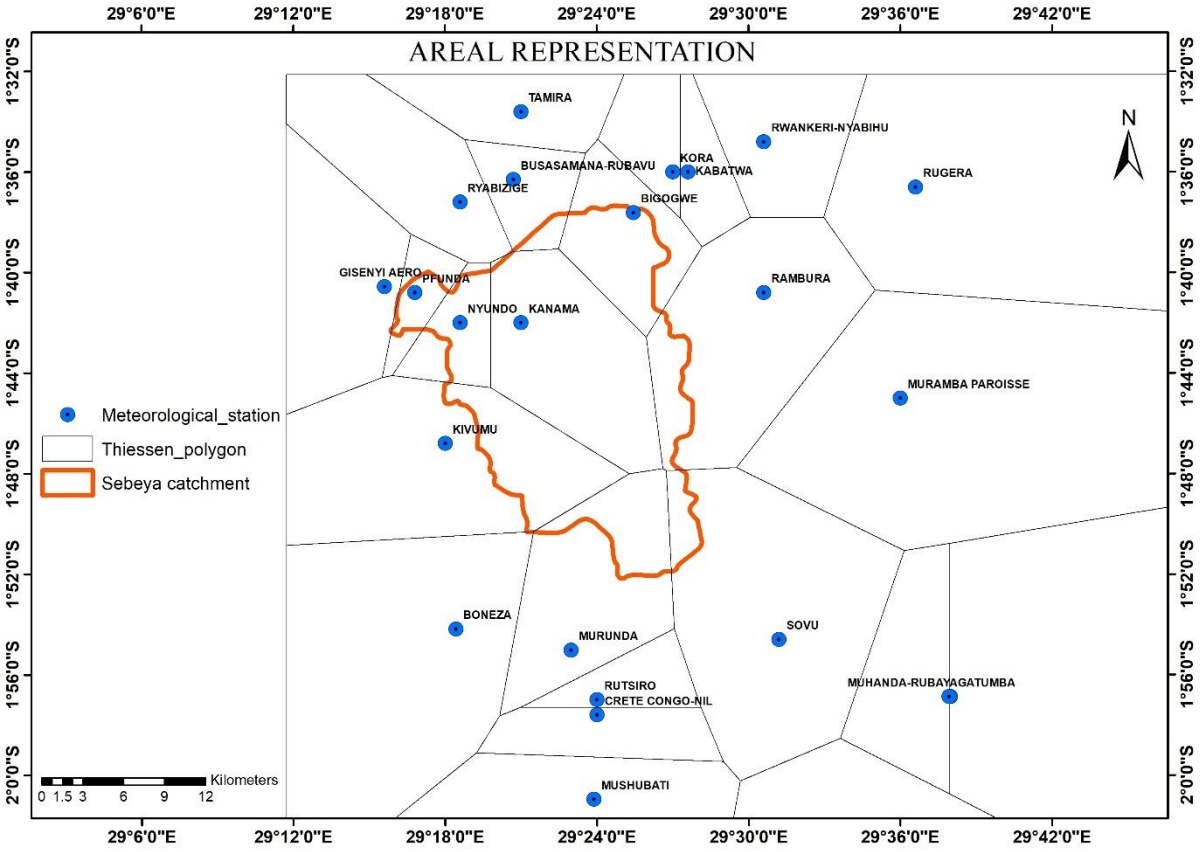

Figure 3.9: The aerial representation of rainfall variables using Thiessen polygons method

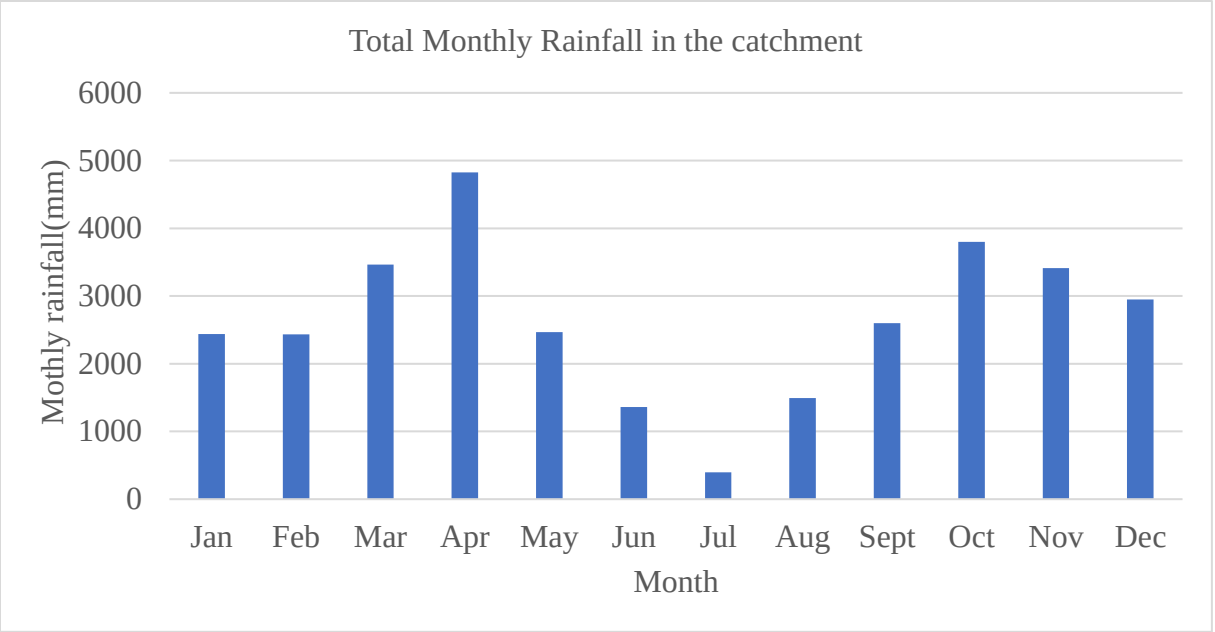

Figure 3.10: Total Monthly rainfall within the catchment from 2014 to 2018

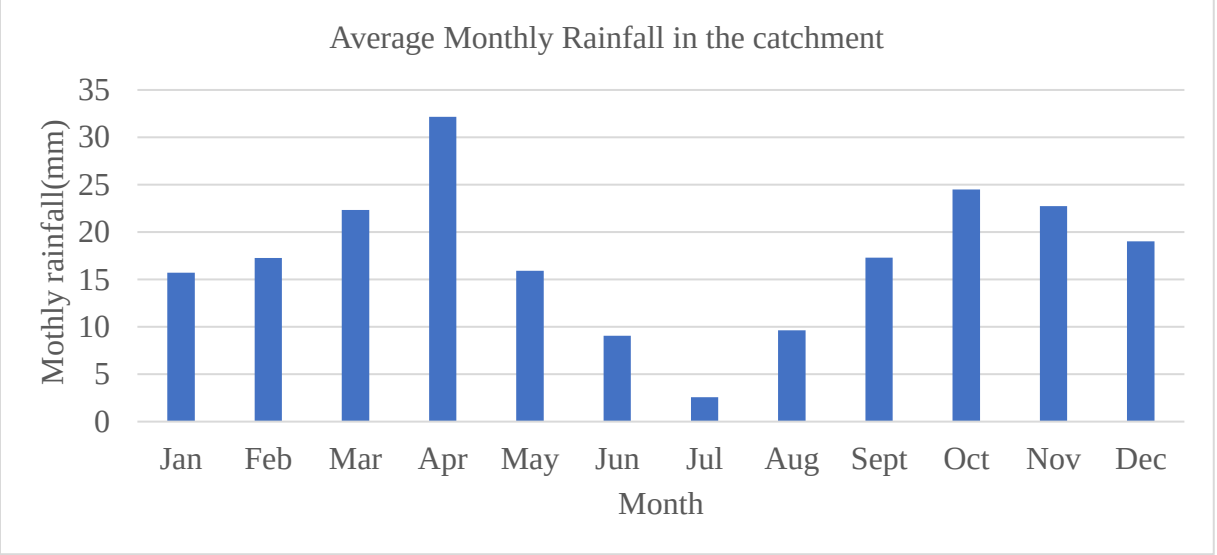

Figure 3.11: Average Monthly rainfall within the catchment from 2014 to 2018

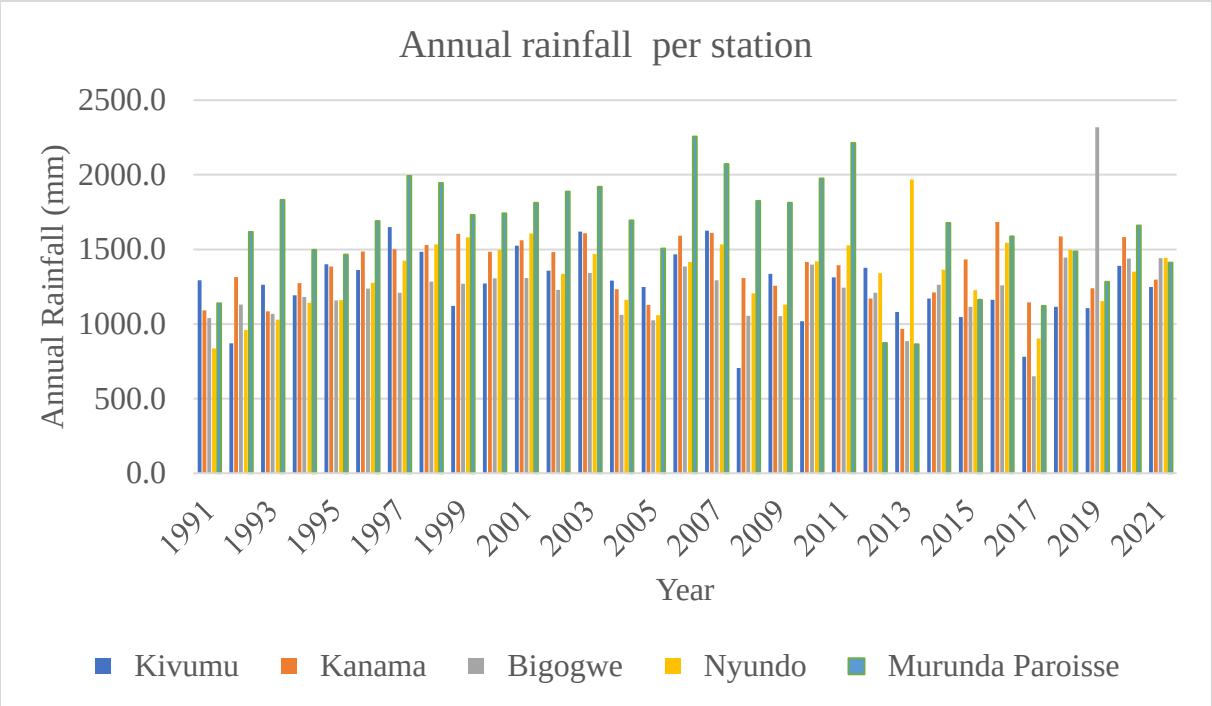

Figure 3.12: Annual rainfall (mm) per station (Kivumu, Kanama, Bigogwe, Nyundo, Murunda Paroisse) in Sebeya catchment from 1991 to 2021.

Table 3.4: Location of meteorological stations

ID	Station Name	Latitude	Longitude	Elevation(m)
1	Murunda	-1.91	29.38	1832
2	Kivumu	-2.05	29.8	1791
3	Kanama	-1.7	29.35	1887
4	Bigogwe	-1.61	29.41	2382
5	Nyundo	-1.70	29.31	1692

3.2 Data Collection

The datasets for this study were gathered from different sources such as governmental institutions, interviews , field visit and observations. Rainfall datasets for Sebeya catchment were collected from the Rwanda Meteorology Agency(METEO) for 30 years from 1991 to 2021. Streamflow datasets were gathered from various hydrological stations within the catchment from Rwanda Water Resources Board (RWB) and Digital Elevation Model datasets with 30 m resolution were downloaded from Shuttle Radar Topography Mission(STRM). Administrative boundaries of Rwanda were obtained from the Humanitarian Data Exchange

(HDX). Land use and land cover images were obtained from National Land Authority. Previous flood event data and reports were collected through field observations, Ministry in charge of Emergency Management (MINEMA) and interviews with local population and leaders.

3.3 Data Pre-processing

To ensure completeness and accuracy of the collected data. All datasets had undergone data cleaning procedures such as handling missing values and outliers' detection, along with normalization and feature selection. For example, Data required for the HEC-HMS model was from 1992-2021. However, Rainfall data obtained from Rwanda Meteorology Agency (METEO) had a data gap for 13 days in July 2018 for all stations in the catchment and this was filled using XL stat software. Techniques such as data interpolation or deletion, tailored to the specific dataset characteristics, were applied as necessary. Furthermore, data conversions or standardizations was conducted to maintain uniformity among the datasets. Stringent validation measures were employed to verify data accuracy, including cross-checking with reliable sources and seeking expert consultation where needed. These steps were crucial to ensure the integrity and reliability of the data used in the analyses done.

3.4 Data Preparation

This step is essential to facilitate HEC-HMS model to create an accurate hydrological model of the Sebeya Catchment. This required the spatial data such as terrain elevation, land cover, soil type, and precipitation patterns, ensuring their coverage across the study area. Additionally, historical streamflow data in excel format was collected to calibrate and validate the model.

Afterwards, a unified spatial framework was established by integrating the various datasets using GIS software for proper georeferencing and alignment. From this structured approach relevant features such as slope, elevation, land cover types and soil properties were obtained.

To assess the performance of the model accurately, the historical flow data was divided into distinct calibration and validation datasets. The calibration dataset was five years from 2014 to 2018 was used to serve as the foundation for model training, enabling the model to learn and adjust their parameters. The 3 years input data for validating the model was used from 2019 to 2021 to evaluate the models' performance, providing an objective measure of its accuracy and predictive capabilities.

3.5 Processing of Rainfall

Rainfall data for 30 years from 1991 to 2021 collected at Kanama station in the Sebeya catchment located at -1.7 latitude and 29.35 longitude with 1887 of elevation. By applying Gumbel's distribution method , the frequency analysis was done to predict the rainfall for 5,10,20 and 50 years return period as shown in the table 3.5. The maximum annual rainfall of the corrected rainfall data and the results of each step to get the probability distribution were shown on Appendix.

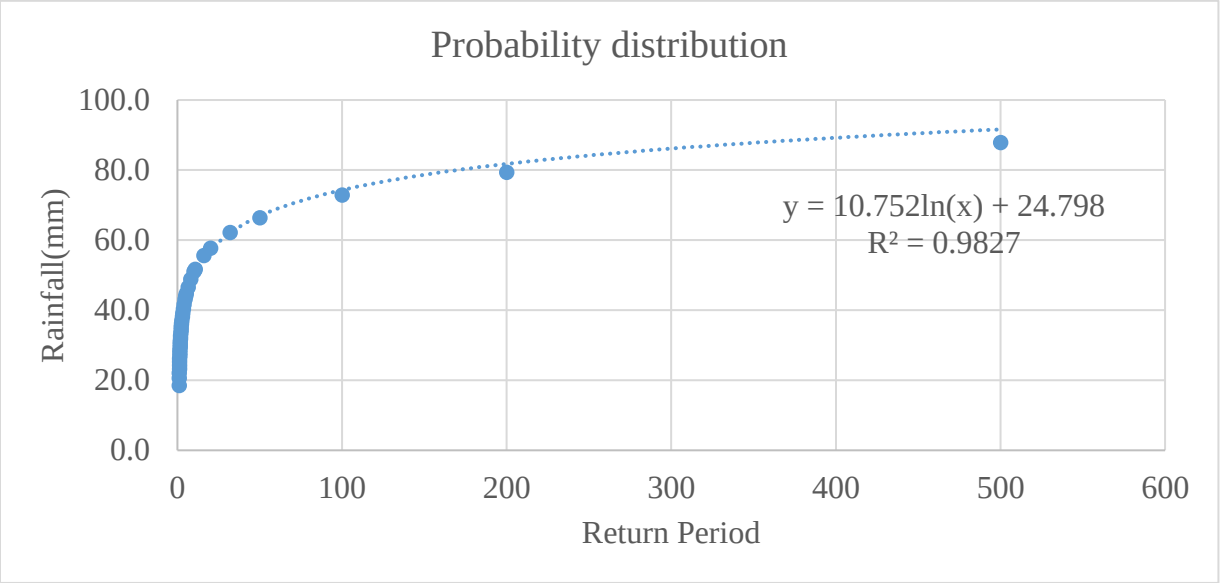

Figure 3.13: Rainfall Frequency Analysis Gumbel's Extreme Value Probability Distribution

Table 3.5: Frequency Precipitation for each return period year

Return Period (years)	Gumbel's factor frequency within each return period (K_T)	Frequency Rainfall (mm)
5	0.86	44.06
10	1.54	51.04
20	2.18	57.74
50	3.02	66.42
100	3.64	72.92
200	4.26	79.39
500	5.09	87.94

3.6 Trend Analysis

3.6.1 Sen's slope test

The Sen's Slope test is suggested by the World Meteorological Organization as part of the process of identifying trends in hydrometeorological data. This test assumes a linear trend and quantifies the change over time. It has a distinct advantage over linear regression in that it is unaffected by the presence of outliers and data errors (Aditya et al., 2021). The Sen's Slope equation for a finite number of N pairs of data samples is expressed as:

$$Q_i = \frac{(x_j - x_i)}{j-i}, i = 1,2,3,\ldots,N$$

Where, x_j and x_i are data values at time j and i (j > i), respectively. If there are n values of x_j in the time series, there will be N = n(n-1)/2 slope estimates (Aditya et al., 2021).

3.6.2 Mann-Kendall test

The Mann-Kendall test is a non-parametric statistical test employed to ascertain a trend in data by analyzing the relative ranks within a certain time period. For this test, the data is not required to satisfy ordinary assumptions (Sa'adi et al., 2019). This test is suggested by the World Meteorological Organization for identifying trends in a collection of hydrological data (Aditya et al., 2021). The Mann-Kendall test statistic is computed as follows:

$$S = \sum_{i=1}^{n=1} \sum_{j=i+1}^{n} \text{sign}(x_j - x_i), \quad \text{sign}(x_j - x_i) = \begin{cases} +1 & (x_j - x_i) > 0 \\ 0 & (x_j - x_i) = 0 \\ -1 & (x_j - x_i) < 0 \end{cases}$$

A positive S number signifies an upward trend, whereas a negative value corresponds to a downward trend. To determine the Z value, the variance of the rainfall is computed. Calculation of variance (S) is performed as follow (Aditya et al., 2021).

$$\text{Var}(S) = \frac{n(n-1)(2n+5) - \sum_{i=1}^{m} t_i(t_i-1)(2t_i+5)}{18}$$

These two types of tests, The Mann-Kendall and Sen's slope tests were performed using RStudio for the monthly, yearly, and seasonal rainfall trend analysis of 5 meteorological stations in this catchment area.

3.7 Model Setup

3.7.1 Setting up project default

Under the Tools Menu, the following setting of methods used were specified:

- Subbasin canopy method
- Subbasin surface method
- Subbasin loss method
- Subbasin transform method
- Subbasin baseflow method
- Reach routing method

This project utilized HEC-HMS 4.11 to perform the rainfall-runoff analysis in order to simulate the runoff volume and peak flows within the catchment. This facilitated in determining the flood risks in the catchment in order to take the possible measures to mitigate socio-culturally, environmental and physically risks. The setting up of a hydrological model in HEC-HMS involves definition of basin model, meteorological inputs, control specifications, and calibration of parameters based on observed data to effectively facilitate the model accuracy that inform flood risk assessments and watershed management strategies. The Figure below describes the steps involved to achieve the main objective of this research.

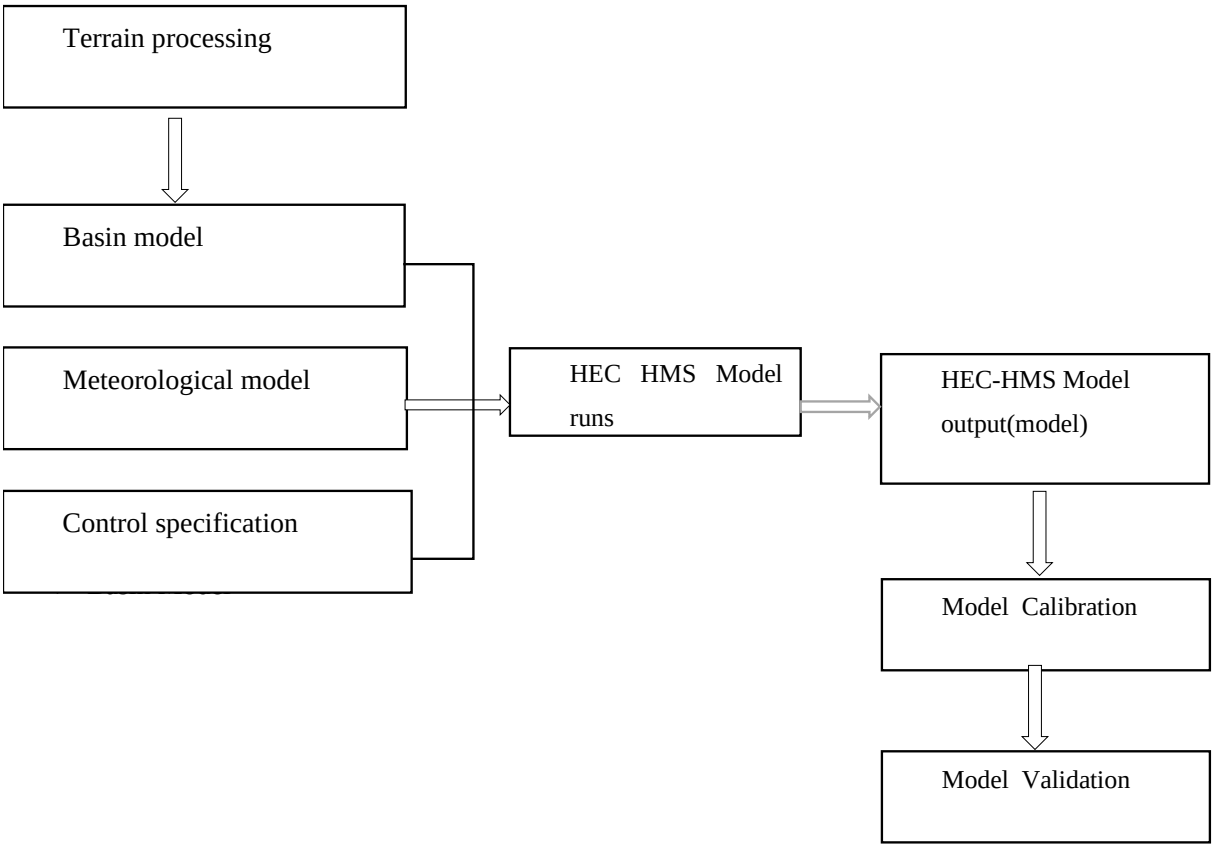

Figure 3.14: HEC-HMS Model procedure

3.7.2 Terrain processing and Basin model

This describes the hydrology on the land surface and it is performed by defining the sub-basins, reach elements, junctions and outlets using the processed Digital Elevation Model(DEM) data. To facilitate the catchment delineation, it required the following steps:

- Setting of coordinate system using GIS menu to be the same as of the DEM used for Terrain data in terrain model.
- Under the GIS Menu, the sinks were filled, Preprocess drainage was done to calculate flow direction and flow accumulation
- Streams identification was done to define stream network with threshold of 5 km^2.
- Break point creation tool was used to define watershed outlet
- Delineate elements in the opened window was done by defining subbasin prefix and reach prefix and inserting junctions within the catchment.
- The hydrological station was imported as shape file from ArcGIS which was used to insert the observed streamflow for calibration and validation.

❖ Meteorological Model

The meteorologic model describes the atmospheric conditions over the basin. This includes methods for simulating various elements of atmospheric boundary conditions. Precipitation is the fundamental process in hydrologic modelling. Precipitation drives the flow of water into the modelled watershed (USACE, 2000).This step was done through the following steps:

- Specifying a time series of rainfall for each meteorological station, and associating this gauge with each individual sub-basin
- In component Editor panel, time window changed to 01st January 2014 to 31st December 2018 for calibration and 01st January 2019 to 31st December 2021 for Validation.
- In component Editor panel, table was filled with the daily rainfall and streamflow data as the time series data.
- The meteorologic model folder in component editor panel, the setting was changed from replacing missing values to default.

❖ Control Specifications:

Set up the control specifications help to define the temporal resolution and extent of simulation (when the simulation will start and stop) and time interval used during the simulation process. The following steps were followed:

- Start date was 01st January 2014 for calibration
- End date was 31st December 2018
- Start and end time was set to be 00:00 with time interval of 1 day
- Simulation run was done by choosing basin, meteorological model and control specification from the list.

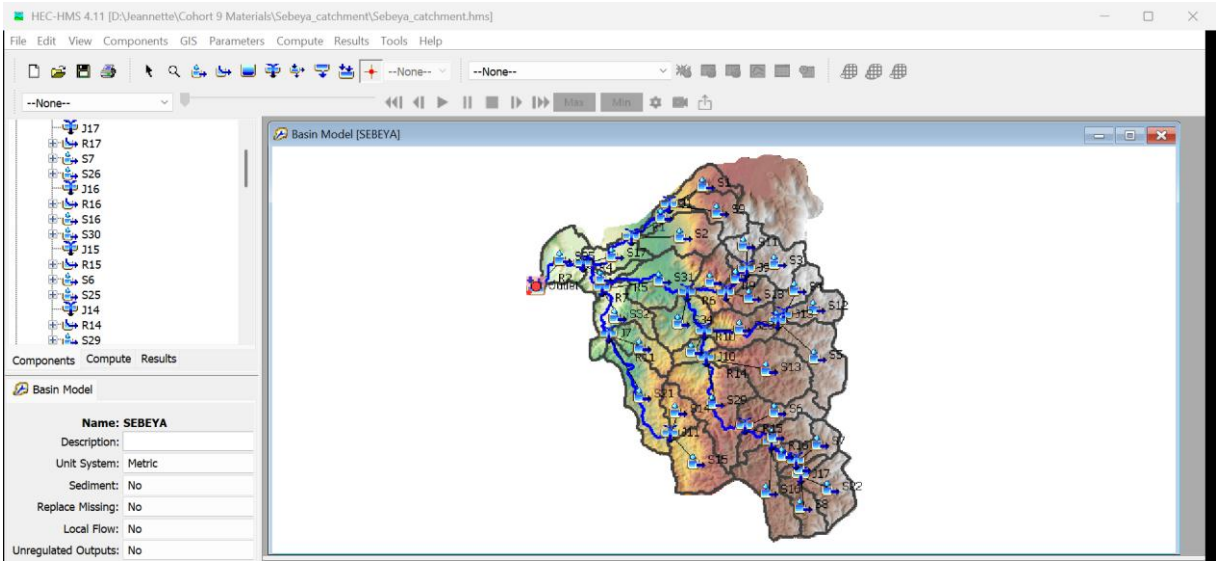

Figure 3.15: Catchment layout in HEC- HMS

3.8 HEC-HMS Calibration and Validation

Calibration is the methodical exploration of parameters using studied hydrometeorological data to find the optimal match of the calculated results to the observed runoff. The term commonly used to describe this search is optimization (USACE HEC,2023). Objective of this comparison is to assess the degree of conformity between the model and the actual hydrologic system. To ensure credible outputs, a hydrological model must be calibrated and validated using stream flow observations. The simulated stream flow must be compared to the observed stream flow to assess the goodness of fit and determine whether the model can accurately forecast and yield reliable outcomes (Ouédraogo et al., 2018). The procedure starts with the collecting data such as rainfall and flow time series data which are necessary for rainfall-runoff models. This iterative process minimizes the differences between predicted and actual hydrographs, enhancing the model's reliability for future predictions of hydrological events. By integrating statistical measures such as Nash-Sutcliffe Efficiency and Root Mean Square Error help in can assessing quantitatively the performance of the model. The validation approach involved utilizing the optimized parameters from a different period and verifying the goodness of fit between the observed and simulated streamflow (Ouédraogo et al., 2018) . Here there is figure shows the procedure for model calibration.

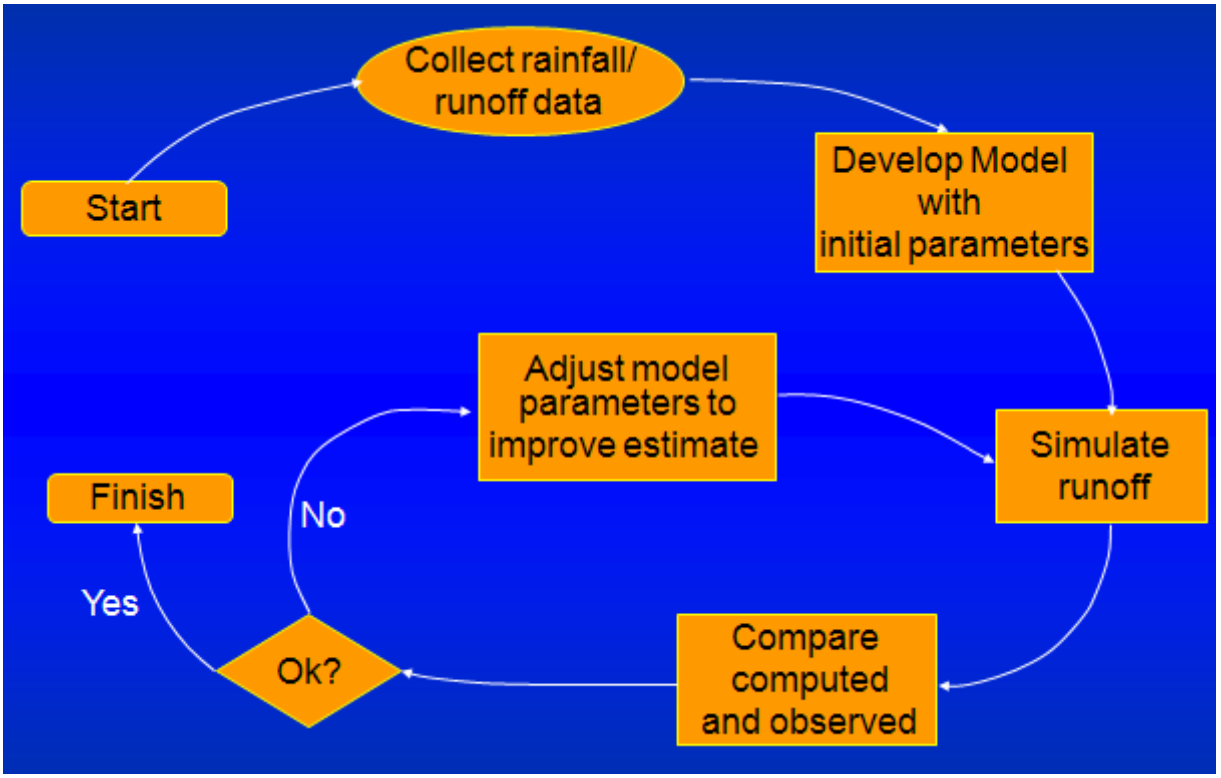

Figure 3.16: Schematic of calibration procedure (ASCE, 2023)

Table 22. Objective functions for calibration.

Criterion	Equation
Sum of absolute errors (Stephenson, 1979)	$Z = \sum_{i=1}^{NQ} \left\| q_O(i) - q_S(i) \right\|$
Sum of squared residuals (Diskin and Simon, 1977)	$Z = \sum_{i=1}^{NQ} \left[q_O(i) - q_S(i) \right]^2$
Percent error in peak	$Z = 100 \left\| \frac{q_S(peak) - q_O(peak)}{q_O(peak)} \right\|$
Peak-weighted root mean square error objective function (USACE, 1998)	$Z = \left\{ \frac{1}{NQ} \left[\sum_{i=1}^{NQ} \left(q_O(i) - q_S(i) \right)^2 \left(\frac{q_O(i) + q_O(mean)}{2 q_O(mean)} \right) \right] \right\}^{1/2}$

Note:

[1] Z = objective function; NQ = number of computed hydrograph ordinates; $q_O(t)$ = observed flows; $q_S(t)$ = calculated flows, computed with a selected set of model parameters; $q_O(peak)$ = observed peak; $q_O(mean)$ = mean of observed flows; and $q_S(peak)$ = calculated peak

Figure 3.17: Objective function for calibration (ASCE, 2023).

3.8.1 Goodness-of-fit indices

HEC-HMS calculates goodness-of-fit indices to compare a calculated hydrograph with an observed hydrograph. The three computed indices used in this research are:

- Mean Absolute Error (MAE).
- Root Mean Square Error (RMSE).
- Nash –Sutcliffe Efficiency Coefficient (NSE).

$$RMSE = \frac{\sqrt{\sum_1^n (Q_{Si} - Q_{Oi})\text{^}2}}{n}$$

$$MAE = \frac{1}{n}\sum_1^n |Q_{Si} - Q_{Oi}|$$

$$NAE = 1 - \frac{\sqrt{\sum_1^n (Q_{Si} - Q_{Oi})\text{^}2}}{(Q_{Oi} - Q_{Mean})\text{^}2}$$

Where:

Q_{oi} is the observed flow

Q_{si} is the simulated flow

$\bar{Q}_{oi}$ is the average of the observed flow

n is the number of data points.

A reduced MAE and RMSE indicate superior model fit and performance; conversely, a higher NAE signifies an improved model fit (NAE typically ranges from 0 to 1) (Jer Lang Hong et al., 2018).

3.9 Rainfall-Runoff Modeling

The HEC-HMS model is a physically based and theoretically semi-distributed model developed to mimic rainfall-runoff processes across a diverse array of geographic locations, ranging from huge river basin water supply and flood hydrology to tiny urban and natural watershed runoffs. It efficiently manages extensive activities associated with hydrological studies, encompassing losses, runoff transformation, open channel routing, meteorological data processing, rainfall-

runoff simulation, and parameter estimate (Hawkins et al., 2008).Many hydrological models are used to mimic rainfall into runoff which consider all of the processes that transform rainfall into runoff. In this study, HEC-HMS 4.11 version model was chosen to achieve the objectives of the research. This package contains different methods such as canopy, surface, loss , transform, base flow and routing method.

3.9.1 Simple canopy method

The basic canopy approach in HEC-HMS calculates interception loss from vegetation. It presumes a constant canopy storage capacity, supplemented by precipitation and diminished by evaporation. This strategy is uncomplicated and necessitates minimal data, rendering it appropriate for regions with scarce information (Scharffenberg et al., 2010). In this method the important parameters were set such as initial storage in %, maximum storage in mm, crop coefficient , evaporation method and uptake method.

- Initial surface storage (%): This is an input representing the percentage of maximum surface storage occupied at the commencement of the simulation. The simulation starts following a period of no rainfall, resulting in the complete evaporation or infiltration of all water held in the basin depression. A value of 0% is suitable in this context. This assumption must be maintained in the selection of simulation periods (Ahbari et al., 2018).
- Maximum surface storage (mm): The estimation is based on the slope (%) of the catchment surface.

3.9.2 Runoff volume calculation(the transform model)

The SCS unit hydrograph method is a rainfall-runoff technique in which excess precipitation is converted to point runoff using the SCS unit hydrograph, developed by the Soil Conservation Service based on the average unit hydrographs produced from measured rainfall and runoff data. The HEC-HMS SCS unit hydrograph approach calculates the peak discharge of the basin based on the lag time of the drainage region (Belay et al., 2022). The lag time (T_{lag}) serves as the sole input for this approach. The duration from the center of mass of surplus precipitation to the peak hydrograph is determined for each watershed using the time of concentration as follows:

T_{lag}= 0.6T_c

where :

T_{lag} is lag time in minute and

T_c is the time of concentration in minute.

The time of concentration can be estimated based on basin characteristics including topography and the length of the reach by Kirpich's formula (Al-Mukhtar & Al-Yaseen, 2019)

$$T_c = 0.0078 \times \frac{L^{0.77}}{S^{0.385}}$$

Where L is the reach length in feet, and S is the slope in (ft/ft).

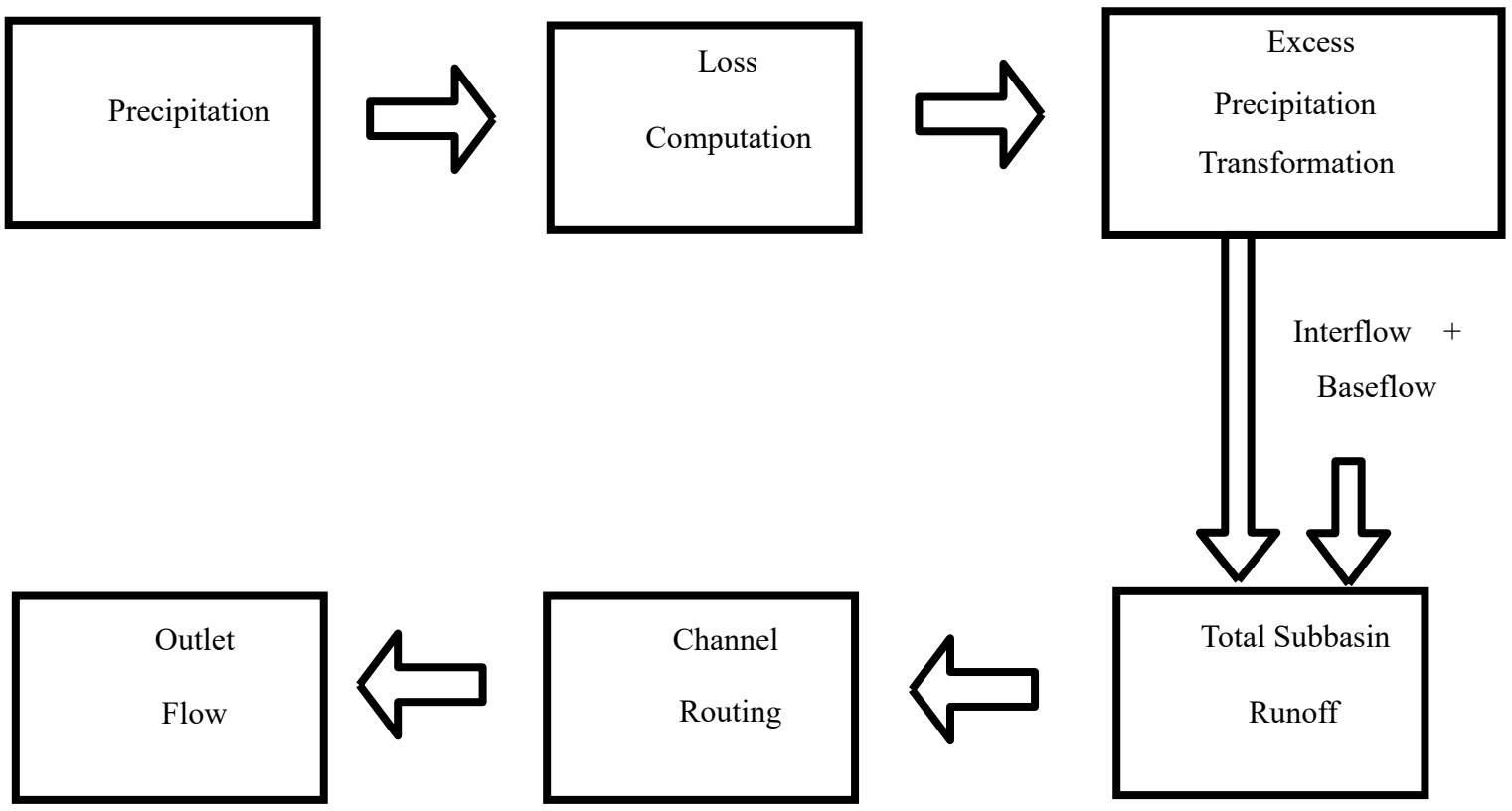

Figure 3.18: Runoff volume computation procedure

3.9.3 Routing method

This is the most basic of the provided routing models. The outflow hydrograph is identical to the inflow hydrograph, except that all ordinates are shifted in time by a designated duration. The flows remain unattenuated; hence the form remains unchanged. This concept is extensively utilized, particularly in urban areas drainage systems.

Mathematically, the downstream ordinates are computed by:

$$O_t = \begin{cases} I_t & t < lag \\ I_{t-lag} & t \geq lag \end{cases}$$

Where:

O_t = outflow hydrograph ordinate at time t; I_t = inflow hydrograph ordinate at time t; and

lag = time by which the inflow ordinates are to be lagged.

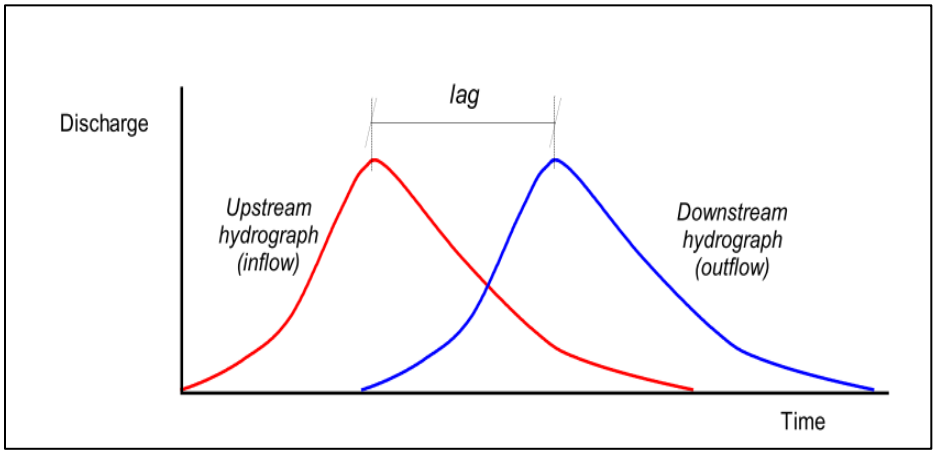

Figure 3.19: Lag example

3.9.4 Base flow computation

The Linear Reservoir Model is a conceptual hydrological concept deployed for modelling the storage and outflow dynamics of a catchment or a segment of the hydrological cycle, including groundwater, surface runoff, or baseflow. The theory is that the discharge from a reservoir is directly proportionate to its storage capacity (HEC, 2023). The model is governed by the following equation:

$$Q = \frac{S}{K}$$

Where: Q is outflow from the reservoir (e.g., streamflow, baseflow)

- S is storage within the reservoir
- K is reservoir time constant (storage coefficient)

3.10 Sensitivity Analysis

A sensitivity analysis is often conducted in the majority of modeling research. Identifying the essential characteristics and the requisite precision for calibration is a vital step. The primary sensitivity analysis technique employs partial differentiation, while the most fundamental way is varying parameter values individually (Al-Mukhtar & Al-Yaseen, 2019). In this project, the more effective parameters were adjusted in the range of ±30 % with 5% intervals. Zelelew and Melesse did a sensitivity analysis by varying the parameter values within a range of ±30% at 5% intervals until achieving a perfect fit between the observed and simulated parameters in the specified hydrograph (Zelelew, 2018). This analysis was performed to understand the complex relationships among model parameters and variables. It is used to identify the parameters that substantially influence model performance and offers an estimation of the exact value of each parameter (Bhuiyan et al., 2017).

3.11 Sampling Method

Several research papers employ Slovin's (or occasionally Sloven's) formula to determine the sample size (Tejada et al., 2012). Let n represent the sample size; Slovin's formula is expressed as:

$$n = \frac{N}{N + Ne^2}$$

Where N is the population size and e is the margin of error (5%)

The populations of three cells which are Mahoko, Nyundo and Rugerero cell were 9543,6975 and 10,006 respectively making total population of 26524. a sample was calculated using sample size calculation provided above. Using the equation above, a sample size of 120 interviewees were calculated to participate in the survey.

3.12 Data Collection

The random method was adopted for data collection. The data collected in each household, local government officers, representative of schools and private company who work and live in the flood prone area within the catchment of different sector such as Kanama, Nyundo and Rugerero sector. Structured questionnaires and interviews were used to collect data. The Rubavu District authorized the research with communicating with executive secretaries in the sectors and cells level for the additional support. In order to maintain the accuracy of the responses, the respondents were informed to the benefits of conducting this research and their participation was fully voluntary.

3.13 Data Analysis

After gathering relevant data, the data were analyzed using Microsoft Excel sheet. The quantitative data acquired from the surveys were examined utilizing descriptive including frequency, count, histogram and percentages.

3.14 Flood Frequency Analysis

Flood frequency analysis is crucial for predicting and calculating Peak Flood Discharge for a specified return period, which is necessary for the management and design of hydrological structures such as bridges, weirs, spillways, and dams (Ray & Desai, 2022). A variety of flood frequency analysis distributions have been employed using hydrological data to estimate flood magnitude and frequency. The flood frequency analysis methods employed in hydrology include the Log Pearson Type-III distribution, Log-Normal distribution, Partial Duration Series, and Gumbel's Distribution (Keast & Ellison, 2013).

3.14.1 Gumbel's distribution

Gumbel is a statistical distribution originating from extreme value theory. The function in this distribution is unrestricted on either side, resulting in a negative flow calculation. This illustrates the distribution of extreme values, whether maximum or minimum, utilized in various distributions and for modelling the distribution of peak levels. This is employed for forecasting earthquakes, floods, and other natural catastrophes. It also simulates operational threats in managing risks associated with products that deteriorate quickly before reaching a specific age (Samantaray & Sahoo, 2020) The Gumbel distribution employed in flood frequency analysis

delineates extreme values, including the maximum or minimum values within a sample. It functions as a fundamental element in numerous distributions and is frequently utilized for modelling the distribution of peak values (Ray & Desai, 2022).

The abbreviated variate (Y_t) for the specified return period (T) has been evaluated using the formula:

$$Y_t = ln\{\ln (T/(T-1)\}$$

The concise mean and reduced standard deviation have been derived using the Gumbel distribution table for the specified sample size (N). The frequency factor is calculated using the formula:

$$K_t = \left(\frac{K_t - K_n}{S_n}\right)$$

where K_t = frequency factor, Y_t reduced variate, Y_n= reduced mean,

S_n= reduced standard deviation. Thus, the predicted discharge (Q_p) is computed using the standard normal distribution formula for diverse return period for respective seasons:

$$Q_p = \mu + K_t\sigma$$

Where Q_p is the predicted discharge

μ is the average of peak discharge

σ is the standard deviation of the peak discharge

Among these methods, Gumbel's distribution was utilized in this research to get the correlation between the possibility of rainfall events and peak discharge for different return periods to be aware of the flood magnitude corresponding to the specified return time.

3.15 HEC RAS Model Set Up

The HEC-RAS (Hydrologic Engineering Center River Analysis System) 5.0.7 software, developed by the US Army Corps, is a commonly employed tool for flood modeling in hydrodynamic simulations (Hadi & Almansori, 2023). This model is capable of conducting one-dimensional steady flow and two-dimensional unsteady flow simulations for the transport of solids and water quality modeling. It does flow analysis utilizing geometric and hydraulic

computation processes over a river network. This research based on running 1D river flow simulations to perform flood inundation analysis as recommended by Dasallas to be simple and useful in practice (Dasallas et al., 2019). The figure below shows the steps followed to perform the analysis.

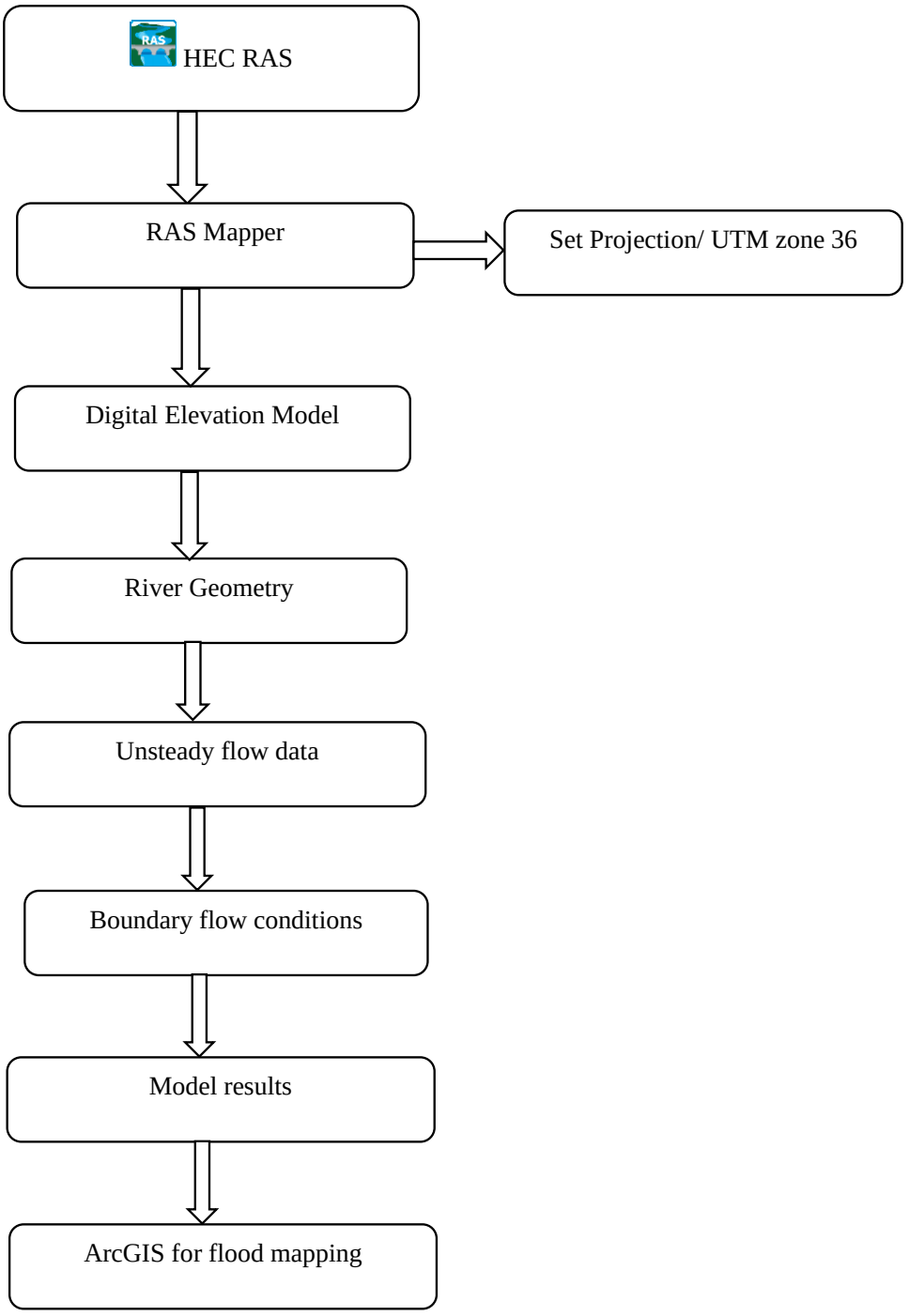

Figure 3.20: HEC-RAS Model step

3.15.1 Data collection and preparation

To create 1D flow HEC-RAS model require the different type data collected from various sources. The fundamental input dataset needed are Digital elevation model , daily observed discharge obtained from Nyundo hydrological station for 2016, manning's roughness coefficient based on CHOW standard and project file of the study area as spatial reference. All this data serves the model in order to get output and evaluation of the model. Hydraulic modelling and inundation mapping are conducted using RAS Mapper, a spatial data integration and mapping tool within HEC-RAS. HEC-RAS Mapper enables the creation of RAS terrains, arrangement of geometric data, extraction of terrain information, and presentation of results through maps and tables (Vashist & Singh, 2023).

Table 3.6: Manning's roughness coefficient ranges according to the CHOW standard (https://www.fsl.orst.edu/geowater/FX3/help/8_Hydraulic_Reference/Mannings_n_Tables.htm).

Land Use	Manning (n)		
	Minimum	Normal	Maximum
Road	1	5	10
Bare soil	0.02	0.03	0.04
Buildings	1	5	10
Grass	0.025	0.035	0.05
Agriculture	0.03	0.04	0.05
Forest	0.11	0.15	0.2
Pasture	0.025	0.03	0.035

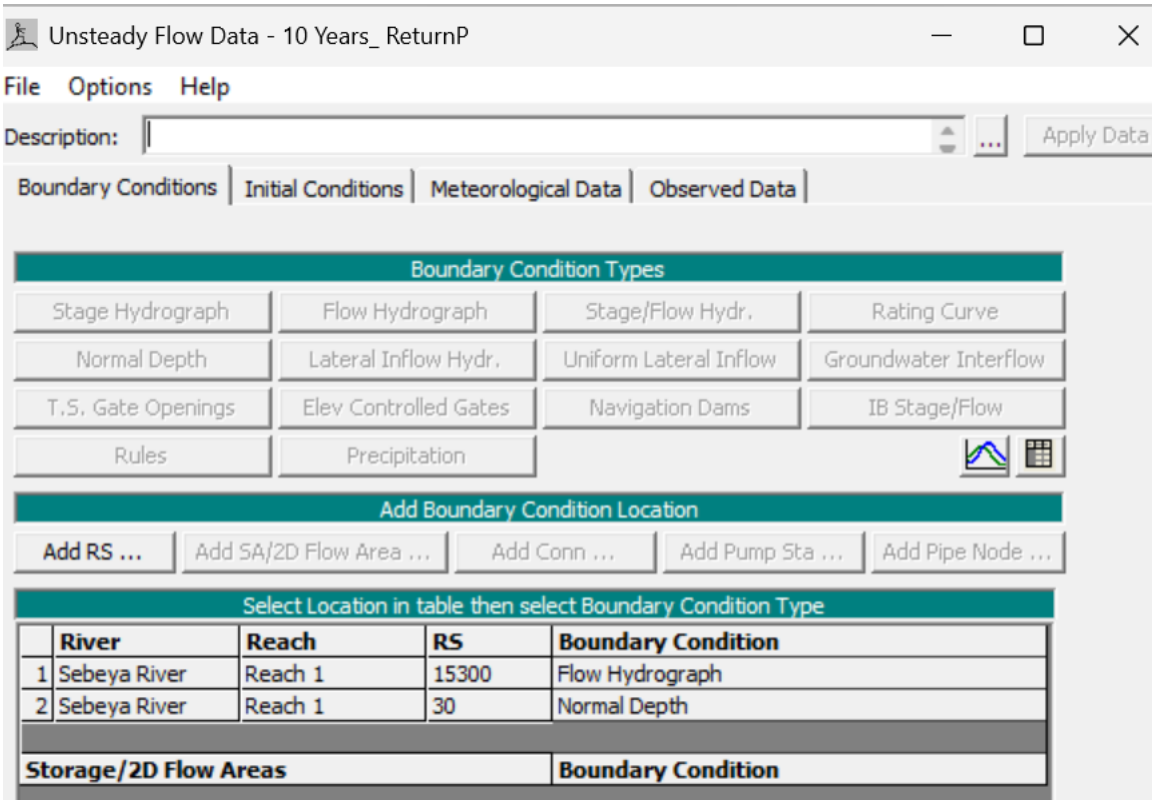

Figure 3.21: Boundary conditions of the model

3.15.2 1D flow cross section and River channel

To create the RAS terrain layer, it is imperative to consider the spatial reference of the study area. This was set to WGS 84 UTM zone 36 S as projection. The DEM of 30 m resolution was used with creating new geometric file. The parameters such as unsteady flow data and surface roughness was obtained from manning roughness input. The cross sections were created for 100 m interval to each cross section to facilitate the coverage of reaches with in the study area, inundation mapping, simulation run time and accuracy.

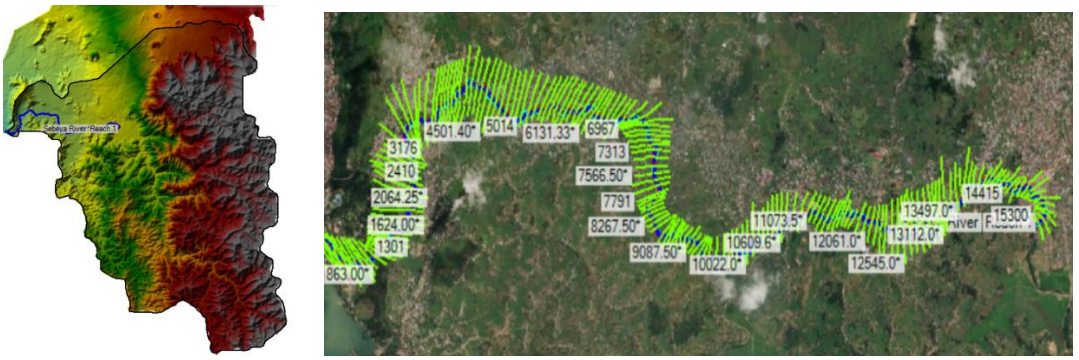

Figure 3.22: 1D cross section and River channel

3.15.3 Unsteady flow analysis and simulation

After generating cross section, the model performed the unsteady flow analysis. The input flow data were added such as discharge for upstream boundaries, the normal depth was added on the downstream boundaries.The computational parameters, including modelling interval, hydrograph output interval, mapping output interval, and detailed output interval, must be provided for the simulations. In unsteady flow computations, the computation interval is a critical parameter utilized. The simulation interval must be selected to adequately uphold the accuracy and stability criteria in accordance with the courant condition (Vashist & Singh, 2023). To maintain the stability and accuracy of the results, the simulation period was set to be 01st May 2020 to 02nd May 2020 and the computation interval of 3 seconds was used in this model.

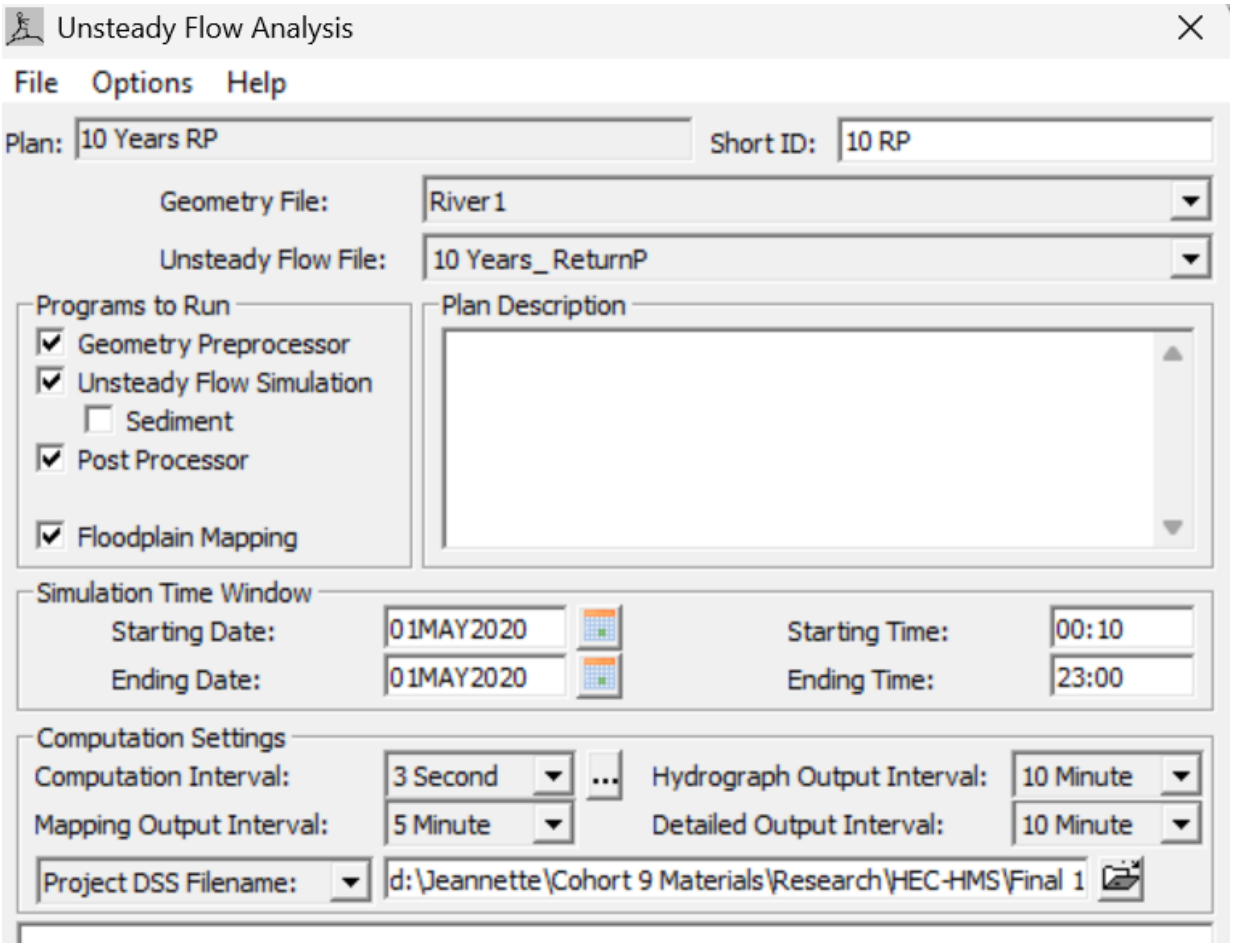

Figure 3.23: Unsteady flow analysis

3.16 Flood Mapping

After generating water depth, velocities, inundation map and water surface extent from HEC-RAS model, the shapefile and raster map were exported to ArcGIS version 10.4 to visualize and identify the areas located in low, medium and high flood zone. This was done by classifying them into categories from low risk to high-risk range as seen in table 3.7 for flood depth, water velocity and inundation extent.

Table 3.7: Flood risk categories

Category (m)	Risk
0 - 1	Very low
1 - 2	Low
2 - 3	Moderate
3 - 4	High
>4	Very high

RESULTS AND DISCUSSION

4.1 Initial Parameters for The Model

Initially, the model has been set with different parameters to different method. This simple canopy showed that it is effective to the model calibration. Here there is summary of initial parameters before calibration.

Simple Canopy [SEBEYA]

Filter: --None--

Subbasin	Initial Storage (%)	Max Storage (MM)	Crop Coefficient	Evapotranspiration	Uptake Method
S16	1	2	1	Wet and Dry Periods	Simple
S11	1	2	1	Wet and Dry Periods	Simple
S40	1	2	1	Wet and Dry Periods	Simple
S26	1	2	1	Wet and Dry Periods	Simple
S21	1	2	1	Wet and Dry Periods	Simple
S31	1	2	1	Wet and Dry Periods	Simple
S30	1	2	1	Wet and Dry Periods	Simple
S39	1	2	1	Wet and Dry Periods	Simple
S5	1	2	1	Wet and Dry Periods	Simple
S25	1	2	1	Wet and Dry Periods	Simple
S9	1	2	1	Wet and Dry Periods	Simple
S38	1	2	1	Wet and Dry Periods	Simple
S20	1	2	1	Wet and Dry Periods	Simple
S24	1	2	1	Wet and Dry Periods	Simple
S15	1	2	1	Wet and Dry Periods	Simple
S23	1	2	1	Wet and Dry Periods	Simple
S27	1	2	1	Wet and Dry Periods	Simple
S33	1	2	1	Wet and Dry Periods	Simple

Figure 4.1: Initial parameters of the model

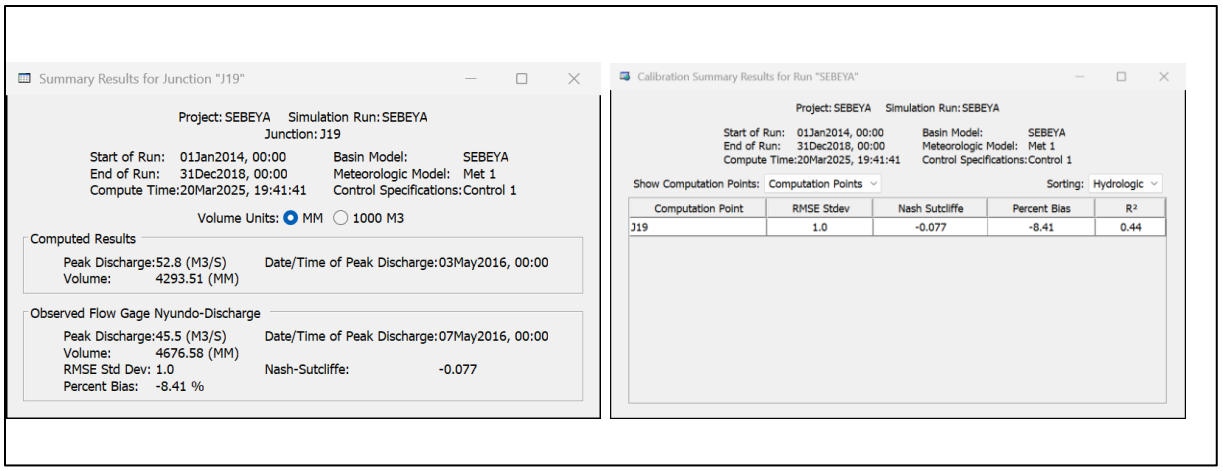

Figure 4.2: Model output before calibration

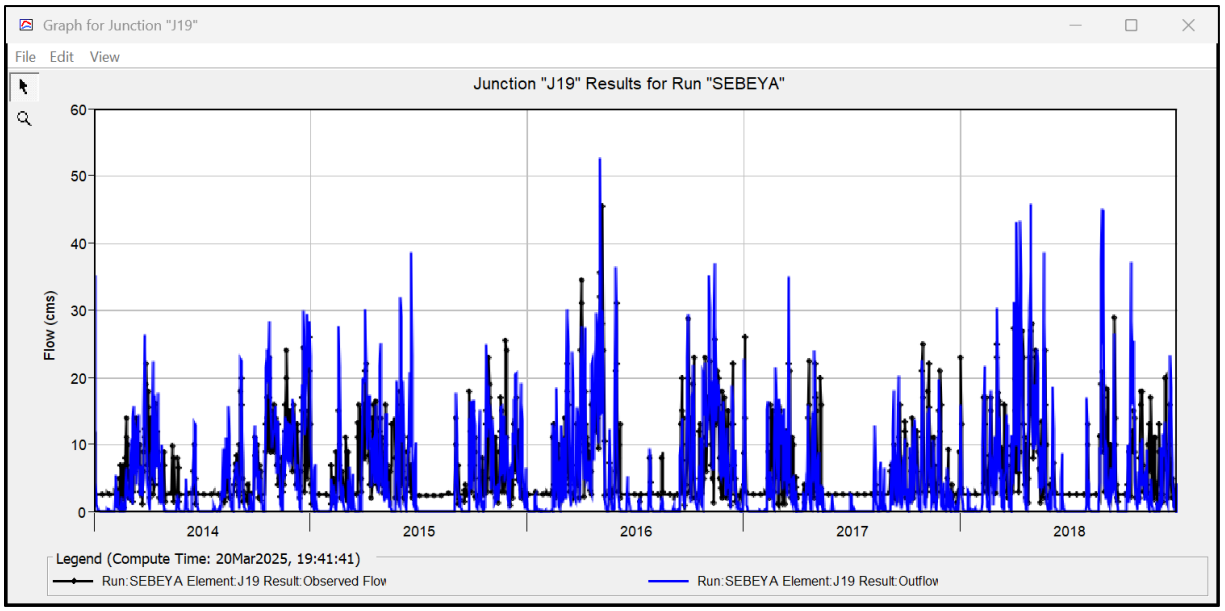

Figure 4.3: Flow hydrograph shows the variation of Streamflow over time before Calibration

4.2 Model Calibration and Validation

4.2.1 Sensitivity analysis

The sensitivity analysis was performed on the model parameters specifically on simple canopy, deficit and constant, baseflow and routing method. The re-run of the model was repeated by increasing and decreasing by ±30 % from the initial value of each parameter while maintaining all other parameters constant at their nominal initial values. The hydrographs resulting from the scenarios of adjusted model parameters were then compared with the baseline model hydrograph. The higher sensitive parameters were found to be crop coefficient, constant rate, lag time and groundwater fraction. The initial deficit, maximum deficit, and constant flow rate were identified as the least sensitive factors, exhibiting minimal variation in flow rates. This aligns with Gebre's study, which identified the storage coefficient as the most sensitive parameter for simulating runoff in the Upper Blue Nile Basin (Gebre, 2015).

Table 4.1: Initial lag time and lag time after sensitive analysis

Reach name	Initial lag time	Lag time after calibration
R18	37	48
R17	51	66
R15	47	62
R14	83	108
R12	45	59
R11	6	8
R10	44	58
R3	136	176
R9	13	17
R8	30	39
R20	35	46
R19	83	108
R16	130	169
R13	100	130
R4	114	148
R2	53	69
R7	107	140
R6	2	3
R5	79	102
R1	71	92

Table 4.2: HEC-HMS model parameters after calibration

Method	Parameters	Calibrated values
Canopy (Simple canopy)	Initial storage (%)	0
	Maximum storage(mm)	2.0
	Crop coefficient	1.2
Baseflow (Linear reservoir)	GW fraction 1	0.5
	GW fraction 2	0.35
Routing (Lag)	Lag time (increased by 30% for each reach)	-

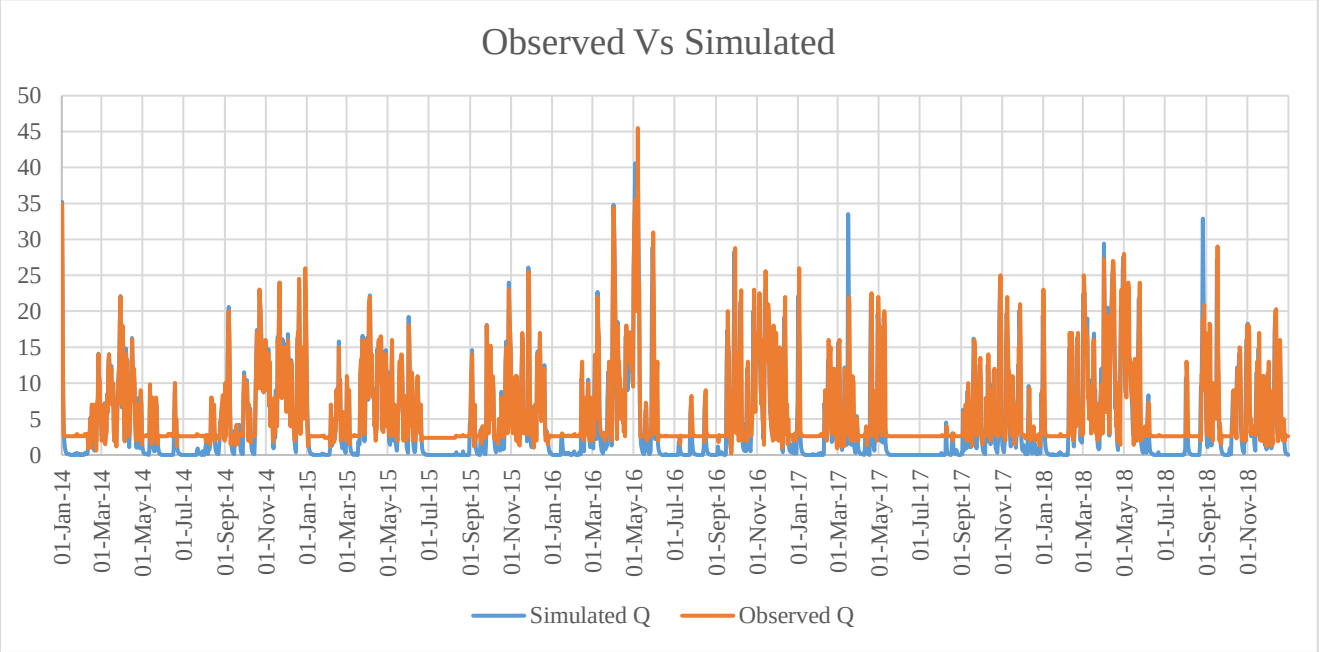

Figure 4.4: Observed and simulated stream flow from 2014 to 2018 after calibration

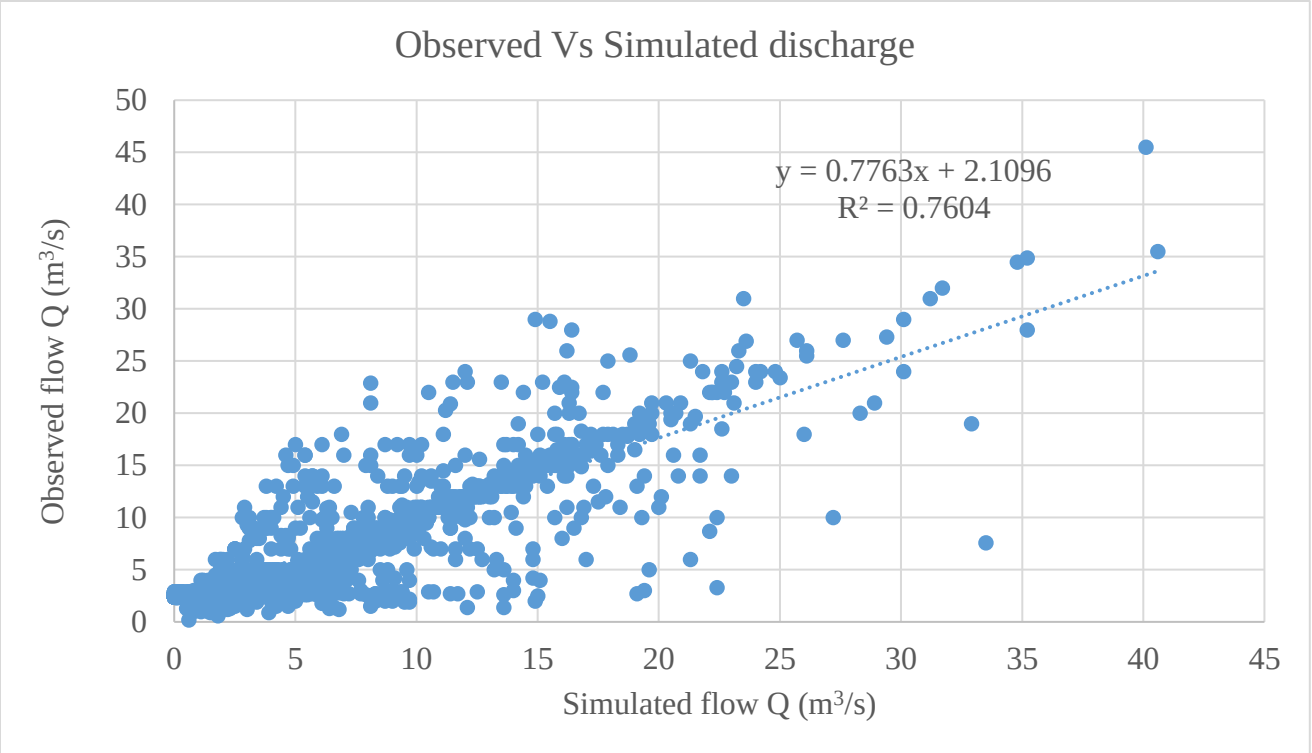

Figure 4.5: Plot of simulated versus observed flow data of the model after calibration

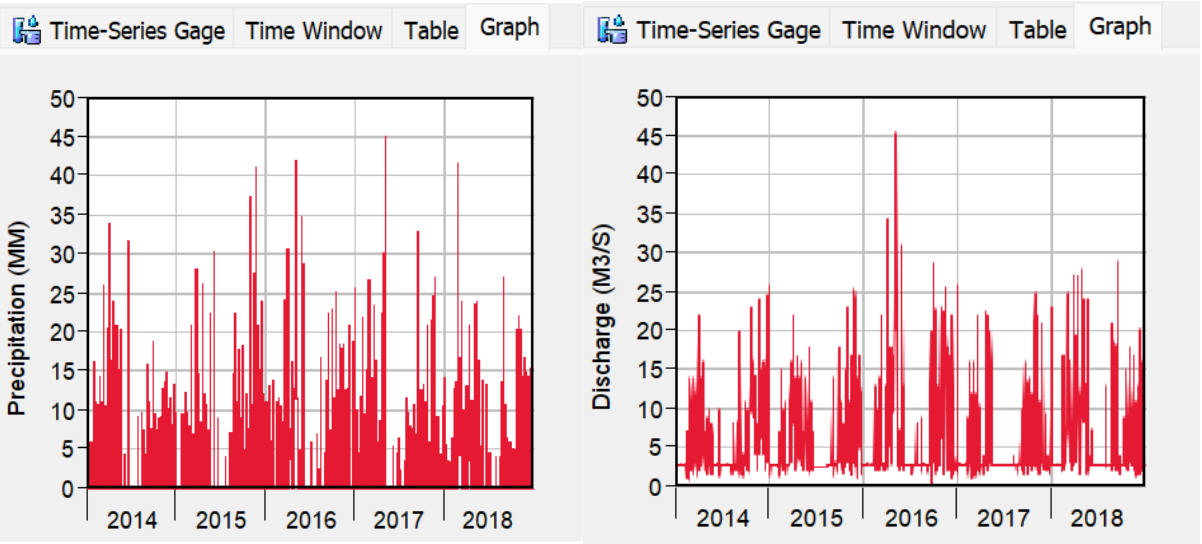

Figure 4.6: Precipitation and Discharge hydrograph after calibration from 2014 to 2018

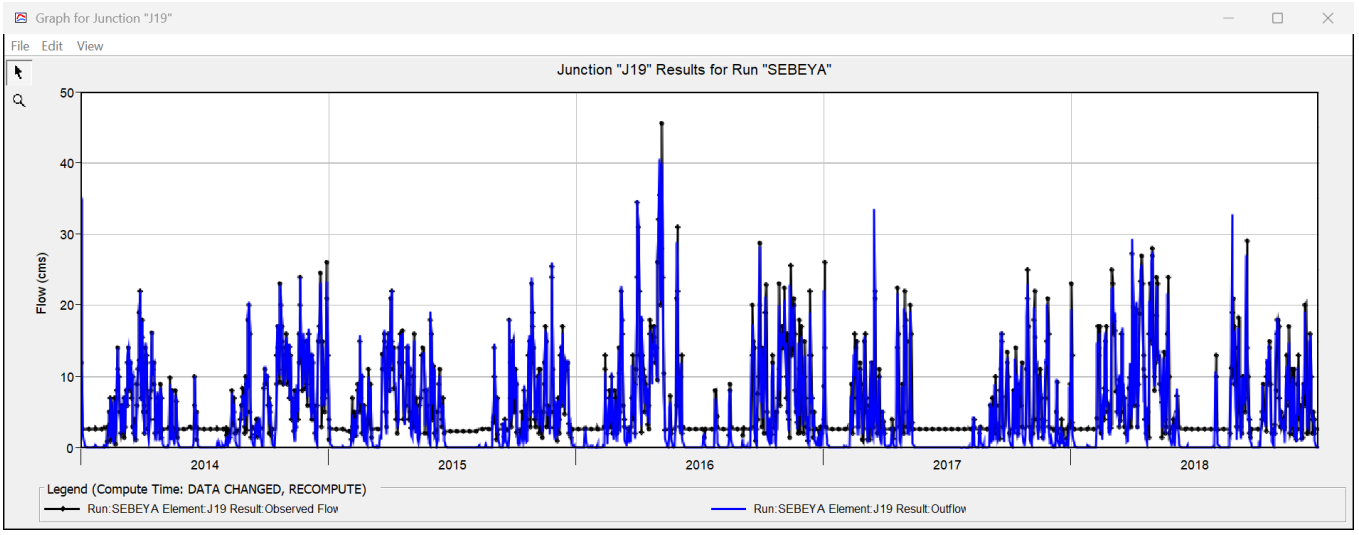

Figure 4.7: Flow hydrograph after model calibration

4.2.2 Model output after calibration and validation

The model has shown that the simulated peak discharge was obtained on 03rd May 2016 with amount of 40.6 m^3/s while the peak observed streamflow was 45.5 m^3/s on 07th May 2016. In addition, this model was validated using the dataset for 3 years from 2019 up to 2021 without changing model parameters. This has shown that the simulated peak flow was obtained to be 45.2 m^3/s on 04th May 2020 and the peak observed streamflow was 47.5m^3/s on 10th May 2020. The performance of the model was good to use with the values shown in the table below:

Table 4.3: Performance of the model

Model output with its assessment criteria			
Criteria	Initial value	Calibration	Validation
Nash–Sutcliffe	-0.08	0.67	0.70
Root Mean Square Error (RMSE)	1.00	0.60	0.80
Correlation coefficient (R^2)	0.44	0.76	0.88

4.3 HEC-HMS Results from Frequency Precipitation Depth

After calibration and validation of the model, the frequency precipitation depths corresponding to each return period were introduced in the model to simulate hydrograph and peak runoff. The

considered return periods were 5,10,20 and 50 years. The figures below show the results from the model where the peak runoff is increasing from low return period to high return period.

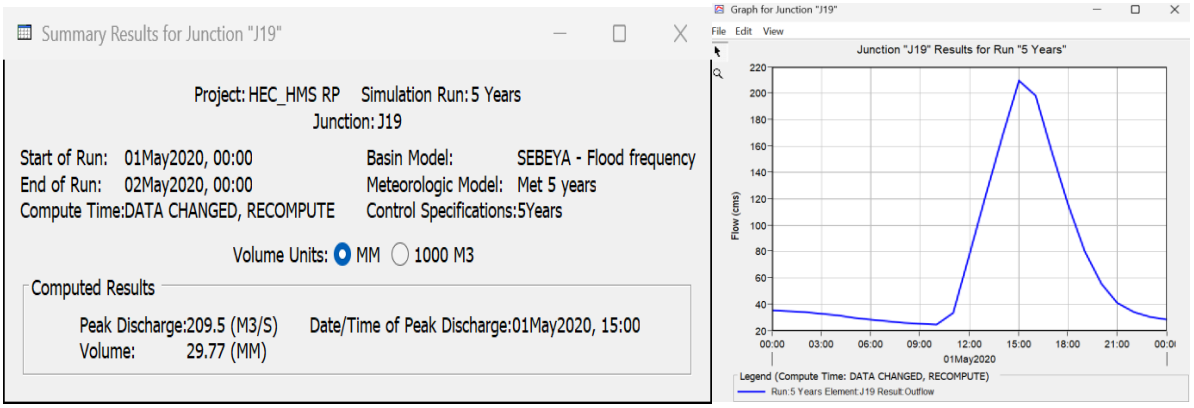

Figure 4.8: 5-year return period hydrograph with corresponding peak discharge

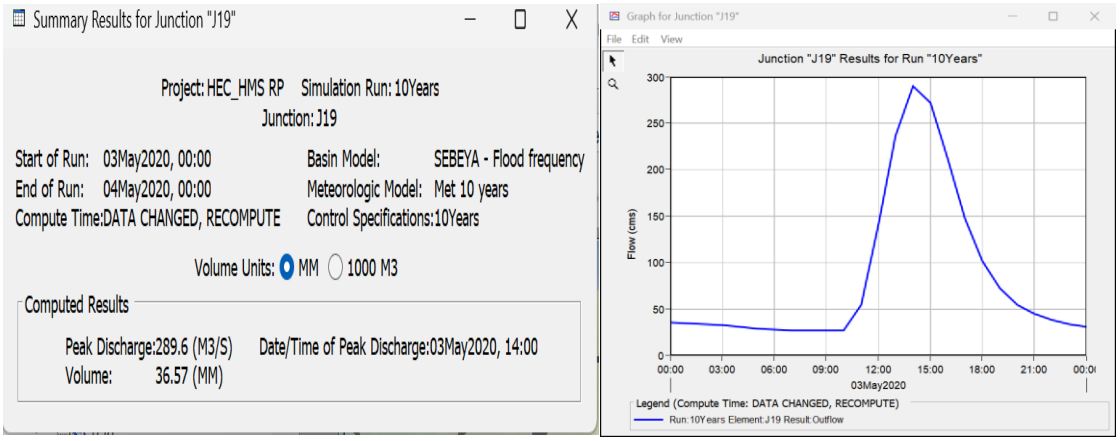

Figure 4.9: 10-year return period hydrograph with corresponding peak discharge

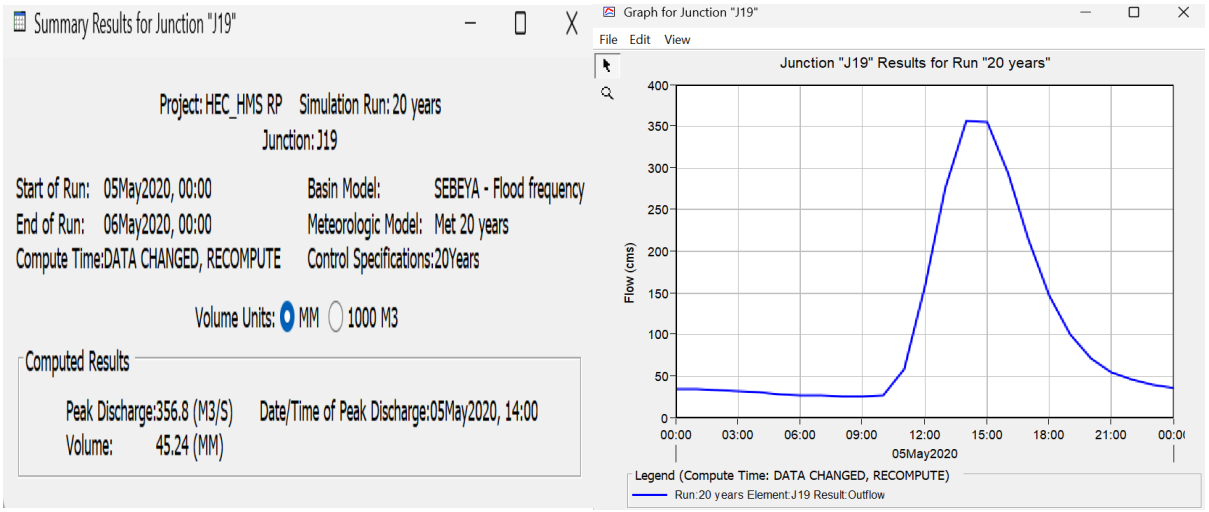

Figure 4.10: 20-year return period hydrograph with corresponding peak discharge

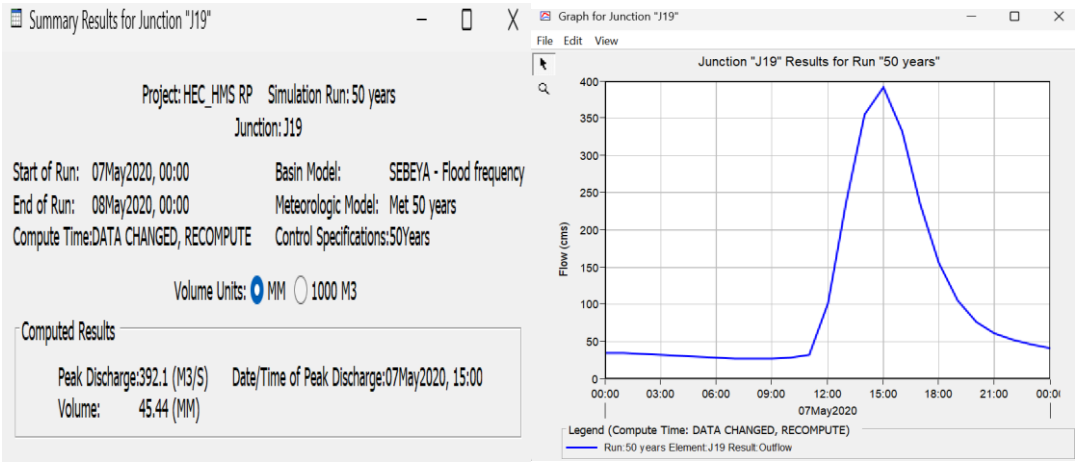

Figure 4.11: 50-year return period hydrograph with corresponding peak discharge

Table 4.4: HEC-HMS simulated peak discharge corresponding to different return period

Return period	Simulated Peak Discharge (m^3/s)
5	209.5
10	289.6
20	356.8
50	392.1

4.4 Trend Analysis

Mann-Kendall and Sen's slope test showing rainfall trends(mm) in the Sebeya catchment at Kivumu, Kanama, Bigogwe, Nyundo and Murunda Paroisse station (1991-2021) are summarized in the table below.

	Mann- Kendall and Sens's slope Test					
	Kivumu Station			Kanama station		
Month	z-value	p-value	sen's slope	z-value	p-value	sen's slope
Jan	-2.890	0.004	-0.086	-0.255	0.799	-0.006
Feb	0.323	0.747	0.010	-0.306	0.760	-0.007
Mar	-1.904	0.057	-0.096	-0.102	0.919	-0.006
Apr	0.935	0.350	0.038	-0.187	0.852	-0.006
May	-1.955	0.051	-0.112	-1.785	0.074	-0.057
Jun	-0.675	0.500	0.000	2.003	0.045	0.051
Jul	1.503	0.133	0.000	2.195	0.028	0.008
Aug	-0.204	0.838	-0.002	0.901	0.367	0.032
Sept	0.697	0.486	0.022	0.714	0.475	0.019
Oct	-1.360	0.174	-0.037	-0.085	0.932	-0.002
Nov	-0.272	0.786	-0.008	-1.666	0.096	-0.072
Dec	0.833	0.405	0.023	-1.054	0.292	-0.033
Annual	-1.530	0.126	-6.607	0.204	0.838	1.250
Dry season(Jul - Aug)	-0.068	0.946	0.000	0.629	0.529	0.769
Short rain season(Sept - Dec)	0.340	0.734	0.900	-0.510	0.610	-1.572
Long rain season(Feb - May)	-1.462	0.144	-5.313	-0.782	0.434	-2.250

	Bigogwe station			Nyundo station			Murunda station		
Month	z-value	p-value	Sen's slope	z-value	p-value	Sen's slope	z-value	p-value	Sen's slope
Jan	-1.921	0.055	-0.049	0.391	0.696	0.015	-0.884	0.377	-0.047
Feb	-0.561	0.575	-0.014	0.374	0.709	0.012	-1.105	0.269	-0.038
Mar	-1.207	0.228	-0.039	1.786	0.074	0.054	-2.076	0.038	-0.070
Apr	1.479	0.139	0.075	0.952	0.341	0.038	-1.241	0.215	-0.087
May	-1.275	0.202	-0.036	-1.020	0.308	-0.019	0.799	0.424	-0.049
Jun	1.742	0.082	0.031	1.819	0.069	0.033	0.710	0.478	0.000
Jul	0.689	0.491	0.002	1.575	0.115	0.007	1.070	0.285	0.000
Aug	0.527	0.598	0.022	0.323	0.747	0.012	0.817	0.414	0.023
Sept	1.395	0.163	0.037	0.527	0.598	0.016	-0.119	0.905	-0.004
Oct	1.258	0.208	0.032	-0.731	0.465	-0.018	0.170	0.865	0.004
Nov	0.238	0.812	0.011	-0.867	0.386	-0.033	-1.615	0.106	-0.089
Dec	-1.836	0.066	-0.045	-0.187	0.852	-0.010	-0.833	0.405	-0.021
Annual	1.904	0.057	7.862	1.427	0.153	7.371	-1.139	0.255	-8.720
Dry season (Jul - Aug)	0.323	0.747	0.700	0.663	0.507	0.925	0.919	0.358	0.986
Short rain season (Sept - Dec)	0.323	0.747	0.700	-0.510	0.610	-1.538	-1.496	0.135	-6.800
Long rain season (Feb - May)	0.323	0.747	0.700	1.530	0.126	4.000	-1.496	0.135	-6.800

4.4.1 Annual rainfall trend analysis

Rainfall data obtained from Rwanda Meteorological Agency (METEO) for Kivumu,Kanama, Bigogwe, Nyundo and Murunda- Paroisse meteorological station indicates a mean annual precipitation from 1991 to 2021 was 1254.5mm,1376.1mm,1235.6mm,1325.8mm and 1637.0mm respectively. Rainfall patterns are greatly influenced by altitude as it can be seen that Bigogwe rainfall station at an elevation of 2382m above sea level receives small amount of rainfall compared to other 4 stations. The Mann-Kendall trend test presented in Table 4.4 detected trends in the annual rainfall totals spanning the research period of 1991-2021. The data obtained from Bigogwe meteorological station had a statistically significant upward(positive) trend with a p-value of 0.05 at 95% confidence interval which falls in p-value range of 0.05 indicating a statistical significance. The Sens's slope of 7.862 mm/year observed indicated a substantial increase in rainfall within the upstream of Sebeya catchment. This shows that there is trajectory increases of precipitation in the catchment which will contribute to the downstream over years. On the other hand, Kanama and Nyundo meteorological station annual rainfall data also indicated a negative trend with a p-value of 0.838 and 0.153 which exceed the 0.05 threshold at 95% confidence interval. The calculated Sen's slope value was at 1.25mm/year and 7.371mm/year indicating a significant increase in precipitation within the upstream, midstream and downstream of the catchment areas. This indicate that there is a real increasing trend in rainfall over time which might be due to different factors.

Table 4.5: Total annual rainfall in different station

	Stations				
Year	**Kivumu**	**Kanama**	**Bigogwe**	**Nyundo**	**Murunda**
1991	1293.2	1090.7	1041.0	836.0	1139.0
1992	871.0	1314.8	1130.0	961.0	1617.0
1993	1264.0	1084.0	1068.0	1029.0	1831.0
1994	1192.0	1274.0	1182.0	1144.0	1498.0
1995	1400.0	1386.0	1158.0	1161.0	1465.0
1996	1361.0	1486.0	1238.0	1277.0	1690.0
1997	1650.0	1502.0	1210.0	1423.0	1992.0
1998	1483.0	1529.0	1284.0	1533.0	1946.0
1999	1122.0	1604.0	1269.0	1581.0	1731.0
2000	1271.0	1484.0	1305.0	1498.0	1741.0
2001	1524.0	1561.0	1309.0	1607.0	1813.0
2002	1357.0	1482.0	1228.0	1336.0	1887.0
2003	1619.0	1609.0	1343.0	1468.0	1920.0
2004	1292.0	1232.0	1062.0	1163.0	1694.0
2005	1248.0	1127.0	1026.0	1059.0	1505.0
2006	1467.0	1591.0	1385.0	1415.0	2256.0
2007	1626.0	1610.0	1293.0	1534.0	2071.0
2008	704.3	1309.0	1055.0	1205.0	1825.0
2009	1337.0	1256.0	1053.0	1131.0	1813.0
2010	1019.6	1416.0	1397.4	1418.9	1976.0
2011	1313.0	1394.6	1244.1	1526.2	2212.4
2012	1377.0	1171.2	1209.6	1340.7	872.6
2013	1080.4	967.3	884.6	1968.5	864.8
2014	1170.8	1211.9	1263.1	1364.4	1678.2
2015	1046.2	1432.7	1115.7	1227.1	1162.0
2016	1162.0	1683.5	1258.2	1544.0	1586.3
2017	781.0	1145.3	649.0	902.5	1121.8
2018	1114.8	1587.2	1445.4	1496.5	1485.4
2019	1106.0	1239.8	2318.1	1154.6	1281.5
2020	1390.2	1582.8	1438.2	1351.3	1660.1
2021	1248.2	1296.4	1442.0	1444.1	1412.1
Average Annual Rainfall	1254.5	1376.1	1235.6	1325.8	1637.0

4.5 Flood Frequency Analysis

This analysis of using different method such as Gumbel's distribution, Log Pearson III Distribution method was employed to predict the streamflow in different years including 5,10,20, 50,100,200 and 500 years return period to be sure on the method which is appropriate in this study area.

4.5.1 Gumbel's distribution method

Table 4.6: Flood frequency distribution of simulated peak flow(m^3/s) using Gumbel distribution method

N^0	Years	Predicted Q (m^3/s)
1	5	105.3
2	10	128.6
3	20	150.9
4	50	179.8
5	100	201.5
6	200	223.1
7	500	251.6

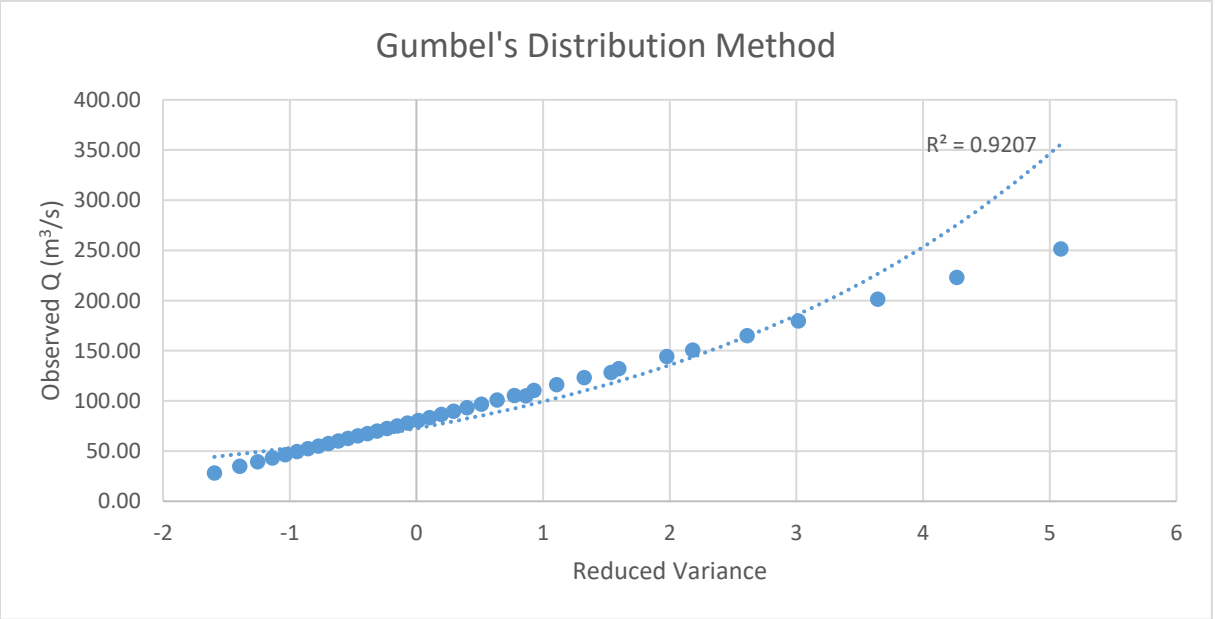

Figure 4.12: Gumbel distribution graph of Maximum annual flows (m3/s) between 1991 to 2021 at Nyundo river gauge station

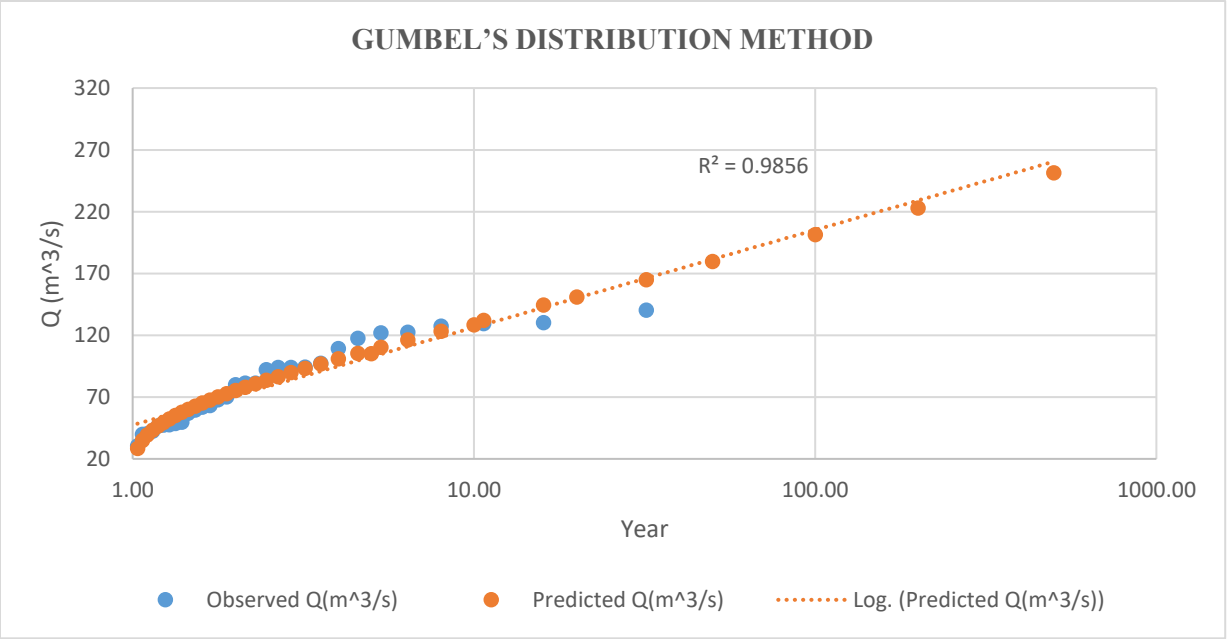

Figure 4.13: Gumbel distribution graph of Maximum annual flows (m3/s) and simulated discharge at Nyundo river gauge station

4.5.2 Log Pearson III method distribution

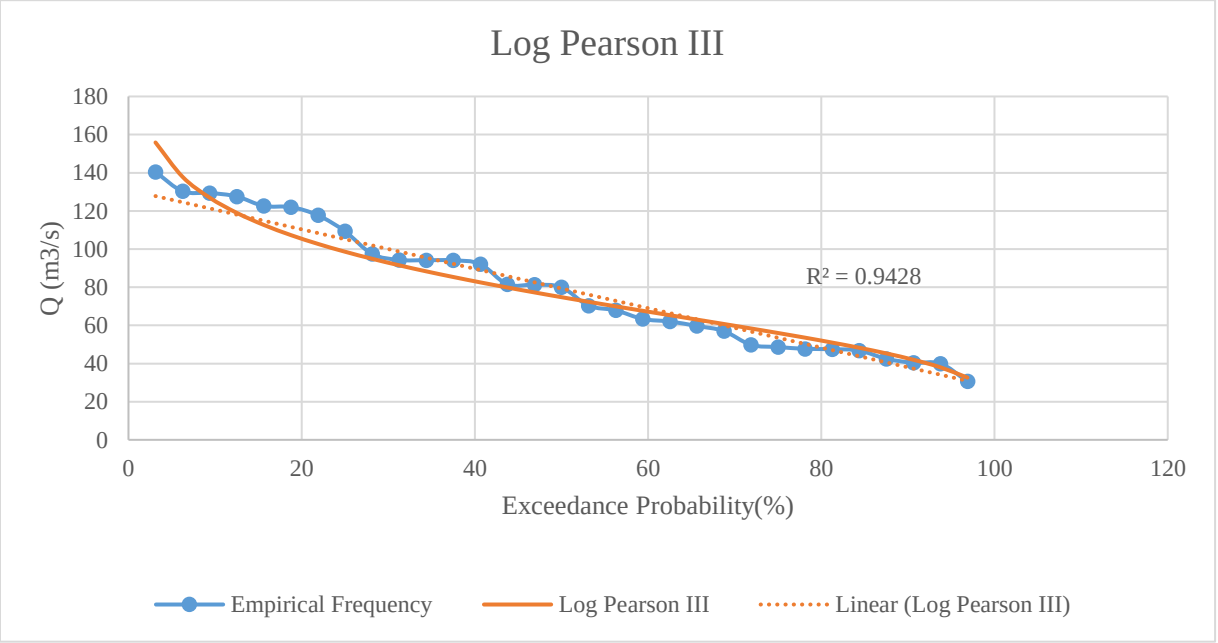

Figure 4.14: Log Pearson III method distribution of Maximum annual flows (m3/s) between 1991 to 2021 at Nyundo river gauge station

Table 4.7: Flood frequency distribution of simulated peak flow(m3/s) and the return periods using Log Pearson III method distribution

N^0	Return Period	Predicted Q(m^3/s)
1	5	103.7
2	10	122.7
3	20	141.0
4	50	164.6
5	100	182.3
6	200	199.9
7	500	223.2

4.5.3 Log Normal distribution method

Table 4.8: Flood frequency distribution of simulated peak flow(m3/s) and the return periods using Log Normal method distribution

N^0	Return Period	Predicted Q(m^3/s)
1	5	102.2
2	10	126.3
3	20	150.5
4	50	183.3
5	100	209.0
6	200	235.7
7	500	375.3

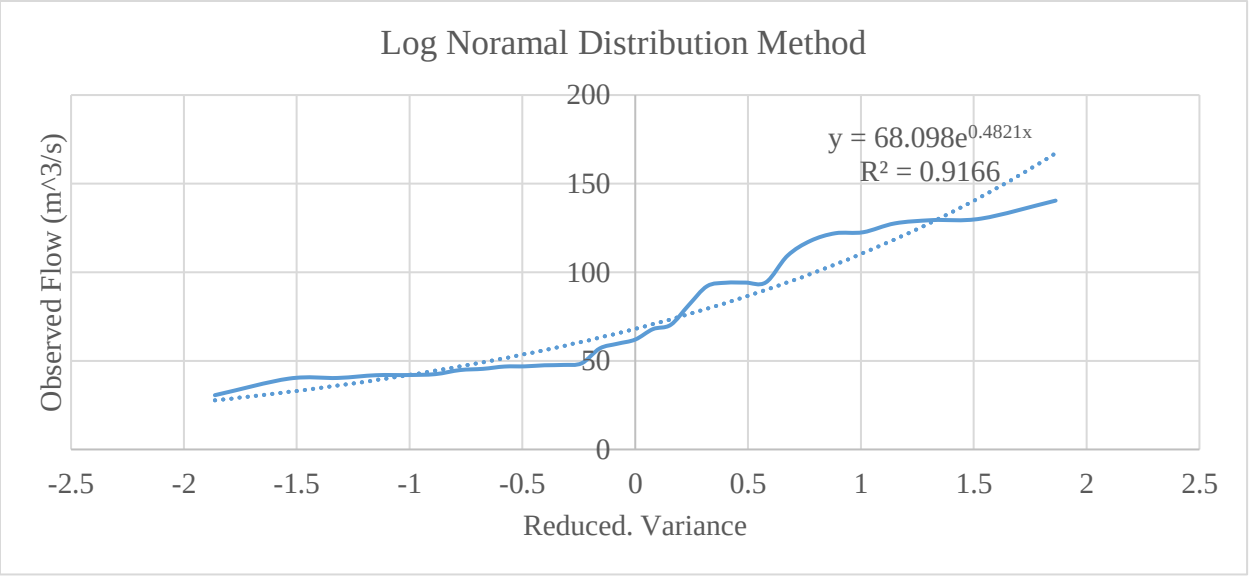

Figure 4.15: Log Normal Distribution graph of Maximum annual flows (m3/s) between 1991 and 2021 at Nyundo station

4.6 Goodness of Fit

This test is employed to determine whether a specific distribution is appropriate for a particular dataset. The quality of fit for the observed dataset is assessed by calculating statistical parameters. The affinity of samples to the anticipated theoretical probability distribution is evaluated. To assess the null hypothesis, it is tested and rejected if the observed statistic exceeds the critical value for the predetermined significance threshold. The Chi-squared, Anderson–Darling (AD), and Kolmogorov–Smirnov (KS) tests are utilized at a significance level of 0.05 (Samantaray & Sahoo, 2020).

The Null hypothesis; Ho: Equal frequencies

Alternative hypothesis; Hi: Unequal frequencies

4.6.1 Gumbel Chi Square Test

Table 4.9: Gumbel Chi square test

Class Interval	Observed Freq. (O_f)	Expected Freq (E_f)	$X^2 = (O_f-E_f)^2/E_f$
0-45.5	8	6.2	0.52
46.5-61.5	7	6.2	0.10
62.0-93.5	5	6.2	0.23
94.0-123.5	7	6.2	0.10
>124	4	6.2	0.78
Total	31		1.74
		Degree of Freedom	4
		C_v	9.48 (H_0 Accepted))

4.6.2 Log Pearson Chi Square Test

Table 4.10: Log Pearson Chi Square Test

Class Interval	Observed Freq. (O_f)	Expected Freq (E_f)	$X^2 = (O_f-E_f)^2/E_f$
0-47.5	11	6.2	3.7
47.5-65	5	6.2	0.2
66-96.6	7	6.2	0.1
97-128.5	5	6.2	0.2
>128	3	6.2	1.7
Total	31		5.9
		Degree of Freedom	4
			9.48
		C_v	(H_0 Accepted)

4.6.3 Log Normal Chi Square Test

Table 4.11: Log Normal Chi Square Test

Class Interval	**Observed Freq. (O_f)**	**Expected Freq (E_f)**	**$X^2 = (O_f-E_f)^2/E_f$**
0-50.7	13	7.8	3.6
51.5-100.5	10	7.8	0.7
106.2-130.5	7	7.8	0.1
>131.5	1	7.8	5.9
Total	31	7.8	10.2
		Degree of Freedom	3
		C_v	7.81 (Rejected)

According to the statistical analysis performed using different method such as Gumbel distribution, Log Pearson Type III distribution and Log Normal distribution, it was observed that the null hypothesis, suggesting equal frequency of flood events, was rejected for one distribution and the rest two were acceptable. This rejection of Log normal distribution method was demonstrated by the Goodness of Fit test, with Chi-square values beyond the crucial threshold at a 5% significance level. The Gumbel and Log Pearson type III distribution demonstrated the better fit where the Chi-square value of 1.74 and 7.9 respectively which is less than the critical threshold of 5%. It was shown that Log normal distribution tended to overestimated flood events over return periods of 50, 100, 200, and 500 years compare to the other distributions. The values of predicted discharge estimated using Gumbel and Log Pearson III distributions exhibited consistency for return periods. These findings suggested that Gumbel

and Log Pearson III distributions can be used to predict the streamflow for certain return periods.

4.7 Land use and Land cover Analysis

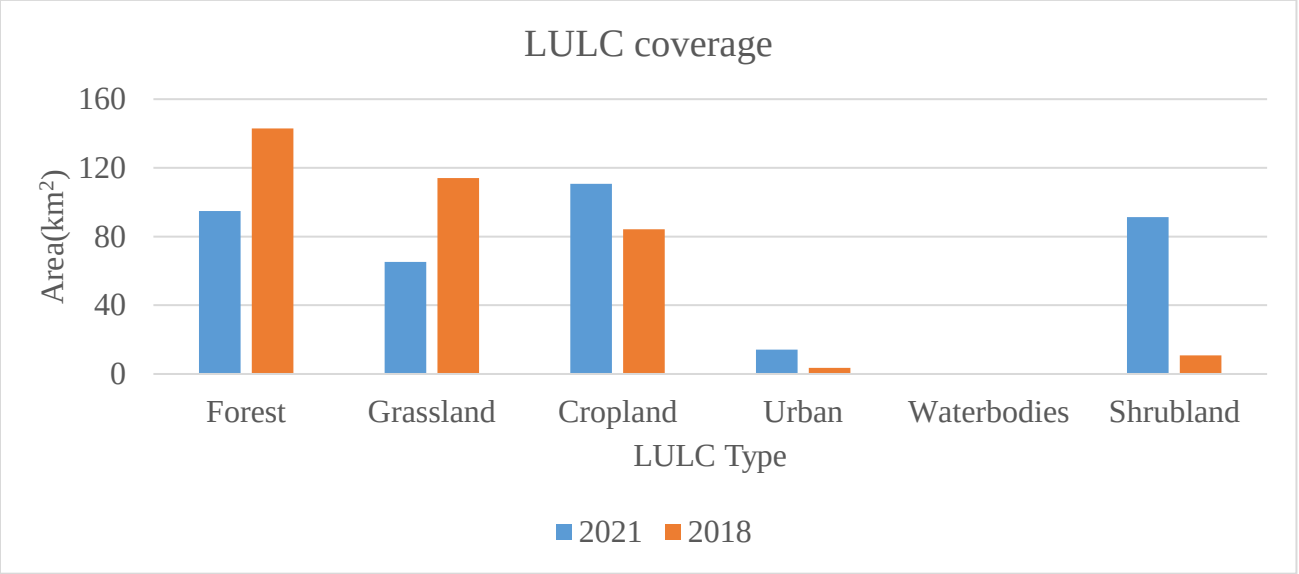

Figure 4.16: Total area of LULC Coverage in Sebeya catchment

Table 4.12: Land use Land cover classes in the Sebeya catchment and changes in area(%)

	2021		2018	
Land use class	Area (Km^2)	Area in (%)	Area (Km^2)	Area in (%)
Forest	94.90	25.96	143.04	39.04
Grassland	65.25	17.85	114.15	31.15
Cropland	110.63	30.26	84.19	22.97
Urban	14.21	3.88	3.53	0.97
Waterbodies	0.01	0.00	0.05	0.01
Shrubland	91.30	24.97	10.81	2.95

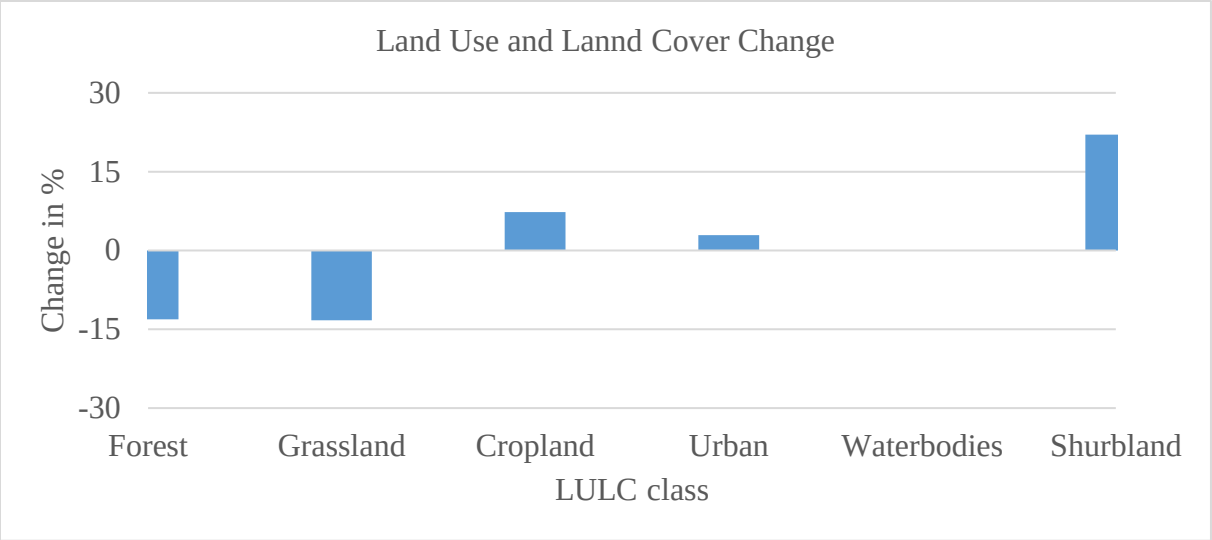

Figure 4.17: Land use and Land cover change in 2021 and 2018

The Sebeya catchment is highly dominated by cropland, forest and grasslands. The LULC from 2018 and 2021 had significant change as seen in figure 4.12. It has shown that the population growth increased in downstream in Rubavu district due to the increase of urban areas. The part of the forest has been converted into cropland and shrubland due to human activities. From the analysis of the supervised classification done on Land use land cover images, Cropland areas covered 110.63km^2(30.26%) in 2021 and 84.19 km^2(22.97%) in 2018. The forest has decreased from 143.04km^2(39.04%) in 2018 to 94.90km^2(25.96%) in 2021. This implies the increase of urban areas from 3.53km^2 to 14.21km^2. This changes lead to the increase of paved surfaces in the watershed may prevent water from infiltrating into the soil, which could accelerate the runoff.

4.8 Description Of Interviewees

The questionnaires collected responses from one person in the family aged 18 or older who was located in Kanama, Nyundo and Rugerero sector in Rubavu District. This area is known as flood prone areas within Sebeya catchment. The findings have shown that 49.2 % of respondents were female and 50.8% were male. The respondents ranged in age from 18 years old.

4.9 Flood Experience

About 96.7% of respondents confirmed that they experienced a flood in their area. The main causes of flooding in this catchment are rainfall counted 96.7%, topography with 88.3%,

urbanization and human activities with 16.7%,25.8% it was confirmed also that year 2023 experienced more significant flood with 93.3% which impacted Agriculture, Buildings, loss of life, Commercial Area ,Livestock and Infrastructures. The results are summarized in the figures below:

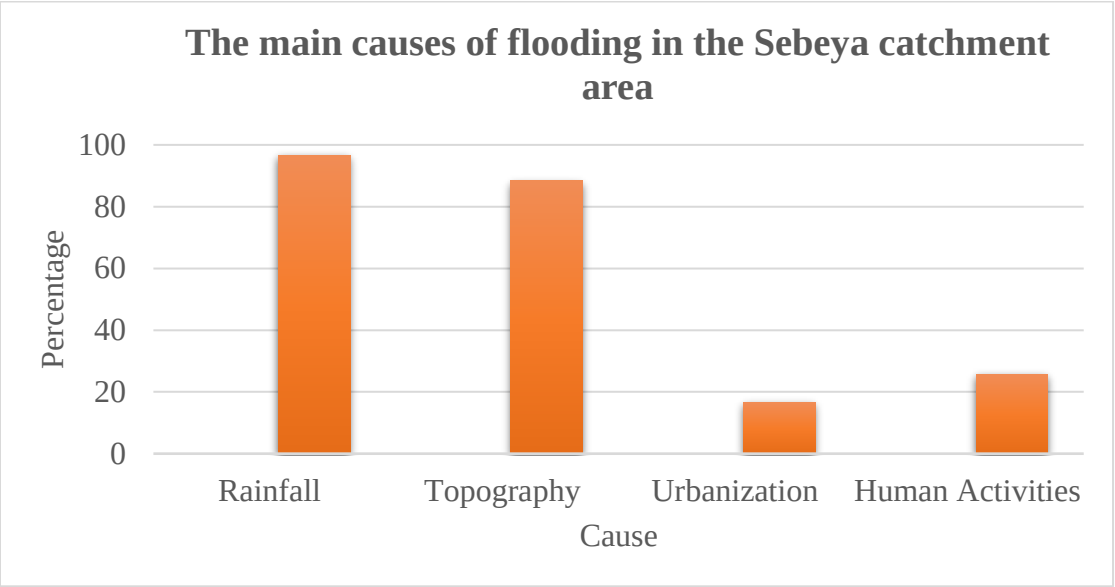

Figure 4.18: The main causes of flooding in the Sebeya catchment area

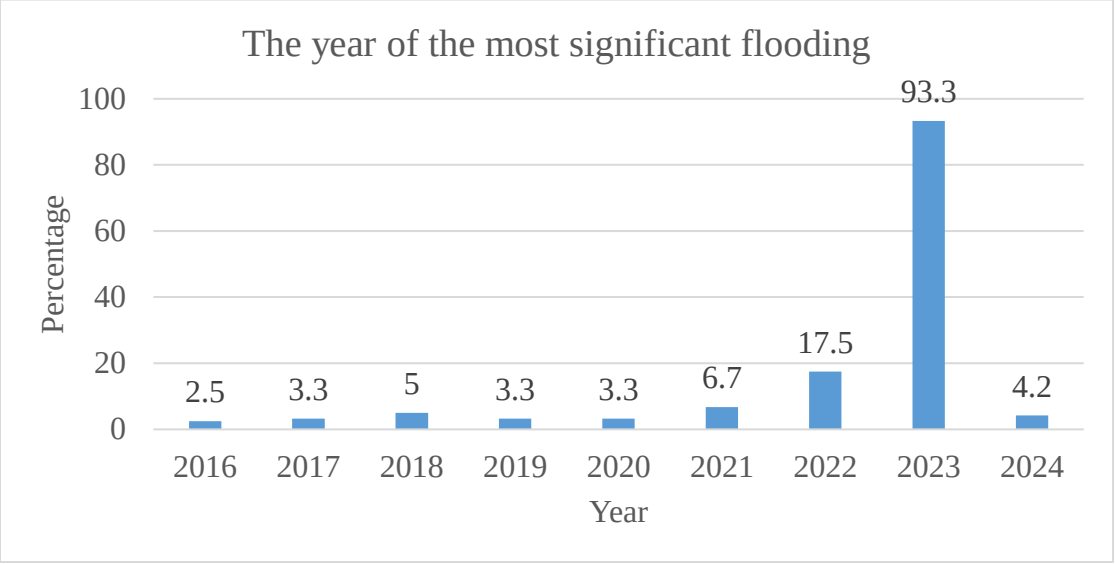

Figure 4.19: The year of the most significant flooding

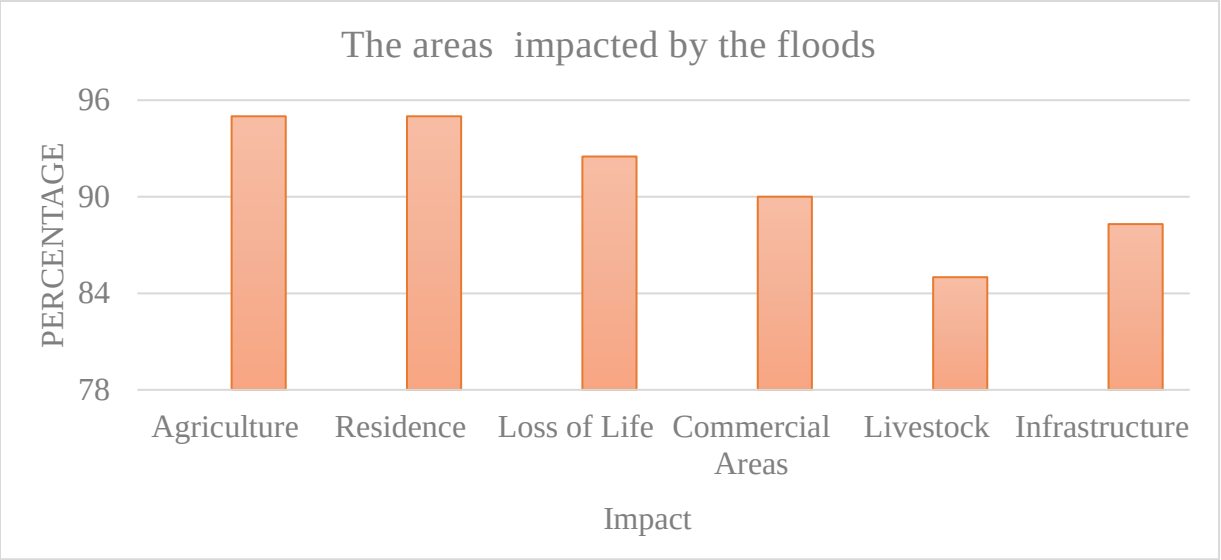

Figure 4.20: The activities impacted by the floods

4.10 Flood Impact and Vulnerability

Most of people live in the district where the questionnaires were collected are in 100 to 500 meters from the river .This accounted 40% 0f the respondents, 22.5% are in 500 to 1000m, 20% are located above 1000m and the rest 17.5% are in less than 100m from the river. The maximum water level of flood reached in their area was ranging between 0 to more than 5 meters. Most of the respondents confirmed that it was less than 1 meter with 55.8%, 29.2% replied that they observed between 1 to 2 meters of flood water. This affected different properties such houses, farmland, infrastructures(e.g., roads, bridges) and commercial buildings. This require the cost for repairs or replacement where the respondents showed that most of the people spent more than 1,000,000 Rwf francs which is 61.7% of the response to overcome these impacts. The results are summarized in the figures below:

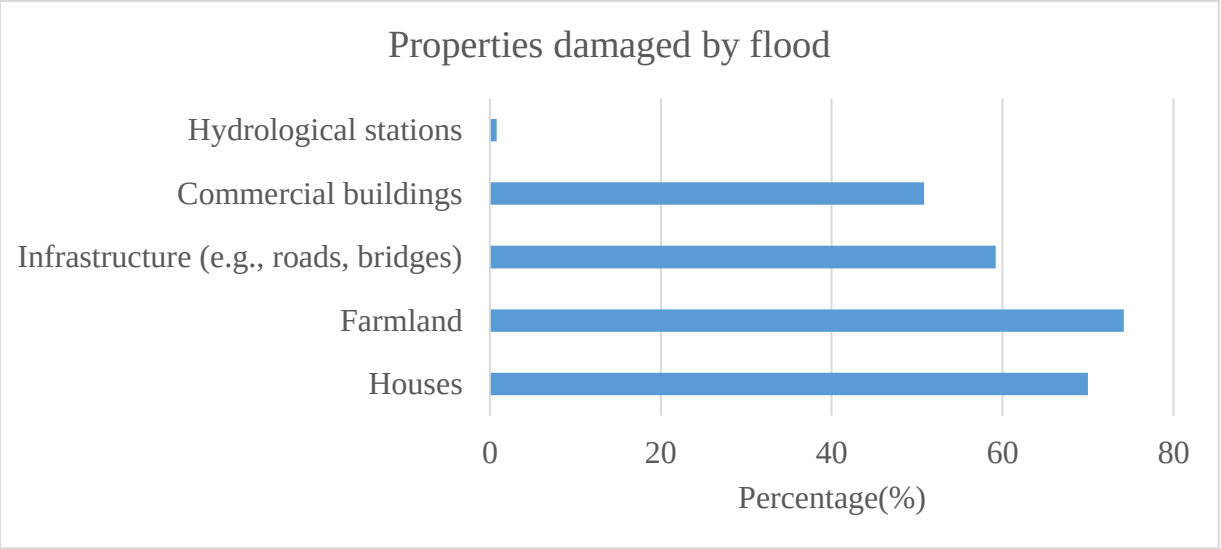

Figure 4.21: Properties damaged by flood

4.11 Flood Information and Preparedness

About 91.7% of the respondents received flood warning notice. There are many communication techniques used in Rwanda such as Radio, Television, phone call, text message, microphone and via email. The most of respondents received notification through Radio and Television where it accounted 84.2% and 40% respectively. It has shown that 90% of the respondents have taken the measures to prevent flood damage to the properties and 10% did not take any prevention measures. The measures which have been taken includes sand bags, drainage channel, relocation, terracing, gabions, ponds and strengthening the house foundation and house roof. The most adaptable measures were found to be drainage channel with 78% of the respondents and sand bags with 34.2%. In order to mitigate flood in this area, the government made the interventions where they provided different type of assistance such as financial aid, relocation and trainings. About 38.3% of the respondents confirmed that they received the financial aids, 29.2% are relocated and 20% participated in the training. Beside these, 28.3% of the responses did not receive any assistance. The figures below are the summary of the responses:

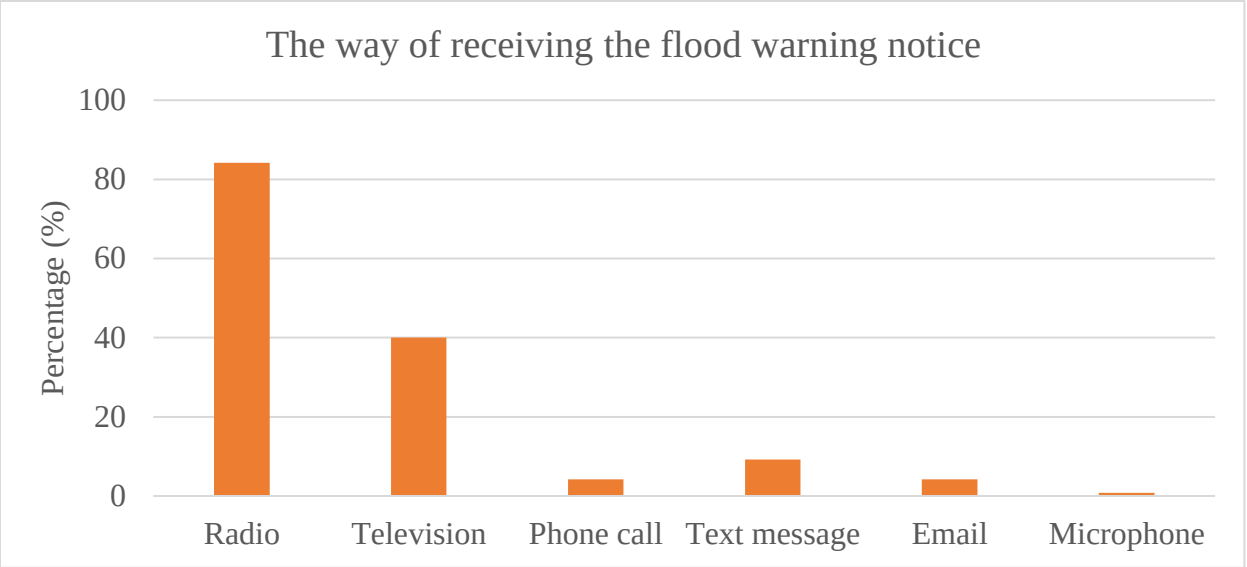

Figure 4.22: The way of receiving the flood warning notice

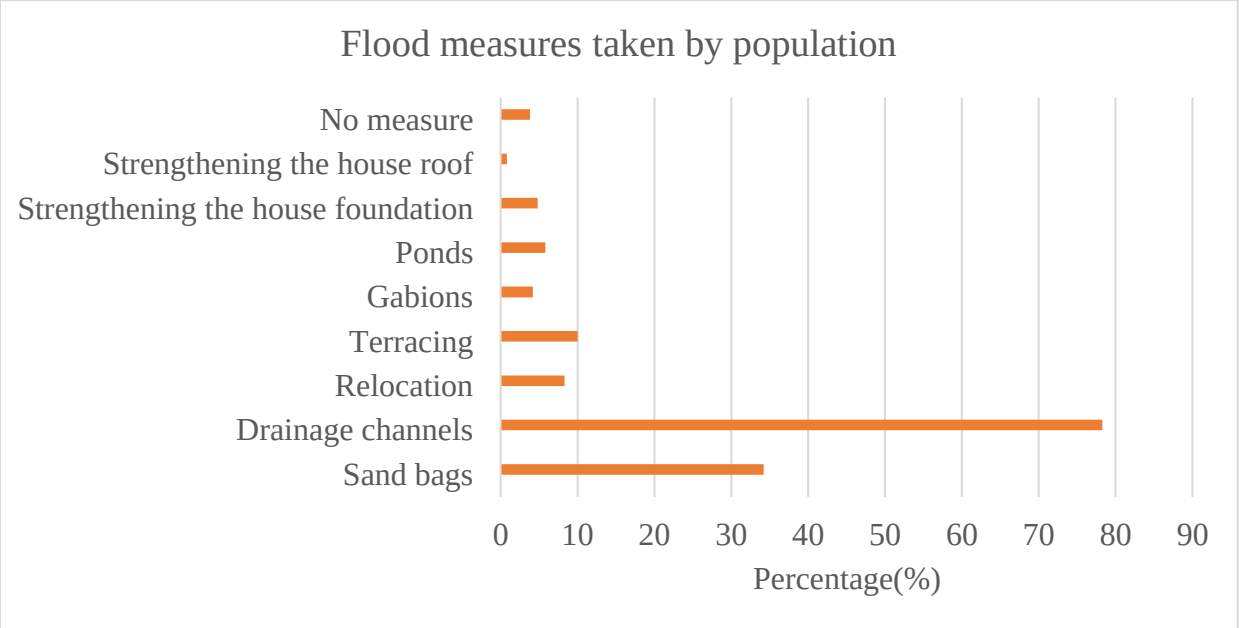

Figure 4.23: Flood measures taken by population

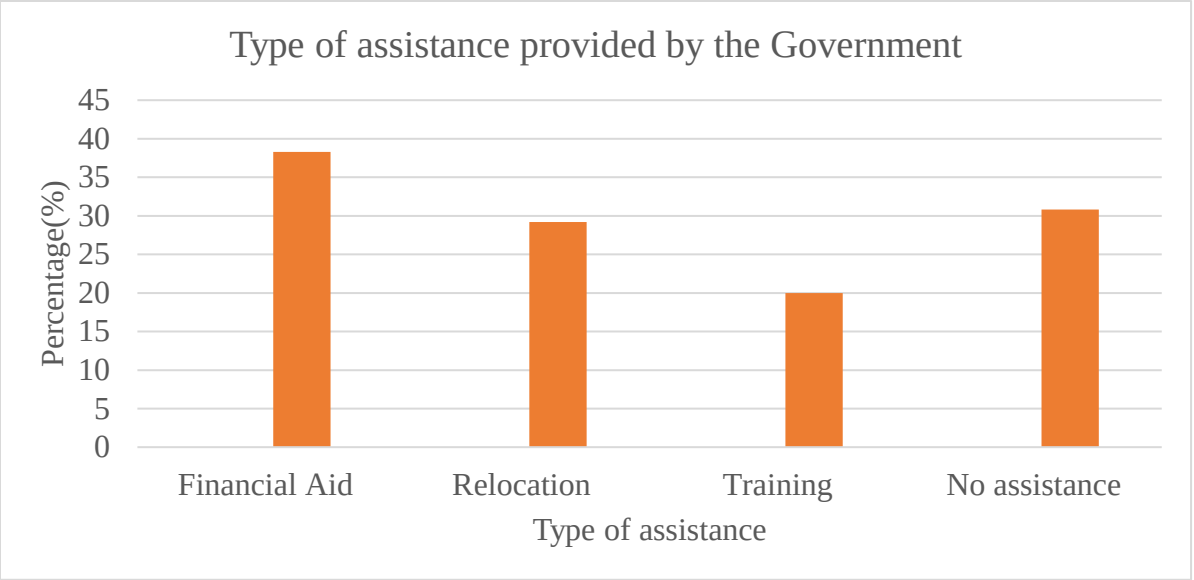

Figure 4.24: Type of assistance provided by the Government

4.12 Flood Mitigation Measures in the Area

Within Sebeya catchment, the responses showed that there are measures implemented by the Government to mitigate flood such as Reservoirs, Dam, Gabions, Ponds, retaining walls, Dykes, Planting trees, Relocation, Terracing, Widening the rivers and Sand bags. The most popular measures implemented are retaining walls with 80%, followed by gabions, sandbags, relocation and dam with 79.2%,78.3%, 75% and 70.8% respectively. In addition, the implemented measures need additional infrastructures such as retaining walls, gabions and relocation which accounted 84.2%, 79.2% and 76.7% respectively to overcome the flood event in this area. Here there are summarized figures from respondents:

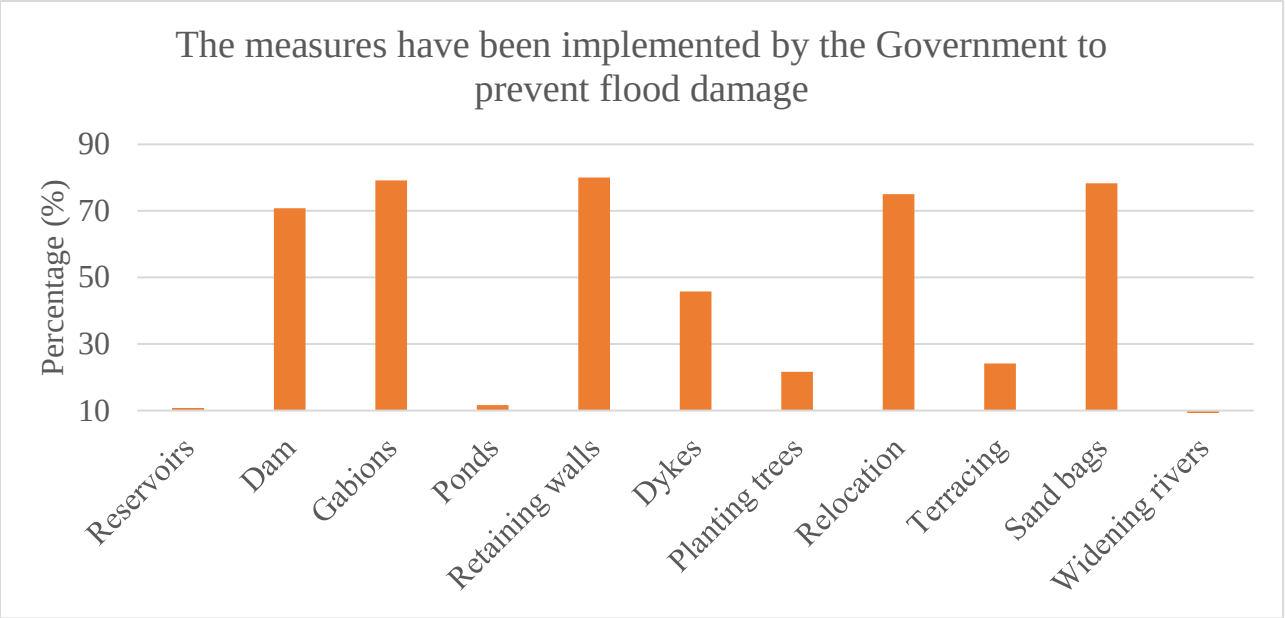

Figure 4.25: The measures have been implemented by the Government to prevent flood damage

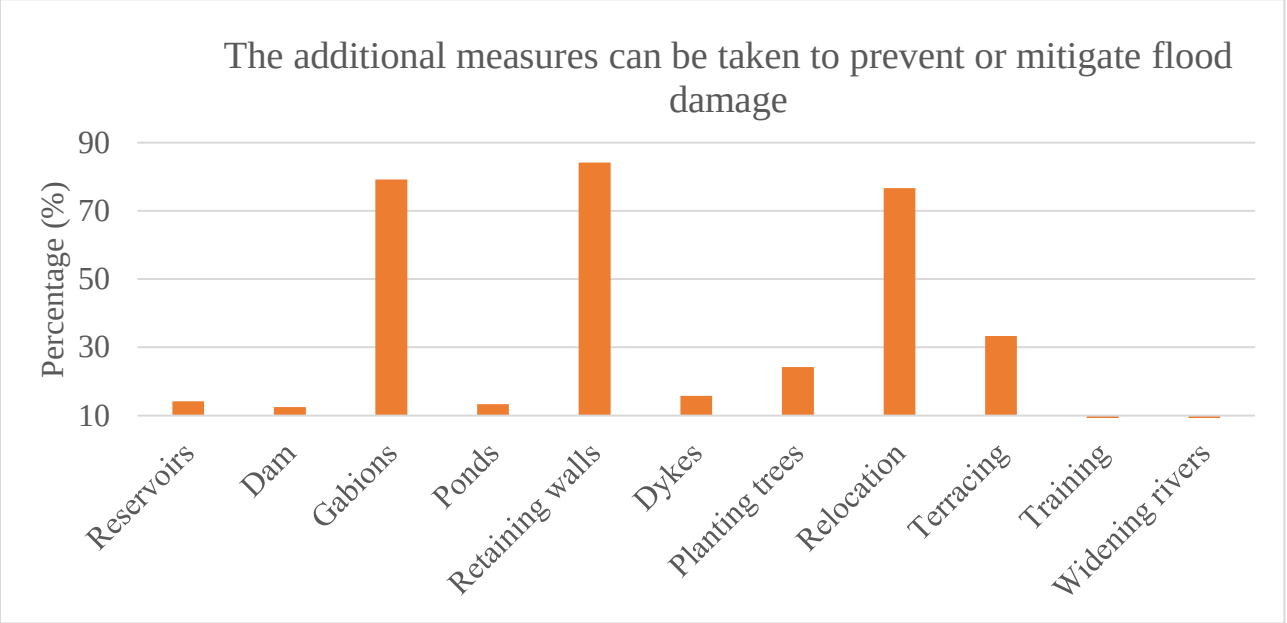

Figure 4.26: The additional measures can be taken to prevent or mitigate flood damage

4.13 Evacuation and Response

During most recent flood events, 64.2% evacuated their home to different places such as schools, churches, friend's home, government shelters and other government aids. About 34.2% of them evacuated to the government shelter and rest 30% were in different location. 85.8% were satisfied to these responses to flood. The areas which found to be very vulnerable to flooding is Mahoko, Nyundo, Pfunda , Kanama, Rugerero, Nyakiriba and Karambo. Here there is figure demonstrate the level of vulnerability according to the responses.

Table 4.13: Level of satisfaction about the response to floods

Level of satisfaction	**Frequency**	**Percentage(%)**
Very Satisfied	12	10
Satisfied	103	85.8
Not Satisfied	4	3.3
Dissatisfied	1	0.8
Total	120	100%

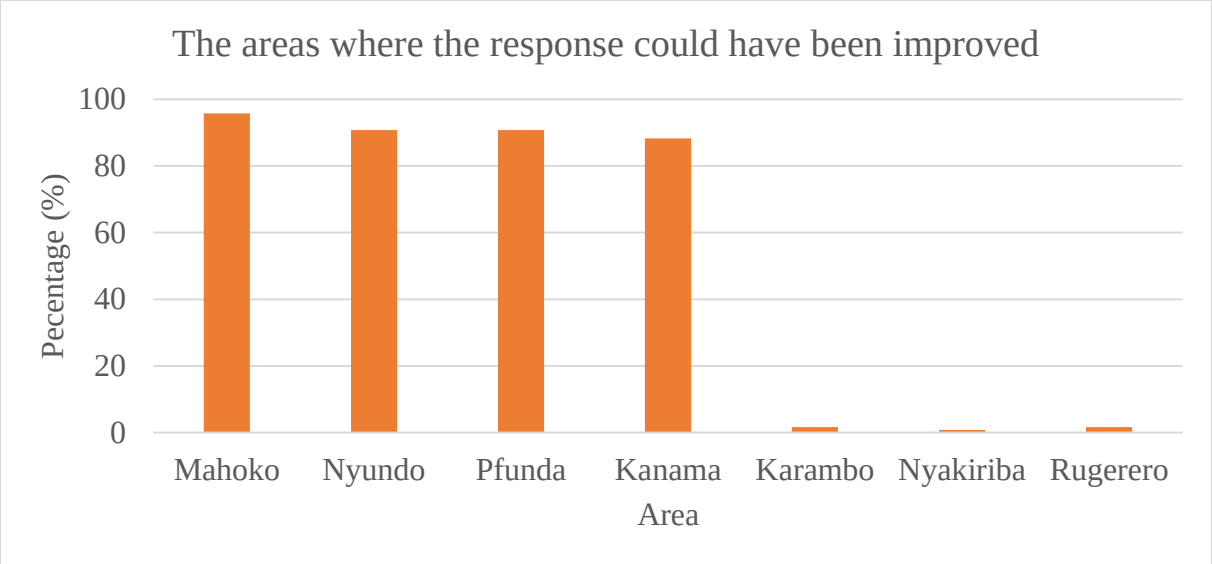

Figure 4.27: The areas where the response could have been improved

4.14 Future Preparedness and Concerns

57.5% of the respondents replied that they are still concerned with flood event and 26.7% are not concerned due to the government relocation. Only 15.8% of the respondents are very concerned to the flood events. About 85% of the respondents feel that they are prepared to the future flood events. They are confident with 79.2%that government have ability to responses of the future floods and the respondents were comfortable with sharing their personal information for the purpose of data collection related to floods events.

4.15 Flood Mapping

Using ArcGIS, the water depth, water surface extent and water velocity were visualized and ranked from low to high-risk zone. According to the output, the maximum water depth and velocity were obtained to the downstream side located in Mahoko cell toward Pfunda and Nyundo region. The inundation mapping done with the model showed that land use and land cover, topography and rainfall are influencing the increase of inundated area. By considering the flood , it is observed that the sectors such as Kanama, Nyundo and Rugerero especially in Mahoko cell, Terimbere and Rugerero cell are mostly affected by flood as shown in figure. The figures below show the flood mapping done in ArcGIS:

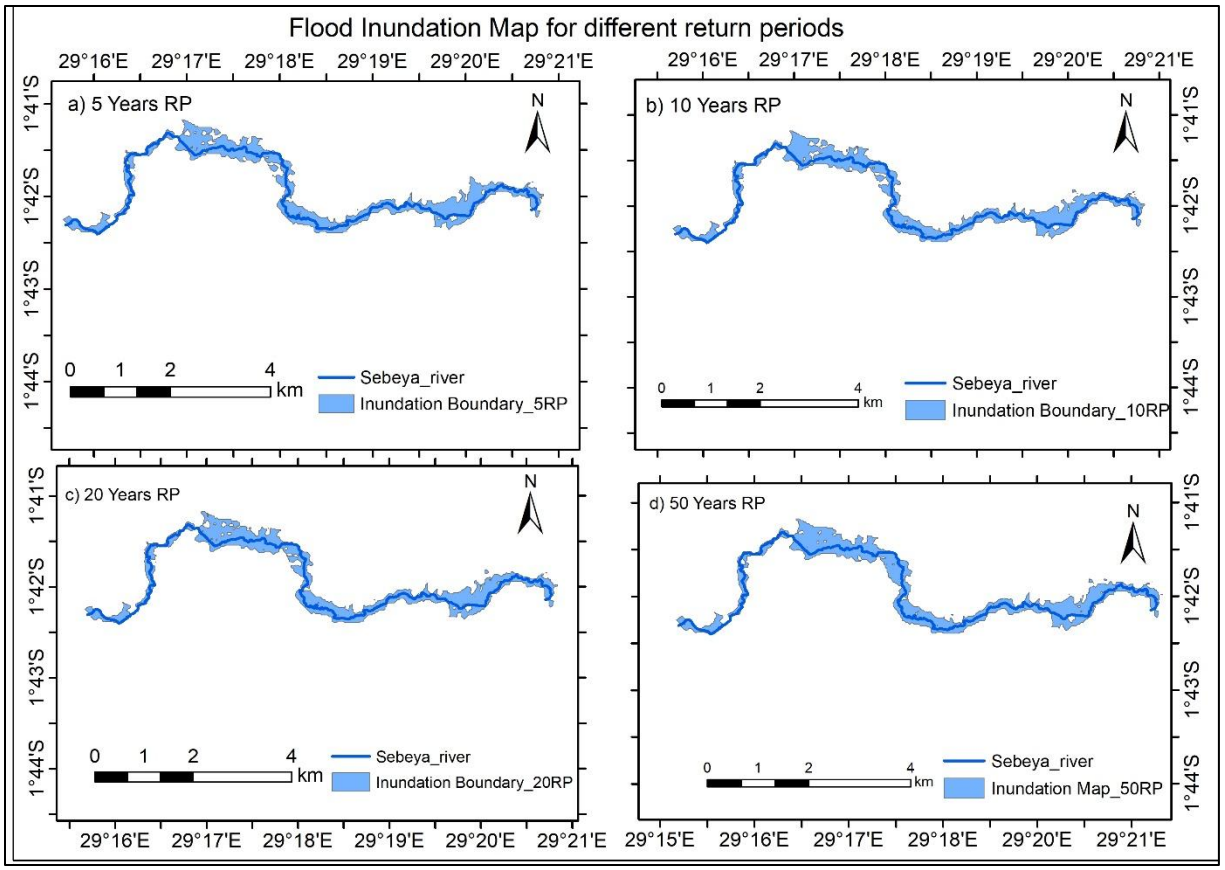

Figure 4.28: Flood inundation maps for different return period

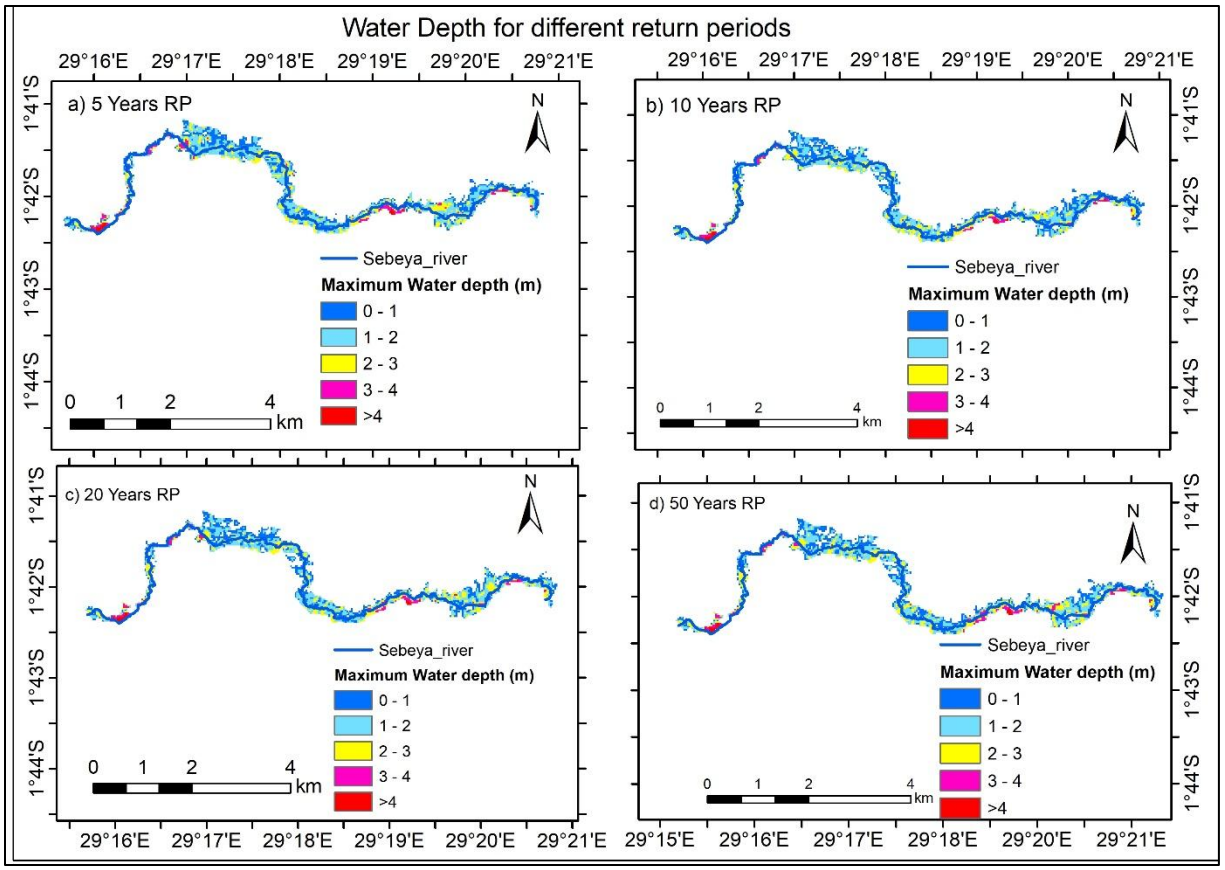

Figure 4.29: Water depth for different return periods

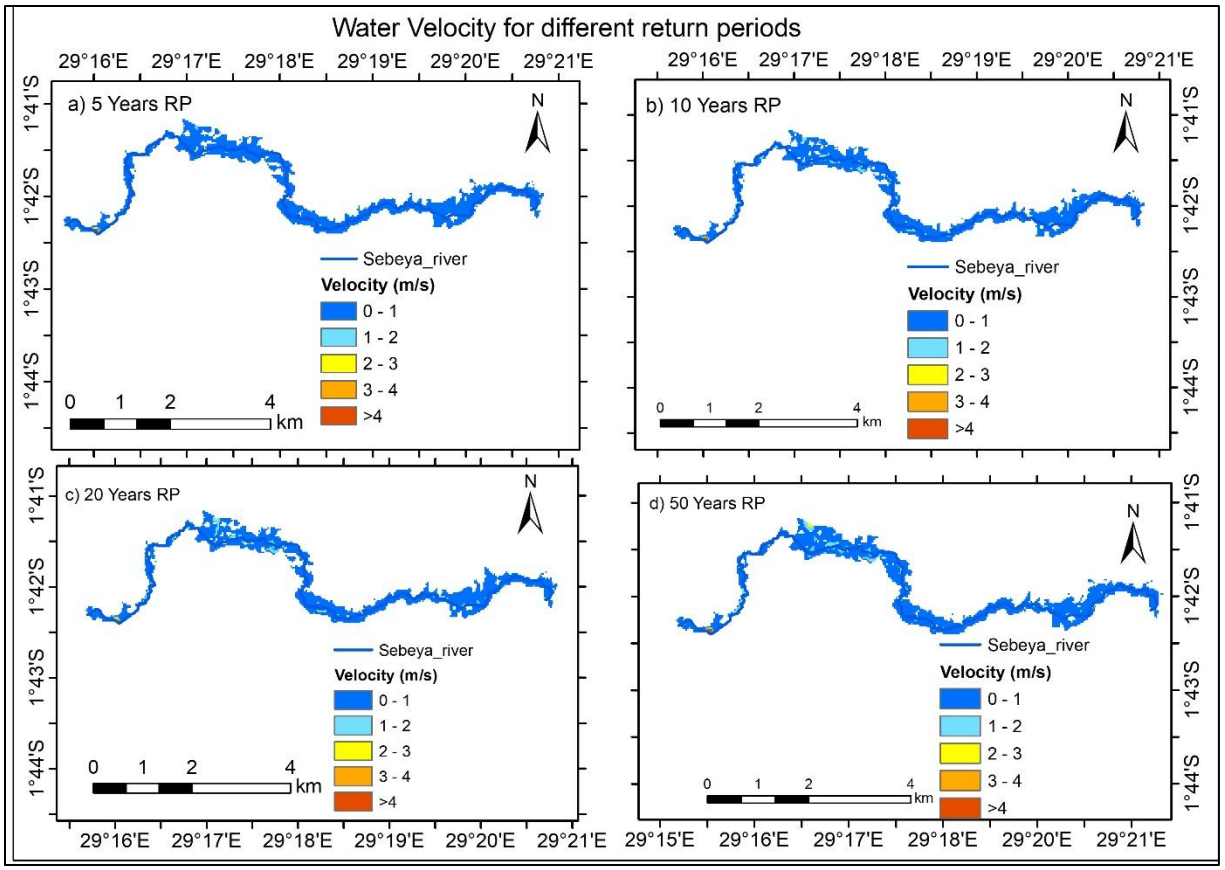

Figure 4.30: Water velocity for different return periods

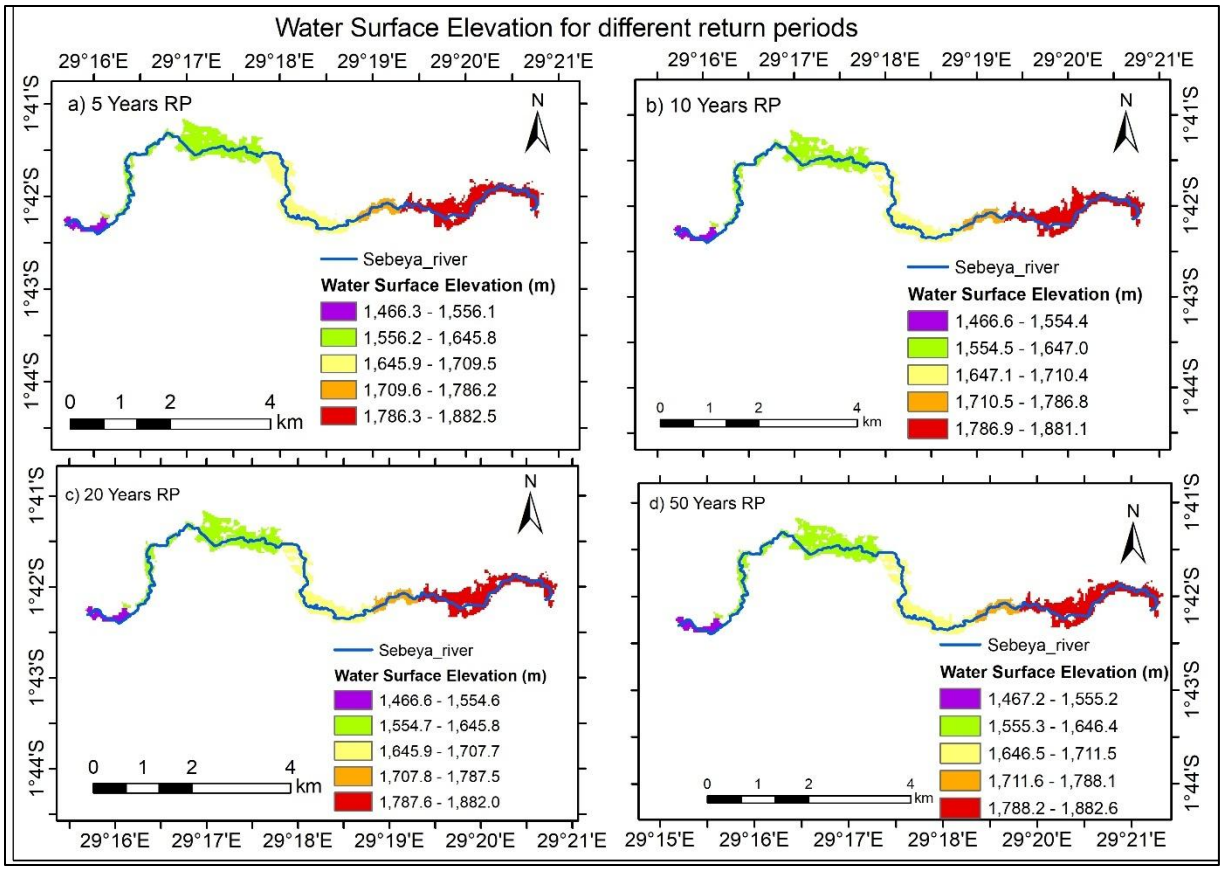

Figure 4.31: Water surface elevation for different return periods

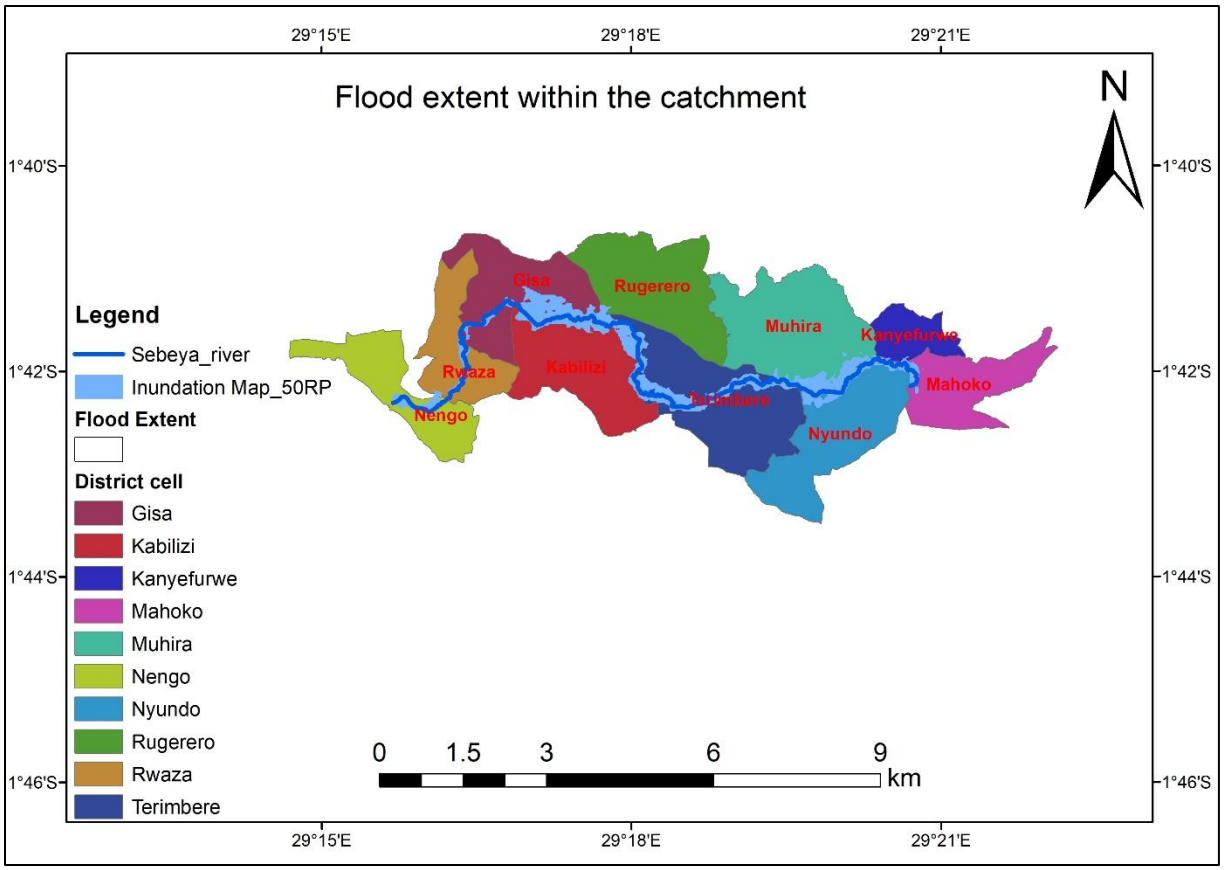

Figure 4.32: Flood extent in the surrounding area

4.16 Floodplain Inundation Area Analysis

The Floodplain inundation maps computed for each return period were presented in figure 4.28 and the corresponding flood inundation areas in hectares (ha) are summarized in the table below:

Table 4.14: Inundated area within Sebeya catchment

Return period	Inundated area (ha)
5	280.82
10	284.75
20	286.82
50	290.16

According to the flood inundation maps, the inundated area possibly expands with an increase in the return period and discharge. The flood inundation area for a 10-year return period has increased by 1.4%(3.9ha) compared to the 5-year return period inundation area. The flood inundation area for a 20-year and 50- year return period has increased by 2.1% (6 hectares) and 3.3 % (9.3ha) respectively compare to 5-year return period.

CONCLUSION AND RECOMMENDATIONS

5.1 Conclusion

5.1.1 Hydrological Model in the Sebeya catchment

To create a detailed hydrological model of the Sebeya Catchment using HEC-HMS, incorporating local hydrological, meteorological, and geographical data for accurate simulation of watershed processes.

The HEC-HMS model was successfully utilized to simulate rainfall-runoff processes within the Sebeya Catchment, using daily rainfall data from multiple gauging stations and daily streamflow records for both model calibration and validation. Initially, there was a significant discrepancy between simulated and observed peak discharges, indicating the need for parameter optimization.

To address this, a sensitivity analysis was performed to identify key model parameters influencing runoff generation. The results revealed that crop coefficient and lag time were among the most sensitive parameters. Following calibration, the model demonstrated a strong agreement between observed and simulated hydrographs.

Model performance metrics were within acceptable ranges, with a Nash-Sutcliffe Efficiency (NSE) of 0.666, RMSE of 0.6, PBIAS of -16.95%, and R^2 of 0.74. According to Yuemei et al. (2008), model simulations can be considered satisfactory when NSE > 0.50, RSR < 0.70, and PBIAS falls within ±25% for streamflow—criteria met in this study.

These findings confirm the suitability of the HEC-HMS model for simulating runoff in the Sebeya Catchment. The calibrated model provides a reliable tool for watershed management planning, enabling informed decision-making for flood mitigation and water resource management in the region.

5.1.2 Community's perception of flood risk in the Sebeya Catchment

To evaluate the community's perception of flood risk in the Sebeya Catchment by integrating local knowledge and experiences with hydrological modeling results, hazard assessments, and analyses of exposure and vulnerability.

Flood risk perception within the Sebeya Catchment was assessed through field-based questionnaires administered in key flood-prone sectors—Kanama, Nyundo, and Rugerero. The findings revealed that flooding has become an annual occurrence, with the most frequently cited causes being intense rainfall, topographical characteristics, rapid urbanization, and unsustainable human activities such as poor land use practices and encroachment on floodplains.

Respondents reported severe and recurring impacts, including loss of life, damage to residential and commercial buildings, agricultural destruction, loss of livestock, and disruption of critical infrastructure. A key observation was that the majority of affected residents live within 100 to 500 meters of the river, placing them in high-exposure zones. This proximity is largely driven by limited financial resources, preventing relocation to safer areas.

By integrating these community insights with hydrological modeling and flood hazard assessments, this objective highlighted the vulnerability and adaptive limitations of local populations. The results underscore the importance of incorporating local knowledge into flood risk management strategies and the urgent need for inclusive, community-driven interventions to reduce flood risk and enhance resilience in the Sebeya Catchment.

5.1.3 Identification and map flood-prone areas based on the assessment

Flood-prone areas within the Sebeya Catchment were successfully identified and mapped using the HEC-RAS hydraulic model in combination with ArcGIS. The HEC-RAS model simulated flood dynamics by generating outputs such as flood extent boundaries, maximum water depth, water surface elevation, and maximum flow velocity. These outputs were spatially visualized in ArcGIS to delineate areas at risk of inundation under varying flood return periods.

The analysis revealed a clear correlation between increasing return periods and expanded flood extent. Compared to the inundation area for a 5-year return period, the flood extent increased by 1.4%, 2.1%, and 3.3% for the 10-year, 20-year, and 50-year return periods, respectively—highlighting the escalating risk posed by higher-magnitude flood events.

Several locations were identified as highly vulnerable to flooding, notably Mahoko, Nyundo, Pfunda, Kanama, Rugerero, Nyakiriba, and Karambo. These areas consistently exhibited high

levels of inundation, underscoring the need for targeted flood risk mitigation and land use planning interventions.

This spatial flood risk mapping provides critical information for decision-makers, enabling proactive measures in urban planning, emergency preparedness, and infrastructure design to reduce vulnerability and enhance resilience across the Sebeya Catchment.

5.2 Recommendations

According to the study's findings, it is essential for decision-makers, practitioners, local community and all stakeholders engaged in future initiatives to consider the following recommendations:

- The major challenge encountered in this study was the quality and availability of the streamflow data to calibrate and validate the model. Only three of 8 hydrological stations had the data record and only one station had the record without many missing values. This led to the poor representation of spatial variability and the model performance was assessed at gauge station. The study recommended the continuous recording for all hydrological station to facilitate the researchers.
- There is need for strengthening Rwanda Water Resources Board (RWB) the institutions in charge of water resources management for good management of flood risk. This also requires the reinforcement of Government and stakeholders for actors such as population, Boards and local government.
- The further studies are recommended to assess the influence of land use on surface runoff since there places within catchment which is dominated by land use and land cover type.
- HEC-RAS model was performed without any calibration of Manning's "n". It would be beneficial to examine the model's sensitivity to the parameter in future research.
- Reinforcing the flood mitigation measures as mentioned during the interview such as retaining walls, Gabions, relocation and constructing reservoirs and dykes in the upstream, widening the rivers and implementing buffer zoning around rivers.
- Increasing of financial support to the people live in flood prone areas to facilitate them in flood management practices such erosion control and rainwater harvesting facilities.

REFERENCES

Aditya, F., Gusmayanti, E., & Sudrajat, J. (2021). Rainfall trend analysis using Mann-Kendall and Sen's slope estimator test in West Kalimantan. IOP Conference Series: Earth and Environmental Science, 893(1). https://doi.org/10.1088/1755-1315/893/1/012006.

Ahbari, A., Stour, L., Agoumi, A., Serhir, N., & Ouidane, B. El. (2018). Estimation of initial values of the HMS model parameters : application to the basin of Bin El Ouidane (Azilal , Morocco). 9(Figure 1), 305–317.

Al-Mukhtar, M., & Al-Yaseen, F. (2019). Modeling water quality parameters using data-driven models, a case study Abu-Ziriq marsh in south of Iraq. Hydrology, 6(1). https://doi.org/10.3390/hydrology6010021

Alexander, D. (1993). Natural Disasters (1st ed.).

Alexander, D. (2020). Disaster risk reduction. Oxford University Press.

Anusha, N., & Bharathi, B. (2020). Flood detection and flood mapping using multi-temporal synthetic aperture radar and optical data. The Egyptian Journal of Remote Sensing and Space Science, 23(2), 207–219.

Asumadu-Sarkodie, S. (2015). Situational Analysis of Flood and Drought in Rwanda. International Journal of Scientific and Engineering Research, 6(8), 960–970. https://doi.org/10.14299/ijser.2015.08.013

Belay, Y. Y., Gouday, Y. A., & Alemnew, H. N. (2022). Comparison of HEC-HMS hydrologic model for estimation of runoff computation techniques as a design input: case of Middle Awash multi-purpose dam, Ethiopia. In Applied Water Science (Vol. 12, Issue 10). https://doi.org/10.1007/s13201-022-01764-7

Bhuiyan, H. A. K. M., McNairn, H., Powers, J., & Merzouki, A. (2017). Application of HEC-HMS in a cold region watershed and use of RADARSAT-2 soil moisture in initializing the model. Hydrology, 4(1), 1–19. https://doi.org/10.3390/hydrology4010009

Brunner, G. W. (2010). HEC-RAS river analysis system: hydraulic reference manual. US Army Corps of Engineers, Institute for Water Resources, Hydrologic ….

Bunganaen, W., Frans, J. H., Seran, Y. A., Legono, D., & Krisnayanti, D. S. (2021). Rainfall-Runoff Simulation Using HEC-HMS Model in the Benanain Watershed, Timor Island. Journal of the Civil Engineering Forum, 7(3), 359. https://doi.org/10.22146/jcef.64782

Chaudhary, M. T., & Piracha, A. (2021). Natural Disasters—Origins, Impacts, Management. Encyclopedia, 1(4), 1101–1131. https://doi.org/10.3390/encyclopedia1040084

Dasallas, L., Kim, Y., & An, H. (2019). Lea Dasallas.pdf. 1–14.

Davies, R. (2023, May 4). Rwanda – Death Toll Rises as Flooding Continues. AFRICA. https://floodlist.com/africa/rwanda-floods-may-2023-update

Dewan, T. H. (2015). Societal impacts and vulnerability to floods in Bangladesh and Nepal. Weather and Climate Extremes, 7, 36–42. https://doi.org/10.1016/j.wace.2014.11.001

Doocy, S., Daniels, A., Murray, S., & Kirsch, T. D. (2013). The Human Impact of Floods: a Historical Review of Events 1980-2009 and Systematic Literature Review. PLoS Currents, APR 2013. https://doi.org/10.1371/currents.dis.f4deb457904936b07c09daa98ee8171a

Du, W., Fitzgerald, G. J., Clark, M., & Hou, X. Y. (2010). Health impacts of floods. Prehospital and Disaster Medicine, 25(3), 265–272. https://doi.org/10.1017/S1049023X00008141

Gaál, L., Szolgay, J., Kohnová, S., Parajka, J., Merz, R., Viglione, A., & Blöschl, G. (2012). Flood timescales: Understanding the interplay of climate and catchment processes through comparative hydrology. Water Resources Research, 48(4), 1–21. https://doi.org/10.1029/2011WR011509

Gebre, S. L. (2015). Application of the HEC-HMS Model for Runoff Simulation of Upper Blue Nile River Basin. Journal of Waste Water Treatment & Analysis, 06(02). https://doi.org/10.4172/2157-7587.1000199

Guarín, G. P., Westen, C. J. van, & Montoya, L. (2015). Community-Based Flood Risk Assessment using GIS for the Town of San Community-Based Flood Risk Assessment Using GIS for the Town of San Sebastián, Guatemala. International Institute for Geoinformation Science and Earth Observation (ITC), January 2004, 29–49. https://www.academia.edu/download/48693265/vanwesten_com.pdf

Hadi, Z. N., & Almansori, N. J. H. (2023). Estimation of Manning coefficient for the section

between Al-Hindiya barrage and Al-Kufa barrage utilizing HEC-RAS. Materials Today: Proceedings, 80, 2595–2601.

Hahirwabasenga, J., Nilsson, E., Larson, M., Bizimana, H., Wali, U. G., & Persson, M. (2024). Flooding in Sebeya catchment, Rwanda - A review of causes, impacts, and management. International Journal of Disaster Risk Reduction, 114(November), 105012. https://doi.org/10.1016/j.ijdrr.2024.105012

Hawkins, R. H., Ward, T. J., Woodward, D. E., & Van Mullem, J. A. (2008). Curve number hydrology: State of the practice.

HEC, U. (2023). Technical Reference Manual. Texas Instruments, December, 155. http://www.hec.usace.army.mil/software/hec-hms/documentation/HEC-HMS_Technical Reference Manual_(CPD-74B).pdf

Hirwa, H., Ngwijabagabo, H., Minani, M., Tuyishime, S. P. C., & Habimana, I. (2023). Geospatial Assessment of Urban Flood Susceptibility Using AHP-Based Multi-Criteria Technique: Case Study of Musanze, Rwanda. Rwanda Journal of Engineering, Science, Technology and Environment, 5(1). https://doi.org/10.4314/rjeste.v5i1.6

IFRC. (2023). Operational Update:Rwanda - Floods and Landslides. Unhcr, December, 1–12.

Ingsrisawang, L., & Potawee, D. (2012). Multiple imputation for missing data in repeated measurements using MCMC and copulas. Proceedings of the International Multi Conference of Engineers and Computer Scientist.

IWRM. (2018). Rwanda Water Boad, IWRM Programme Rwanda: Sebeya Catchment Plan (2018-2024). October 2018, 184. https://waterportal.rwb.rw/sites/default/files/2018-11/Sebeya Catchment Plan 2018-2024.pdf

Jakob, M., & Church, M. (2011). The trouble with floods. Canadian Water Resources Journal, 36(4), 287–292. https://doi.org/10.4296/cwrj3604928

Jamal, S., & Ali, A. (2023). A comparative study of automatic drainage network extraction using ASTER GDEM, SRTM DEM and Cartosat-1 DEM in parts of Kosi basin, Bihar, India. Journal of Umm Al-Qura University for Engineering and Architecture, 14(1), 45–56. https://doi.org/10.1007/s43995-023-00014-4

Janicka, E., & Kanclerz, J. (2023). Assessing the Effects of Urbanization on Water Flow and Flood Events Using the HEC-HMS Model in the Wirynka River Catchment, Poland. Water (Switzerland), 15(1). https://doi.org/10.3390/w15010086

Jer Lang Hong, Suzana Shafie, Irena Naubi, Siew Fang Yong, & Kee An Hong. (2018). Muskingum and Lag Method River Routing Parameters for Klang River At Kuala Lumpur City Centre Derived Using Recorded Hydrographs. The Journal of The Institution of Engineers, Malaysia, 79(2), 1–8. https://doi.org/10.54552/v79i2.1

Kam, P. M., Aznar-Siguan, G., Schewe, J., Milano, L., Ginnetti, J., Willner, S., McCaughey, J. W., & Bresch, D. N. (2021). Global warming and population change both heighten future risk of human displacement due to river floods. Environmental Research Letters, 16(4). https://doi.org/10.1088/1748-9326/abd26c

Karamage. (2016). USLE-based assessment of soil erosion by water in the nyabarongo river catchment, Rwanda. International Journal of Environmental Research and Public Health, 13(8), 1–16. https://doi.org/10.3390/ijerph13080835

Karamage, F., Shao, H., Chen, X., Ndayisaba, F., Nahayo, L., Kayiranga, A., Omifolaji, J. K., Liu, T., & Zhang, C. (2016). Deforestation effects on soil erosion in the Lake Kivu Basin, D.R. Congo-Rwanda. Forests, 7(11), 1–17. https://doi.org/10.3390/f7110281

Karamage, F., Zhang, C., Fang, X., Liu, T., Ndayisaba, F., Nahayo, L., Kayiranga, A., & Nsengiyumva, J. B. (2017). Modeling rainfall-runoffresponse to land use and land cover change in Rwanda (1990-2016). Water (Switzerland), 9(2). https://doi.org/10.3390/w9020147

Karamage, F., Zhang, C., Ndayisaba, F., Shao, H., Kayiranga, A., Fang, X., Nahayo, L., Nyesheja, E. M., & Tian, G. (2016). Extent of cropland and related soil erosion risk in Rwanda. Sustainability (Switzerland), 8(7). https://doi.org/10.3390/su8070609

Kayode, S. J., Yakubu, S., Ologunorisa, T. E., & Kola-Olusanya, A. (2017). A post-disaster assessment of riverine communities impacted by a severe flooding event. Ghana Journal of Geography, 9(1), 17–41.

Keast, D., & Ellison, J. (2013). Magnitude frequency analysis of small floods using the annual and partial series. Water (Switzerland), 5(4), 1816–1829.

https://doi.org/10.3390/w5041816

Khan, M. S., Kim, M., Bang, H.-C., & Kim, D. (2014). A Study of Environment Monitoring using CCTV for on-Road Safety.

Koneti, S., Sunkara, S. L., & Roy, P. S. (2018). Hydrological modeling with respect to impact of land-use and land-cover change on the runoff dynamics in Godavari river basin using the HEC-HMS model. ISPRS International Journal of Geo-Information, 7(6). https://doi.org/10.3390/ijgi7060206

Majoro, F., Mukamwambali, C., Mugabushaka, A., Mwizerwa, F., Ingabire, T., & Nkundabose, J. P. (2020). Sebeya Catchment Inventory in Rwanda. 16(4), 141–163. www.ijsrm.humanjournals.comwww.ijsrm.humanjournals.com

Majoro, F., & Wali, U. G. (2022). Analyzing Various Factors Affecting Farmers' Willingness to Adopt Soil Erosion Control Measures in the Sebeya Catchment, Rwanda. Sustainability (Switzerland), 14(19). https://doi.org/10.3390/su141912895

Majoro, F., Wali, U. G., Munyaneza, O., Naramabuye, F.-X., Bugenimana, E. D., & Mukamwambali, C. (2021). Farmers Perceptions on Soil Erosion in Sebeya Catchment, Rwanda. EPH - International Journal of Agriculture and Environmental Research, 7(2), 17–24. https://doi.org/10.53555/eijaer.v6i2.66

Mendas, A. (2010). The contribution of the digital elevation models and geographic information systems in a watershed hydrologic research. Applied Geomatics, 2(1), 33–42. https://doi.org/10.1007/s12518-010-0017-x

MIDIMAR. (2015). The National Risk Atlas of Rwanda The National Risk Atlas of Rwanda. January 2015, 193.

MINEMA. (2018). Republic of Rwanda National Contingency Plan for Industrial. September, 1–43.

MINEMA. (2023). REPORT FOR THE DISASTER RISK REDUCTION AND MANAGEMENT. March.

MoE. (2024). REPUBLIC OF RWANDA Sebeya Catchment Management Plan (2018-2024). October 2018.

Munawar, H. S., Hammad, A. W. A., & Waller, S. T. (2022). Remote Sensing Methods for Flood Prediction: A Review. Sensors, 22(3). https://doi.org/10.3390/s22030960

Nadeem, M. U., Waheed, Z., Ghaffar, A. M., Javaid, M. M., Hamza, A., Ayub, Z., Nawaz, M. A., Waseem, W., Hameed, M. F., Zeeshan, A., Qamar, S., & Masood, K. (2022). Application of HEC-HMS for flood forecasting in hazara catchment Pakistan, south Asia. International Journal of Hydrology, 6(1), 7–12. https://doi.org/10.15406/ijh.2022.06.00296

Nsangou, D., Kpoumié, A., Mfonka, Z., Ngouh, A. N., Fossi, D. H., Jourdan, C., Mbele, H. Z., Mouncherou, O. F., Vandervaere, J. P., & Ndam Ngoupayou, J. R. (2022). Urban flood susceptibility modelling using AHP and GIS approach: case of the Mfoundi watershed at Yaoundé in the South-Cameroon plateau. Scientific African, 15, e01043. https://doi.org/10.1016/j.sciaf.2021.e01043

Ntakiyimana, C., Zhang, Y., & Twagirayezu, G. (2022). Road Flooding in Kigali City, Rwanda: Causes, Effects on Road Transportation and Mitigation Measures. Polish Journal of Environmental Studies, 31(4), 3735–3744. https://doi.org/10.15244/pjoes/146215

O'Connell, P. E., Ewen, J., O'Donnell, G., & Quinn, P. (2007). Is there a link between agricultural land-use management and flooding? Hydrol. Earth Syst. Sci., 11(1), 96–107. https://doi.org/10.5194/hess-11-96-2007

Ogato, G. S., Bantider, A., Abebe, K., & Geneletti, D. (2020). Geographic information system (GIS)-Based multicriteria analysis of flooding hazard and risk in Ambo Town and its watershed, West shoa zone, oromia regional State, Ethiopia. Journal of Hydrology: Regional Studies, 27(January), 100659. https://doi.org/10.1016/j.ejrh.2019.100659

Oleyiblo, J. O., & Li, Z. J. (2010). Application of HEC-HMS for flood forecasting in Misai and Wan'an catchments in China. Water Science and Engineering, 3(1), 14–22. https://doi.org/10.3882/j.issn.1674-2370.2010.01.002

Ouédraogo, W. A. A., Raude, J. M., & Gathenya, J. M. (2018). Continuous modeling of the Mkurumudzi River catchment in Kenya using the HEC-HMS conceptual model: Calibration, validation, model performance evaluation and sensitivity analysis. Hydrology, 5(3). https://doi.org/10.3390/hydrology5030044

Peker, İ. B., Gülbaz, S., Demir, V., Orhan, O., & Beden, N. (2024). Integration of HEC-RAS and HEC-HMS with GIS in Flood Modeling and Flood Hazard Mapping. Sustainability (Switzerland), 16(3). https://doi.org/10.3390/su16031226

Ray, S. K., & Desai, V. R. (2022). Flood Frequency Analysis of Jamsholaghat Sub- basin using Three Methods and its Comparison. Ijcrt.Org, 10(3), 36–42. https://doi.org/10.1729/Journal.29433

Rehman, A., Ma, H., Ahmad, M., Irfan, M., Traore, O., & Chandio, A. A. (2021). Towards environmental Sustainability: Devolving the influence of carbon dioxide emission to population growth, climate change, Forestry, livestock and crops production in Pakistan. Ecological Indicators, 125, 107460. https://doi.org/10.1016/j.ecolind.2021.107460

RoR. (2020). Republic of Rwanda Updated Nationally Determined. 96.

Rutagengwa, J. D., Nahayo, L., Philbert, M., Yambabariye, E., & Nsanzabaganwa, J. (2020). Spatial Analysis of Flood Hazard for the Risk Reduction in Rwanda. Journal of Environment Protection and Sustainable Development, 6(3), 57–65. http://www.aiscience.org/journal/jepsdhttp://creativecommons.org/licenses/by/4.0/

Sa'adi, Z., Shahid, S., Ismail, T., Chung, E. S., & Wang, X. J. (2019). Trends analysis of rainfall and rainfall extremes in Sarawak, Malaysia using modified Mann–Kendall test. Meteorology and Atmospheric Physics, 131(3), 263–277. https://doi.org/10.1007/S00703-017-0564-3/METRICS

Samantaray, S., & Sahoo, A. (2020). Estimation of flood frequency using statistical method: Mahanadi River basin, India. H2Open Journal, 3(1), 189–207. https://doi.org/10.2166/h2oj.2020.004

Scharffenberg, W., Ely, P., Daly, S., Fleming, M., & Pak, J. (2010). Hydrologic modeling system (HEC-HMS): Physically-based simulation components. 2nd Joint Federal Interagency Conference, June, 1–8.

Shah, S. A., Seker, D. Z., Hameed, S., & Draheim, D. (2019). The rising role of big data analytics and IoT in disaster management: recent advances, taxonomy and prospects. IEEE Access, 7, 54595–54614.

Sharafati, A., Yaseen, Z. M., & Shahid, S. (2021). A novel simulation–optimization strategy for stochastic-based designing of flood control dam: A case study of Jamishan dam. Journal of Flood Risk Management, 14(1), e12678.

Tejada, J. J., Raymond, J., & Punzalan, B. (2012). On the Misuse of Slovin's Formula. The Philippine Statistician, 61(1), 8.

Thywissen, K. (2006). Core terminology of disaster reduction: A comparative glossary. Measuring Vulnerability to Natural Hazards: Towards Disaster Resilient Societies, 448–496.

Uddin, K., Gurung, D. R., Giriraj, A., & Shrestha, B. (2013). Application of remote sensing and GIS for flood hazard management: a case study from Sindh Province, Pakistan. American Journal of Geographic Information System, 2(1), 1–5.

UNDRR. (2019). United Nations Office for Disaster Risk Reduction To download the full report visit : https://gar.unisdr.org To share your comments and news on the GAR on Twitter and Facebook , please use # GAR2019.

UNDRR. (2020). Hazard definition & classification review: Technical Report. Hazard Definition & Classification Reviewazard Definition & Classification Review, 88. https://www.undrr.org/publication/hazard-definition-and-classification-review

USACE. (2000). Hydrologic Modeling System Technical Reference Manual. Hydrologic Modeling System HEC-HMS Technical Reference Manual, March, 148.

Vashist, K., & Singh, K. K. (2023). HEC-RAS 2D modeling for flood inundation mapping: a case study of the Krishna River Basin. Water Practice and Technology, 18(4), 831–844. https://doi.org/10.2166/wpt.2023.048

Wisner. (2018). At Risk: Natural Hazards, People's Vulnerability and Disasters.

WMO. (2021). State of the Global Climate 2020 (Issue 1264). https://library.wmo.int/index.php?lvl=notice_display&id=21880#.YHg0ABMzZR0

Yu, Q., Wang, Y., & Li, N. (2022). Extreme Flood Disasters: Comprehensive Impact and Assessment. Water (Switzerland), 14(8), 1–14. https://doi.org/10.3390/w14081211

Yuemei, H., Xiaoqin, Z., Jianguo, S., & Jina, N. (2008). Conduction between left superior pulmonary vein and left atria and atria fibrillation under cervical vagal trunk stimulation. Colombia Medica, 39(3), 227–234. https://doi.org/10.25100/cm.v39i3.590

Zelelew, D. G. (2018). Applicability of a Spatially Semi-Distributed Hydrological Model for Watershed Scale Runoff Estimation in Northwest Ethiopia. 10–12. https://doi.org/10.3390/w10070923

Zeufack, A. G., Calderon, C., Ntumba Kabundi, A., Kubota, M., Korman, V., & Canales, C. C. (2021). Africa's Pulse, No. 23, October 2021. In Africa's Pulse, No. 23, October 2021 (Vol. 24, Issue October). https://doi.org/10.1596/978-1-4648-1805-9

APPENDIX

Completing miss data of Water levels

Quantitative data:

Summary statistics (Before treatment):

Variable	Observations	Obs. with missing data	Obs. without missing data	Minimum	Maximum	Mean	Std. deviation
Year	4018	0	4018	2011.000	2021.000	2016.000	3.163
Month	4018	2	4016	1.000	12.000	6.523	3.450
Date	4018	0	4018	1.000	31.000	15.730	8.802
Water level(m)	4018	1501	2517	0.036	3.000	1.103	0.356

Summary statistics (Post treatment):

Variable	Observations	Obs. with missing data	Obs. without missing data	Minimum	Maximum	Mean	Std. deviation
Year	4018	0	4018	2011.000	2021.000	2016.000	3.163
Month	4018	0	4018	1.000	12.000	6.523	3.449
Date	4018	0	4018	1.000	31.000	15.730	8.802
Water level(m)	4018	0	4018	0.036	3.000	1.103	0.282

Log Pearson distribution method for discharge prediction

Year	Q_{max}	Sorted	Discharge(m^3/s)	Rank m	Probability (%)	Log10Q	K	Fitted Y	Antilog Y(Q)
1991	127.6	30.64	140.42	1	3.125	2.147429	1.780117	2.192801	155.883917
1992	39.99	39.99	130.31	2	6.25	2.114978	1.487765	2.13943	137.857409
1993	140.4	40.35	129.43	3	9.375	2.112035	1.291843	2.103663	126.958844
1994	92.17	41.9	127.59	4	12.5	2.105817	1.137828	2.075546	118.999782
1995	94.17	42	122.58	5	15.625	2.08842	1.007529	2.051759	112.657262
1996	122	42.5	122.03	6	18.75	2.086467	0.892467	2.030754	107.338041
1997	117.7	44.81	117.72	7	21.875	2.07085	0.787934	2.01167	102.723594
1998	94.09	45.5	109.31	8	25	2.03866	0.691009	1.993976	98.6224622
1999	129.4	46.8	97.45	9	28.125	1.988782	0.599733	1.977313	94.9101572
2000	59.68	46.9	94.32	10	31.25	1.974604	0.512706	1.961425	91.5008485
2001	62.03	47.5	94.17	11	34.375	1.973913	0.428873	1.946121	88.3325583
2002	40.35	47.71	94.09	12	37.5	1.973543	0.347406	1.931248	85.3587866
2003	57.02	48.65	92.17	13	40.625	1.96459	0.26762	1.916683	82.5434672
2004	48.65	57.02	81.49	14	43.75	1.911104	0.18893	1.902317	79.8577676
2005	109.3	59.68	81.37	15	46.875	1.910464	0.110809	1.888056	77.2779605
2006	94.32	62.03	79.98	16	50	1.902981	0.032767	1.873808	74.7839438
2007	46.8	67.92	70.34	17	53.125	1.847202	-0.04568	1.859488	72.3581605
2008	122.6	70.34	67.92	18	56.25	1.831998	-0.12502	1.845004	69.9847637
2009	67.92	81.49	63.36	19	59.375	1.801815	-0.20577	1.830261	67.6489225
2010	81.49	92.17	62.03	20	62.5	1.792602	-0.28853	1.815154	65.33619
2011	130.3	94.09	59.68	21	65.625	1.775829	-0.37394	1.79956	63.0318605
2012	70.34	94.17	57.02	22	68.75	1.756027	-0.46283	1.783333	60.7202348
2013	47.71	94.32	49.81	23	71.875	1.697317	-0.55618	1.766291	58.3836806
2014	44.81	109.3	48.65	24	75	1.687083	-0.65529	1.748198	56.0013051
2015	30.64	117.7	47.71	25	78.125	1.678609	-0.76191	1.728734	53.54691

2016	45.5	122	47.51	26	81.25	1.676785	-0.87851	1.707447	50.9855675
2017	42	122.6	46.8	27	84.375	1.670246	-1.00885	1.683654	48.2673625
2018	41.9	127.6	42.5	28	87.5	1.628389	-1.15901	1.656239	45.3146789
2019	46.9	129.4	40.35	29	90.625	1.605844	-1.34015	1.623171	41.9924228
2020	47.5	130.3	39.99	30	93.75	1.601951	-1.57647	1.58003	38.0215358
2021	42.5	140.4	30.64	31	96.875	1.486289	-1.94197	1.513304	32.6064866
n	31								
x-bar	1.868								
G	-0.197								
STDEV	0.183								
Mean	75.42								
Std	34.63								
Skew	0.532								
Yn	0.537								
Sn	1.116								

Log Normal method for discharge prediction

Year	Q	Q_{max}	Rank	Frequency F(X)	Reduced Variance
1991	30.64	30.64	1	0.03125	-1.862731867
1992	39.99	39.99	2	0.0625	-1.534120544
1993	40.35	40.35	3	0.09375	-1.318010897
1994	41.9	41.9	4	0.125	-1.15034938
1995	42	42	5	0.15625	-1.009990169
1996	42.5	42.5	6	0.1875	-0.887146559
1997	44.81	44.81	7	0.21875	-0.776421761
1998	45.5	45.5	8	0.25	-0.67448975
1999	46.8	46.8	9	0.28125	-0.579132162
2000	46.9	46.9	10	0.3125	-0.488776411
2001	47.5	47.5	11	0.34375	-0.402250065
2002	47.71	47.71	12	0.375	-0.318639364
2003	48.65	48.65	13	0.40625	-0.237202109
2004	57.02	57.02	14	0.4375	-0.157310685
2005	59.68	59.68	15	0.46875	-0.078412413
2006	62.03	62.03	16	0.5	0
2007	67.92	67.92	17	0.53125	0.078412413
2008	70.34	70.34	18	0.5625	0.157310685
2009	81.49	81.49	19	0.59375	0.237202109
2010	92.17	92.17	20	0.625	0.318639364
2011	94.09	94.09	21	0.65625	0.402250065
2012	94.17	94.17	22	0.6875	0.488776411
2013	94.32	94.32	23	0.71875	0.579132162
2014	109.31	109.3	24	0.75	0.67448975
2015	117.72	117.7	25	0.78125	0.776421761
2016	122.03	122	26	0.8125	0.887146559
2017	122.58	122.6	27	0.84375	1.009990169
2018	127.59	127.6	28	0.875	1.15034938
2019	129.43	129.4	29	0.90625	1.318010897
2020	130.31	130.3	30	0.9375	1.534120544
2021	140.42	140.4	31	0.96875	1.862731867

Gumbel method for discharge prediction

Year	Q_{max}	Ranked Q	sorted	Rank m	p=m/(n+1)	Return Period(T)	Y_t	K_t	Q_t
1991	127.6	140.4	30.6	1	0.0	32.0	3.4	2.6	165.8
1992	40.0	130.3	40.0	2	0.1	16.0	2.7	2.0	143.8
1993	140.4	129.4	40.4	3	0.1	10.7	2.3	1.6	130.7
1994	92.2	127.6	41.9	4	0.1	8.0	2.0	1.3	121.2
1995	94.2	122.6	42.0	5	0.2	6.4	1.8	1.1	113.8
1996	122.0	122.0	42.5	6	0.2	5.3	1.6	0.9	107.5
1997	117.7	117.7	44.8	7	0.2	4.6	1.4	0.8	102.2
1998	94.1	109.3	45.5	8	0.3	4.0	1.2	0.6	97.4
1999	129.4	97.5	46.8	9	0.3	3.6	1.1	0.5	93.1
2000	59.7	94.3	46.9	10	0.3	3.2	1.0	0.4	89.2
2001	62.0	94.2	47.5	11	0.3	2.9	0.9	0.3	85.6
2002	40.4	94.1	47.7	12	0.4	2.7	0.8	0.2	82.2
2003	57.0	92.2	48.7	13	0.4	2.5	0.7	0.1	79.0
2004	48.7	81.5	57.0	14	0.4	2.3	0.6	0.0	75.9
2005	109.3	81.4	59.7	15	0.5	2.1	0.5	-0.1	73.0
2006	94.3	80.0	62.0	16	0.5	2.0	0.4	-0.2	70.1
2007	46.8	70.3	67.9	17	0.5	1.9	0.3	-0.2	67.4
2008	122.6	67.9	70.3	18	0.6	1.8	0.2	-0.3	64.7
2009	67.9	63.4	81.5	19	0.6	1.7	0.1	-0.4	62.0
2010	81.5	62.0	92.2	20	0.6	1.6	0.0	-0.5	59.3
2011	130.3	59.7	94.1	21	0.7	1.5	-0.1	-0.5	56.7
2012	70.3	57.0	94.2	22	0.7	1.5	-0.2	-0.6	54.1
2013	47.7	49.8	94.3	23	0.7	1.4	-0.2	-0.7	51.4
2014	44.8	48.7	109.3	24	0.8	1.3	-0.3	-0.8	48.6
2015	30.6	47.7	117.7	25	0.8	1.3	-0.4	-0.9	45.8
2016	45.5	47.5	122.0	26	0.8	1.2	-0.5	-0.9	42.8
2017	42.0	46.8	122.6	27	0.8	1.2	-0.6	-1.0	39.6
2018	41.9	42.5	127.6	28	0.9	1.1	-0.7	-1.1	36.0
2019	46.9	40.4	129.4	29	0.9	1.1	-0.9	-1.3	32.0
2020	47.5	40.0	130.3	30	0.9	1.1	-1.0	-1.4	27.1
2021	42.5	30.6	140.4	31	1.0	1.0	-1.2	-1.6	20.2
n	31.0								
Max	140.4								
Min	30.6								
Median	62.0								
Mean	75.4								
Std	34.6								
Skew	0.5								
Yn	0.5								
Sn	1.1								

5-Year P = 44.1mm							10-Year P = 51mm				
Time(hr)	Rainfall fraction	Rainfall distribution	Incremental	Increasing order	Q_{Peak} @ 24 Hours	Time(hr)	Rainfall fraction	Rainfall distribution	Incremental	Increasing order	QPeak @ 24 Hours
0	0.000	0	0	0	0	0	0.000	0	0	0	0
1	0.013	0.5733	0.5733	0.1764	0.1764	1	0.013	0.663	0.663	0.204	0.459
2	0.024	1.0584	0.4851	0.1764	0.3969	2	0.024	1.224	0.561	0.204	0.561
3	0.037	1.6317	0.5733	0.3969	0.5292	3	0.037	1.887	0.663	0.459	0.612
4	0.049	2.1609	0.5292	0.441	0.5292	4	0.049	2.499	0.612	0.51	0.663
5	0.062	2.7342	0.5733	0.4851	0.5733	5	0.062	3.162	0.663	0.561	0.663
6	0.081	3.5721	0.8379	0.5292	0.7056	6	0.081	4.131	0.969	0.612	0.918
7	0.099	4.3659	0.7938	0.5292	0.8379	7	0.099	5.049	0.918	0.612	0.969
8	0.122	5.3802	1.0143	0.5292	1.1907	8	0.122	6.222	1.173	0.612	1.377
9	0.149	6.5709	1.1907	0.5733	1.764	9	0.149	7.599	1.377	0.663	2.04
10	0.182	8.0262	1.4553	0.5733	3.3075	10	0.182	9.282	1.683	0.663	3.825
11	0.257	11.3337	3.3075	0.5733	10.0548	11	0.257	13.107	3.825	0.663	11.628
12	0.485	21.3885	10.0548	0.7056	10.5399	12	0.485	24.735	11.628	0.816	12.189
13	0.724	31.9284	10.5399	0.7938	4.0572	13	0.724	36.924	12.189	0.918	4.692
14	0.816	35.9856	4.0572	0.8379	2.5578	14	0.816	41.616	4.692	0.969	2.958
15	0.874	38.5434	2.5578	0.8379	1.4553	15	0.874	44.574	2.958	0.969	1.683
16	0.914	40.3074	1.764	1.0143	0.8379	16	0.914	46.614	2.04	1.173	1.173
17	0.926	40.8366	0.5292	1.1907	0.7938	17	0.926	47.226	0.612	1.377	0.969
18	0.942	41.5422	0.7056	1.4553	0.5733	18	0.942	48.042	0.816	1.683	0.816
19	0.961	42.3801	0.8379	1.764	0.5733	19	0.961	49.011	0.969	2.04	0.663
20	0.965	42.5565	0.1764	2.5578	0.5292	20	0.965	49.215	0.204	2.958	0.612

21	0.975	42.9975	0.441	3.3075	0.4851	21	0.975	49.725	0.51	3.825	0.612
22	0.984	43.3944	0.3969	4.0572	0.441	22	0.984	50.184	0.459	4.692	0.51
23	0.996	43.9236	0.5292	10.0548	0.3969	23	0.996	50.796	0.612	11.628	0.204
24	1.000	44.1	0.1764	10.5399	0.1764	24	1.000	51	0.204	12.189	0.204

20-Year P = 57.7mm						50-Year P = 66.4 mm					
Time(hr)	Rainfall fraction	Rainfall distribution	Incremental	Increasing order	QPeak @ 24 Hours	Time(hr)	Rainfall fraction	Rainfall distribution	Incremental	Increasing order	QPeak @ 24 Hours
0	0.000	0	0	0	0	0	0.000	0	0	0	0
1	0.013	0.7501	0.7501	0.2308	0.2308	1	0.013	0.8632	0.8632	0.2656	0.2656
2	0.024	1.3848	0.6347	0.2308	0.577	2	0.024	1.5936	0.7304	0.2656	0.664
3	0.037	2.1349	0.7501	0.5193	0.6347	3	0.037	2.4568	0.8632	0.5976	0.7968
4	0.049	2.8273	0.6924	0.577	0.6924	4	0.049	3.2536	0.7968	0.664	0.7968
5	0.062	3.5774	0.7501	0.6347	0.7501	5	0.062	4.1168	0.8632	0.7304	0.8632
6	0.081	4.6737	1.0963	0.6924	0.9232	6	0.081	5.3784	1.2616	0.7968	1.0624
7	0.099	5.7123	1.0386	0.6924	1.0963	7	0.099	6.5736	1.1952	0.7968	1.2616
8	0.122	7.0394	1.3271	0.6924	1.3271	8	0.122	8.1008	1.5272	0.7968	1.5272
9	0.149	8.5973	1.5579	0.7501	1.9041	9	0.149	9.8936	1.7928	0.8632	2.1912
10	0.182	10.5014	1.9041	0.7501	3.3466	10	0.182	12.0848	2.1912	0.8632	3.8512
11	0.257	14.8289	4.3275	0.7501	13.1556	11	0.257	17.0648	4.98	0.8632	6.1088
12	0.485	27.9845	13.1556	0.9232	13.7903	12	0.485	32.204	15.1392	1.0624	15.8696
13	0.724	41.7748	13.7903	1.0386	5.3084	13	0.724	48.0736	15.8696	1.1952	15.1392

14	0.816	47.0832	5.3084	1.0963	4.3275	14	0.816	54.1824	6.1088	1.2616	4.98
15	0.874	50.4298	3.3466	1.0963	2.308	15	0.874	58.0336	3.8512	1.2616	2.656
16	0.914	52.7378	2.308	1.3271	1.5579	16	0.914	60.6896	2.656	1.5272	1.7928
17	0.926	53.4302	0.6924	1.5579	1.0963	17	0.926	61.4864	0.7968	1.7928	1.2616
18	0.942	54.3534	0.9232	1.9041	1.0386	18	0.942	62.5488	1.0624	2.1912	1.1952
19	0.961	55.4497	1.0963	2.308	0.7501	19	0.961	63.8104	1.2616	2.656	0.8632
20	0.965	55.6805	0.2308	3.3466	0.7501	20	0.965	64.076	0.2656	3.8512	0.8632
21	0.975	56.2575	0.577	4.3275	0.6924	21	0.975	64.74	0.664	4.98	0.7968
22	0.984	56.7768	0.5193	5.3084	0.6347	22	0.984	65.3376	0.5976	6.1088	0.7304
23	0.996	57.4692	0.6924	13.1556	0.5193	23	0.996	66.1344	0.7968	15.1392	0.5976
24	1.000	57.7	0.2308	13.7903	0.2308	24	1.000	66.4	0.2656	15.8696	0.2656

FLOOD RISK ASSESSMENT: INTERVIEW QUESTIONS IN THE SEBEYA CATCHMENT

Background and Purpose of the Questionnaire

This questionnaire is designed as part of a flood risk assessment study in the Sebeya catchment area. The purpose is to gather valuable data from local residents regarding their experiences with flooding, the impact of floods on their homes and livelihoods, and their perceptions of flood risks and mitigation measures. The responses will contribute to understanding the main causes of flooding, the effectiveness of current flood management practices, and the preparedness of communities in the region. Topics covered include flood impacts on agriculture, infrastructure, and property, flood response and evacuation measures, as well as community resilience and future preparedness for flooding events. The findings will inform future flood management strategies and improve community-based disaster risk reduction in the Sebeya catchment.

Personal Information

1. **Gender**
    - Male
    - Female
    - Other (please specify): _____
2. **Age Group**
    - Less than 20 years
    - 20 - 30 years
    - 30 - 40 years
    - 40 - 50 years
    - 50 - 60 years
    - Above 60 years
3. **Marital Status**
    - Married
    - Unmarried
    - Divorced
    - Widowed
    - Separated
4. **Occupation**
    - Student
    - Farmer
    - Employee (Government/Private)
    - Self-employed
    - Construction Worker
    - Public Service Employee
    - Other (please specify): _____
5. **Level of Education**
    - Primary
    - High School
    - University

- Informal Education
- None

6. **Location**
   - Rural
   - Urban

Flood Experience

7. **Have you experienced a flood in your area?**
   - Yes
   - No
8. **What are the main causes of flooding in the Sebeya catchment area? (Select all that apply)**
   - Rainfall
   - Topography
   - Urbanization
   - Human Activities
   - Other (please specify): _____
9. **Which year did you experience the most significant flooding? (Select all that apply)**
   - 2016
   - 2017
   - 2018
   - 2019
   - 2020
   - 2021
   - 2022
   - 2023
   - 2024
10. **What areas were impacted by the floods? (Select all that apply)**
    - Agriculture
    - Buildings
    - Loss of Life
    - Commercial Areas
    - Livestock
    - Infrastructure
    - Other (please specify): _____

Flood Impact and Vulnerability

11. **How far is your residence from the river?**
    - Less than 100 m
    - 100 - 500 m
    - 500 - 1000 m

- Above 1000 m

12. **Is there a dam or reservoir near your residence?**
    - Yes
    - No
13. **Is your residence located in a flood-prone area?**
    - Yes
    - No
14. **During the most recent flood event, what was the maximum water level reached in your area?**
    - Less than 1 meter
    - 1 - 3 meters
    - 3 - 5 meters
    - More than 5 meters
15. **Did floodwaters enter your home or property?**
    - Yes
    - No
16. **Were there any damages to your property due to the flood?**
    - Yes
    - No
17. **If yes, what property was damaged? (Select all that apply)**
    - Houses
    - Farmland
    - Infrastructure (e.g., roads, bridges)
    - Commercial buildings
    - Other (please specify): _____
18. **What is the estimated cost of repairs or replacements (RWF)?**
    - Below 100,000
    - 100,000 - 300,000
    - 300,000 - 500,000
    - 500,000 - 700,000
    - 700,000 - 900,000
    - Above 1,000,000

Flood Information and Preparedness

19. **Did you receive information about the flood warning or evacuation notice?**
    - Yes
    - No
20. **How did you receive information about the flood warning or evacuation notice? (Select all that apply)**
    - Radio
    - Television
    - Phone call
    - Text message
    - Email
    - Other (please specify): _____

21. **Have you taken any measures to prevent or mitigate flood damage to your property?**
    - Yes
    - No
22. **If yes, what measures have you taken? (Select all that apply)**
    - Sand bags
    - Drainage channels
    - Relocation
    - Terracing
    - Gabions
    - Ponds
    - Other (please specify): _____
23. **Have you received any assistance or information from the government or NGOs regarding flood mitigation?**
    - Yes
    - No
24. **If yes, what type of assistance or information was provided? (Select all that apply)**
    - Financial Aid
    - Relocation
    - Training
    - Other (please specify): _____

Flood Mitigation Measures in the Area

25. **What measures have been implemented to prevent or mitigate flood damage in your area? (Select all that apply)**
    - Reservoirs
    - Dams
    - Gabions
    - Ponds
    - Retaining walls
    - Dykes
    - Planting trees
    - Relocation
    - Terracing
    - Sand bags
    - Other (please specify): _____
26. **What additional measures can be taken to prevent or mitigate flood damage in your area? (Select all that apply)**
    - Reservoirs
    - Dams
    - Gabions
    - Ponds
    - Retaining walls
    - Dykes

- Planting trees
- Relocation
- Terracing
- Other (please specify): _____

Evacuation and Response

27. **Did you evacuate your home or property during the most recent flood event?**
    - Yes
    - No
28. **If yes, where did you evacuate to?**
    - Church
    - School
    - Relative or friend's home
    - Government Shelter
    - Other (please specify): _____
29. **How satisfied were you with the response to the flood?**
    - Very satisfied
    - Satisfied
    - Not satisfied
    - Very dissatisfied
30. **Were there any areas where you feel that the response could have been improved?**
    - Yes
    - No
31. **If yes, please select the areas where the response could have been improved (Select all that apply)**
    - Mahoko
    - Nyundo
    - Pfunda
    - Kanama
    - Other (please specify): _____

Future Preparedness and Concerns

32. **How concerned are you about the possibility of future floods in your area?**
    - Very concerned
    - Somewhat concerned
    - Not concerned
33. **Do you feel that your community is well prepared to respond to future floods?**
    - Yes
    - No
34. **How confident are you in the ability of the government or NGOs to respond to future floods?**

- Very confident
- Somewhat confident
- Not at all confident

35. **How comfortable are you with sharing your personal information for the purpose of data collection related to flood events?**
    - Very comfortable
    - Somewhat comfortable
    - Not at all comfortable
36. **Is there any other information related to flood events or flood preparedness that you would like to share?**

- _____
  _____
  _____
  _____
  _____